

# ITERATIVE SOLVERS IN ADAPTIVE FEM

ADAPTIVITY YIELDS QUASI-OPTIMAL COMPUTATIONAL RUNTIME

PHILIPP BRINGMANN, ANI MIRAÇI, AND DIRK PRAETORIUS

**ABSTRACT.** This chapter provides an overview of state-of-the-art adaptive finite element methods (AFEMs) for the numerical solution of second-order elliptic partial differential equations (PDEs), where the primary focus is on the optimal interplay of local mesh refinement and iterative solution of the arising discrete systems. Particular emphasis is placed on the thorough description of the essential ingredients necessary to design adaptive algorithms of optimal complexity, i.e., algorithms that mathematically guarantee the optimal rate of convergence with respect to the overall computational cost and, hence, time. Crucially, adaptivity induces reliability of the computed numerical approximations by means of a-posteriori error control. This ensures that the error committed by the numerical scheme is bounded from above by computable quantities. The analysis of the adaptive algorithms is based on the study of appropriate quasi-error quantities that include and balance different components of the overall error. Importantly, the quasi-errors stemming from an adaptive algorithm with contractive iterative solver satisfy a centerpiece concept, namely, full R-linear convergence. This guarantees that the adaptive algorithm is essentially contracting this quasi-error at each step and it turns out to be the cornerstone for the optimal complexity of AFEM. The unified analysis of the adaptive algorithms is presented in the context of symmetric linear PDEs. Extensions to goal-oriented, non-symmetric, as well as non-linear PDEs are presented with suitable nested iterative solvers fitting into the general analytical framework of the linear symmetric case. Numerical experiments highlight the theoretical results and emphasize the practical relevance and gain of adaptivity with iterative solvers for numerical simulations with optimal complexity.

## 1. MOTIVATION

**1.1. Concept of adaptivity and historical overview.** The design of modern numerical schemes for approximating the solution to partial differential equations (PDEs) proceeds in certain steps. First, the equation is transformed into a suitable *variational formulation*. This provides the mathematical framework allowing to verify existence and uniqueness of the solution. Second, the *discretization* of the formulation is typically based on dissecting the underlying domain into a computational mesh, choosing an appropriate finite element space, e.g., consisting of globally continuous piecewise polynomials of a given degree, and solving the discretized variational formulation for this discrete space. Such a scheme is called finite element method (FEM) and results in a system of equations with a finite number of unknowns to be solved on a computer. However, generating and refining the mesh is crucial for the quality of the discrete solution in approximating

---

2020 *Mathematics Subject Classification.* 41A25, 65N15, 65N30, 65N50, 65Y20.

*Key words and phrases.* Adaptive finite element method, iterative solver, a-posteriori error control, optimal convergence rates, cost-optimality.

**Acknowledgment.** This research was funded by the Austrian Science Fund (FWF) projects [10.55776/F65](#) (SFB F65 “Taming complexity in PDE systems”), [10.55776/I6802](#) (international project I6802 “Functional error estimates for PDEs on unbounded domains”), and [10.55776/P33216](#) (standalone project P33216 “Computational nonlinear PDEs”).

the unavailable – and possibly singular – solution to the PDE. Indeed, the accuracy of the approximation will be heavily spoiled by singularities of the solution, if they are not sufficiently resolved by the mesh. Third, *iterative solvers* are of utmost importance to compute a numerical approximation. In particular, once the discrete problem is translated to a system of linear equations, the choice of the algebraic solver is essential for memory- and time-efficient simulations. Moreover, non-linear discrete problems must be linearized and, clearly, the interaction of linearization and inexact solution of the resulting systems of linear equations pose additional challenges to the structure of the numerical scheme and its analysis.

From a practical point of view, numerical simulations must not only ensure *reliability* (i.e., a guaranteed user-specified accuracy) but should moreover provide *efficiency* (i.e., considerably short and, potentially, minimal computing time). For this purpose, computable *a-posteriori error estimators* play a major role. They are evaluated after computing a numerical approximation to the solution with the aim of assessing its quality and, thereby, deciding whether a desired accuracy has been achieved or not. Moreover, they enable the efficient usage of computational resources (like memory consumption and computing time) by steering the adaptive mesh-refinement process and balancing different parts of the error like discretization error, linearization error, and algebraic solver error. The newly refined mesh allows to compute a more accurate approximation which in turn, through the a-posteriori estimator, allows to further refine the mesh where needed. The continuation of this *nested iterative process*, while yielding ever better numerical results, is inherently cumulative in nature. On the one hand, these algorithms allow for the best possible accuracy with respect to the dimension of the discrete spaces of approximation, i.e., *rate-optimality*. On the other hand, the additional computational effort for the mesh refinement should pay off to achieve the desired error threshold within the shortest possible runtime and, thus, keeping the computational cost minimal, i.e., *cost-optimality*. In both cases, the analysis is not built upon the study of the error itself, but on (essentially equivalent) *quasi-error* quantities consisting of the a-posteriori estimator and other error components.

In order to achieve such optimality results, the need for suitable iterative solvers and appropriate stopping criteria balancing reasonable computational cost and good accuracy becomes centerpiece. In practice, the approximation should be constructed in a number of operations proportional to the dimension of the discrete space (resp. number of simplices in the triangulation), i.e., at *linear cost*, while ensuring an *error contraction* property with respect to the previous available approximation. Finally, the overall number of iterative solver steps is controlled thanks to the *a-posteriori* estimator through an adaptive *stopping criterion*.

Before introducing the model problem in Section 1.2, this final paragraph recalls key contributions from the academic history of the field, where we refer, in particular, to the exhaustive review [BBCO24]. Some first pioneering works on the mathematics of adaptive mesh refinement include [BR78; ZR79; GKZB83]. Since adaptive algorithms do not drive the mesh size to zero in the whole domain, their convergence is not guaranteed by the classical a-priori error analysis, see, e.g., [BS08b; EG21]. While convergence was already addressed in [BV84] for one-dimensional problems, the first convergence results of adaptive FEMs for two or higher space dimensions were provided by [Dör96; MNS00]. Eventually, the notion of nonlinear approximation classes enabled the proof of optimal convergence rates with respect to the dimension of the discrete space, see [BDD04;

[Ste07]. The succeeding generalizations to a myriad of applications led to a summarizing axiomatic framework in [CFPP14] and the role of adaptive stopping criteria being emphasized in [EV13]. While even the early contributions like [Ste07] address the iterative algebraic solution, all convergence results remain subject to the assumption of the iterative solution being sufficiently close to the exact algebraic solution; see, e.g., [Ste07; CFPP14]. This severe algorithmic restriction was removed for the proof of full R-linear convergence in [GHPS21a] for energy-contractive iterative solvers and in [BFM<sup>+</sup>23] for general contractive solvers.

**1.2. Symmetric second-order model problem.** The focus of the present chapter is initially drawn to symmetric second-order linear elliptic PDEs as a model problem with further extensions, discussed at the end of the chapter. Let  $\Omega \subset \mathbb{R}^d$ ,  $d \in \mathbb{N}$ , denote the computational domain, which is mathematically assumed to be a bounded Lipschitz domain with polytopal boundary  $\partial\Omega$ . This chapter employs the notation of Lebesgue and Sobolev spaces as used in standard textbooks on PDEs, e.g., [Eva98, Sect. 5]. Given a symmetric coefficient tensor  $\mathbf{A} \in [L^\infty(\Omega)]_{\text{sym}}^{d \times d}$  and load functions  $f \in L^2(\Omega)$  and  $\mathbf{f} \in [L^2(\Omega)]^d$ , we consider the elliptic boundary value problem of seeking  $u^* \in \mathcal{X} := H_0^1(\Omega)$  such that

$$-\operatorname{div}(\mathbf{A}\nabla u^*) = f - \operatorname{div} \mathbf{f} \text{ in } \Omega \quad \text{and} \quad u^* = 0 \text{ on } \Gamma := \partial\Omega. \quad (1)$$

We assume that  $\mathbf{A}$  is uniformly elliptic in the sense that the minimal and maximal eigenvalues are uniformly bounded almost everywhere, i.e.,

$$0 < \operatorname{ess\,inf}_{x \in \Omega} \lambda_{\min}(\mathbf{A}(x)) \leq \operatorname{ess\,sup}_{x \in \Omega} \lambda_{\max}(\mathbf{A}(x)) < \infty. \quad (2)$$

Then, we define the bilinear form  $a : \mathcal{X} \times \mathcal{X} \rightarrow \mathbb{R}$  using the dot notation henceforth designating the vector-product in the sense of

$$a(u, v) := \int_{\Omega} (\mathbf{A}\nabla u) \cdot \nabla v \, dx = \sum_{i,j=1}^d \int_{\Omega} \mathbf{A}_{ij} \partial_i u \partial_j v \, dx \text{ for all } u, v \in \mathcal{X} = H_0^1(\Omega).$$

The uniform bounds (2) ensure that  $a(\cdot, \cdot)$  is a scalar product on  $\mathcal{X}$  and thus induces an energy norm denoted as  $\|\cdot\|$ . The Riesz–Fischer theorem [Eva98, Thm. 2 in § D.2] guarantees existence and uniqueness of the solution  $u^* \in \mathcal{X}$  to (1) and the equivalent variational formulation

$$a(u^*, v) = \int_{\Omega} (f v + \mathbf{f} \cdot \nabla v) \, dx = \int_{\Omega} f v \, dx + \sum_{i=1}^d \int_{\Omega} \mathbf{f}_i \partial_i v \, dx =: F(v) \text{ for all } v \in \mathcal{X}. \quad (3)$$

The discretization of problem (3) employs a conforming simplicial mesh  $\mathcal{T}_H$  of  $\Omega$ , i.e., triangles for  $d = 2$  and tetrahedra for  $d = 3$ . Conformity means that  $\bigcup_{T \in \mathcal{T}_H} T = \overline{\Omega}$  and that the intersection of two different simplices is either empty or a common lower-dimensional sub-simplex, e.g., a common vertex or edge for  $d = 2$  or a common vertex, edge, or face for  $d = 3$ . The usual conforming finite element space of globally continuous and piecewise polynomial functions of degree at most  $p \in \mathbb{N}$  reads

$$\mathcal{X}_H := \{v_H \in \mathcal{X} : v_H|_T \text{ is a polynomial of degree } \leq p, \text{ for all } T \in \mathcal{T}_H\}. \quad (4)$$

This leads to the discrete formulation seeking the unique solution  $u_H^* \in \mathcal{X}_H$  to

$$a(u_H^*, v_H) = F(v_H) \quad \text{for all } v_H \in \mathcal{X}_H. \quad (5)$$

Although the index  $H$  historically originates from meshes with a quasi-uniform mesh size  $H$ , this notation indicates all discrete objects throughout this chapter also with

respect to highly graded meshes. Related discrete objects have the same index, e.g.,  $v_H$  is a discrete function in the space  $\mathcal{X}_H$  corresponding to the triangulation  $\mathcal{T}_H$ . Different indices are used to distinguish between different triangulations and the corresponding discrete objects, e.g.,  $\mathcal{T}_H, \mathcal{T}_h, \mathcal{T}_\ell$ , etc.

**1.3. Outline of the chapter.** In the following, the algorithm and its constituting modules are presented in Section 2. The main results on optimality are showcased in Section 2.7. Section 3 highlights the numerical performance of the presented adaptive algorithm for a variety of test cases and confirms its optimality results in accordance with the theory. The proofs of the main results are presented in detail in Section 4. The Sections 5–7 are devoted to extending the model problem (1) to a goal-oriented framework, or a setting exhibiting non-symmetry or non-linearity. Throughout, particular emphasis is put on the algorithmic decision for the termination of the iterative solver and its cost-optimal interplay with adaptive mesh refinement. An additional focus is on parameter-robust convergence, where mathematics guarantees convergence without any constraints on the choice of fine-tuned parameters.

## 2. ADAPTIVE MESH-REFINING ALGORITHM

This section discusses the assumptions on the modules SOLVE, ESTIMATE, MARK, and REFINED as employed in the adaptive algorithm. The module REFINED is presented first since the successively improved sequence of meshes is fundamental for the discretization and computation in the remaining modules. The formulation of the algorithm follows in Subsection 2.5 as well as the introduction of the notions of quasi-errors and computational cost in Subsection 2.6 below. Subsection 2.7 presents the convergence and complexity results.

**2.1. Module REFINED.** The convergence analysis of adaptive FEM crucially depends on a mesh-refinement strategy which avoids over-refinement and the degeneration of the shapes of simplices. From an analytical perspective, the standard choice is newest-vertex bisection (NVB). This strategy is denoted by `refine`( $\cdot$ ) throughout this chapter. A visualization in the two-dimensional case is given in Figure 1. Let  $\mathcal{T}_h = \text{refine}(\mathcal{T}_H, \mathcal{M}_H)$  denote the coarsest conforming triangulation of  $\Omega$  obtained from  $\mathcal{T}_H$  by bisecting at least all marked elements of  $\mathcal{M}_H \subseteq \mathcal{T}_H$ . A suitable closure procedure ensures that no hanging nodes (or hanging edges in 3D) exist in the refined mesh  $\mathcal{T}_h$ . This requirement is subject to an appropriate enumeration and connectivity of the vertices of the initial mesh  $\mathcal{T}_0$ ; see [Ste08] for  $d \geq 2$ . The recent work [DGS23] introduced an initialization strategy for arbitrary initial meshes  $\mathcal{T}_0$  for all  $d \geq 2$ ; see also the seminal work [Mit91] for  $d \geq 2$  for admissible  $\mathcal{T}_0$  as well as [KPP13] for the case  $d = 2$  and any initial mesh. The existence of hanging nodes cannot be avoided for hexahedral meshes, imposing additional difficulties in the analysis; see, e.g., [BN10, Sect. 6.3] for details.

Without a second argument,  $\mathcal{T}_h \in \text{refine}(\mathcal{T}_H)$  represents all triangulations  $\mathcal{T}_h$  obtainable by finitely many steps (including zero) of NVB refinements (with arbitrary marked elements in each step). We define  $\mathbb{T} := \text{refine}(\mathcal{T}_0)$  as the set of all meshes which can be generated from the initial simplicial mesh  $\mathcal{T}_0$  of  $\Omega$  by use of `refine`( $\cdot$ ). NVB-generated meshes are indeed locally nested, i.e., for any two simplices  $T \in \mathcal{T} \in \mathbb{T}$  and  $T' \in \mathcal{T}' \in \mathbb{T}$  with  $|T \cap T'| > 0$ , in the sense of the  $d$ -dimensional measure, it holds either  $T = T'$  or  $T \subsetneq T'$  or  $T' \subsetneq T$ . Moreover, the NVB refinement ensures that all meshes  $\mathcal{T}_H \in \mathbb{T}$  are uniformly shape regular. This means that for  $\rho_T$  being the radius of the largest

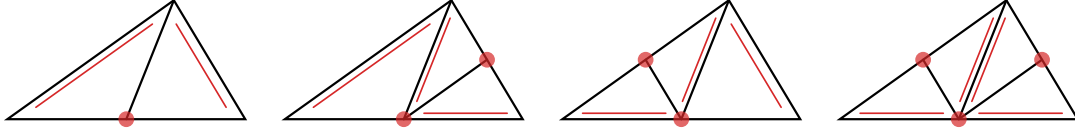


FIGURE 1. Visualization in 2D of the finite number of patterns of new triangles obtained by NVB. Each triangle has an associated refinement edge to be bisected in case the triangle is marked for refinement. NVB marks edges, here indicated by red dots, in order to avoid hanging nodes. The red line indicates the new refinement edge – opposite to the newest vertex – on the new triangles.

ball inscribed in  $T$  and  $\text{diam}(T)$  being the diameter of  $T$ , there exists a shape-regularity constant  $\gamma > 0$  such that

$$\gamma := \sup_{\mathcal{T} \in \mathbb{T}} \max_{T \in \mathcal{T}} \frac{\text{diam}(T)}{\rho_T} < \infty. \quad (6)$$

Every  $\mathcal{T}_H \in \mathbb{T}$  corresponds to an associated finite element space  $\mathcal{X}_H \subsetneq \mathcal{X}$  defined via (4). Note that, for  $\mathcal{T}_H, \mathcal{T}_h \in \mathbb{T}$  with  $\mathcal{T}_h \in \text{refine}(\mathcal{T}_H)$ , there holds nestedness of the spaces  $\mathcal{X}_H \subseteq \mathcal{X}_h$ .

Throughout this chapter, the tilde notation  $A \lesssim B$  abbreviates  $A \leq C B$  for a constant  $C > 0$  that is independent of the mesh size, but might depend on  $\mathcal{T}_0$  (and, thus, the shape-regularity parameter  $\gamma$ ), the input data  $\mathbf{A}$ ,  $f$ , and  $\mathbf{f}$ , as well as on the polynomial degree  $p$  of the discretization. Moreover,  $A \approx B$  represents the equivalence  $A \lesssim B$  and  $B \lesssim A$ .

Our analysis relies on the following properties of the mesh refinement:

**(R1) splitting property:** Each refined element is split into finitely many children, i.e., for all  $\mathcal{T}_H \in \mathbb{T}$  and all  $\mathcal{M}_H \subseteq \mathcal{T}_H$ , the triangulation  $\mathcal{T}_h = \text{refine}(\mathcal{T}_H, \mathcal{M}_H)$  satisfies that

$$\#(\mathcal{T}_H \setminus \mathcal{T}_h) + \#\mathcal{T}_H \leq \#\mathcal{T}_h \lesssim \#(\mathcal{T}_H \setminus \mathcal{T}_h) + \#(\mathcal{T}_H \cap \mathcal{T}_h);$$

**(R2) overlay estimate:** For all meshes  $\mathcal{T}_H \in \mathbb{T}$  and  $\mathcal{T}_h, \mathcal{T}_{h'} \in \text{refine}(\mathcal{T}_H)$ , there exists a common refinement  $\mathcal{T}_h \oplus \mathcal{T}_{h'} \in \text{refine}(\mathcal{T}_h) \cap \text{refine}(\mathcal{T}_{h'}) \subseteq \text{refine}(\mathcal{T}_H)$  such that

$$\#(\mathcal{T}_h \oplus \mathcal{T}_{h'}) \leq \#\mathcal{T}_h + \#\mathcal{T}_{h'} - \#\mathcal{T}_H;$$

**(R3) mesh-closure estimate:** For each sequence  $(\mathcal{T}_\ell)_{\ell \in \mathbb{N}_0}$  of successively refined meshes, i.e.,  $\mathcal{T}_{\ell+1} := \text{refine}(\mathcal{T}_\ell, \mathcal{M}_\ell)$  with  $\mathcal{M}_\ell \subseteq \mathcal{T}_\ell$  for all  $\ell \in \mathbb{N}_0$ , it holds that

$$\#\mathcal{T}_\ell - \#\mathcal{T}_0 \lesssim \sum_{j=0}^{\ell-1} \#\mathcal{M}_j.$$

We refer to [BDD04; Ste07; Ste08; CKNS08; KPP13; GSS14] for the validity of (R1)–(R3) for NVB-refinement algorithms. In particular, it follows from the splitting property (R1) that the computation of  $\mathcal{T}_h = \text{refine}(\mathcal{T}_H, \mathcal{M}_H)$  can be realized at linear cost  $\mathcal{O}(\#\mathcal{T}_H)$ , i.e., the number of operations is bounded by a fixed multiple of the number of elements in  $\mathcal{T}_H$ . Figure 2 illustrates the overlay  $\mathcal{T}_h \oplus \mathcal{T}_{h'}$  of two meshes. The estimate (R2) can be seen by noting that each coarse simplex  $T \in \mathcal{T}_H$  has children in  $\mathcal{T}_h$ , and  $\mathcal{T}_{h'}$ , respectively, which can be represented by two binary trees thanks to the structure of NVB refinement. Moreover, note that mesh closure is in general *non-local*, i.e., the number of new simplices

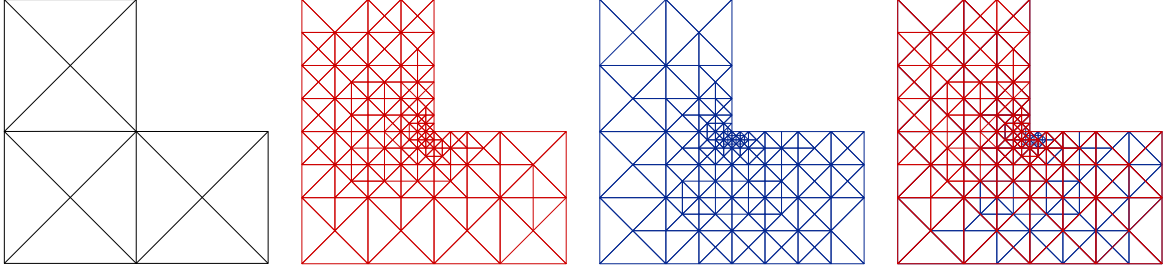


FIGURE 2. Example in 2D of the overlay of two distinct triangulations  $\mathcal{T}_h$  and  $\mathcal{T}_{h'}$ , represented in red and blue. The meshes stem from the refinement of the same coarse mesh  $\mathcal{T}_H$ , represented in black, and their overlay  $\mathcal{T}_h \oplus \mathcal{T}_{h'}$ , i.e., the coarsest common refinement, is illustrated in the rightmost figure.

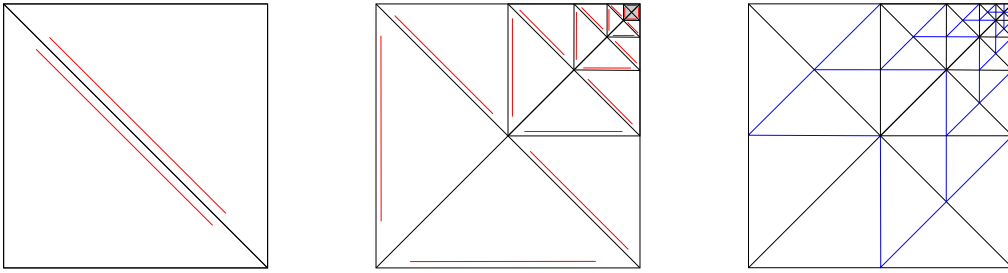


FIGURE 3. Example in 2D of non-locality of the mesh closure. From the initial triangulation  $\mathcal{T}_0$  in the left, iterative NVB refinement leads to the middle triangulation  $\mathcal{T}_\ell$ . Only four elements (highlighted in gray, each refinement edge represented by a red line) of  $\mathcal{T}_\ell$  are marked for refinement. Nonetheless, each triangle of  $\mathcal{T}_\ell$  is bisected at least once for the new triangulation  $\mathcal{T}_{\ell+1}$  in the right to be conforming (and avoid hanging nodes) and thus the refinement propagates through the entire mesh.

arising in one refinement step cannot be bound by the number of marked elements alone; see Figure 3 for an example. Nonetheless, the estimate (R3) ensures control on the number of generated elements over a mesh hierarchy by the sum of marked elements.

**2.2. Module SOLVE.** Recall that even when the linear system arising from the discretization (5) is symmetric and positive definite, its exact solution is in practice prohibitively expensive. Thus, an iterative solver will be used to compute an approximation. One step of the iterative solver for the numerical solution of the discrete problem (5) is formally denoted as an operator  $\Psi_H : \mathcal{X}^* \times \mathcal{X}_H \rightarrow \mathcal{X}_H$ , i.e.,  $u_H^k := \Psi_H(F; u_H^{k-1})$  is the new approximation constructed by one solver step from the available approximation  $u_H^{k-1}$  and the right-hand side  $F$  in the so-called dual space  $\mathcal{X}^* \equiv H^{-1}(\Omega)$  consisting of all linear and continuous forms  $F : \mathcal{X} \rightarrow \mathbb{R}$ . A crucial assumption for the later convergence analysis is the strict contraction of the algebraic solver in the energy norm, defined by

$$\| \| u \| \| := \langle A \nabla u, \nabla u \rangle_{L^2(\Omega)}^{1/2} := \left( \int_{\Omega} \mathbf{A} \nabla u \cdot \nabla u \, dx \right)^{1/2} \quad \text{for all } u \in \mathcal{X}.$$

This means that there exists some uniform constant  $0 < q_{\text{alg}} < 1$  at each iteration, i.e.,

$$\| \| u_H^* - u_H^k \| \| \leq q_{\text{alg}} \| \| u_H^* - u_H^{k-1} \| \| . \quad (\text{C})$$

Examples for such solvers include conjugate gradient methods with optimal additive Schwarz or BPX-type preconditioners [CNX12] or optimal geometric multigrid methods which respect the multilevel structure of locally graded meshes of the later adaptive algorithm. For the latter, we refer to [WZ17] for discretizations with  $p = 1$  as well as to [IMPS24] for higher-order robust solvers and also [SMPZ08]. Note that, here, the exact discrete solution  $u_H^*$  is never computed but only approximated by  $u_H^k$ . However, the contraction (C) and the triangle inequality imply that

$$\frac{1 - q_{\text{alg}}}{q_{\text{alg}}} \|\|u_H^* - u_H^k\|\| \leq \|\|u_H^k - u_H^{k-1}\|\| \leq (1 + q_{\text{alg}}) \|\|u_H^* - u_H^{k-1}\|\|. \quad (7)$$

This means that  $\|\|u_H^k - u_H^{k-1}\|\|$  provides a (computable) a-posteriori estimator for the algebraic error  $\|\|u_H^* - u_H^k\|\|$ . Hence, this estimator allows to stop the algebraic solver when the algebraic error is dominated by a fixed factor  $\lambda_{\text{alg}} > 0$  times the discretization error measured by some computable quantity  $\eta_H(u_H^k)$ , i.e.,

$$\|\|u_H^k - u_H^{k-1}\|\| \leq \lambda_{\text{alg}} \eta_H(u_H^k). \quad (8)$$

This can be interpreted as numerically balancing the error contributions: When the algebra is sufficiently resolved, the solver should be stopped and a new mesh-refinement step should take place. The final index of the iterative solver being the minimal  $k \in \mathbb{N}$ , where (8) is satisfied, is denoted by  $\underline{k}[H]$ . In this notation, the dependency on the discretization parameter  $H$  is omitted if it is clear from the context. The contraction (C) immediately establishes a bound for the distance between the initial iterate  $u_H^0$  and the final iterate  $u_H^{\underline{k}}$

$$\|\|u_H^{\underline{k}} - u_H^0\|\| \leq \|\|u_H^* - u_H^{\underline{k}}\|\| + \|\|u_H^* - u_H^0\|\| \leq (1 + q_{\text{alg}}^{\underline{k}[H]}) \|\|u_H^* - u_H^0\|\| \leq 2 \|\|u_H^* - u_H^0\|\|. \quad (9)$$

Note that one solver step of the optimally preconditioned conjugate gradient method [CNX12] or the geometric multigrid method [WZ17; IMPS24] can indeed be implemented at linear cost  $\mathcal{O}(\#\mathcal{T}_H)$ .

**2.3. Module ESTIMATE.** To account for the discretization error, i.e., the inaccuracy of the numerical scheme in approximating the continuous solution  $u^*$  to (3), we use a residual-based a-posteriori estimator. To formulate the latter, we require additional regularity of the data. More precisely, we assume that  $\mathbf{A}|_T$  and  $\mathbf{f}|_T$  are Lipschitz continuous for all  $T \in \mathcal{T}_H$ . Since  $v_H \in \mathcal{X}_H$  is a globally continuous,  $\mathcal{T}_H$ -piecewise polynomial of degree  $p \in \mathbb{N}$ , its gradient  $\nabla v_H$  is in general a discontinuous  $\mathcal{T}_H$ -piecewise polynomial of degree  $p - 1 \in \mathbb{N}_0$ . In particular,  $\mathbf{A}\nabla v_H$  can jump across the  $(d - 1)$ -dimensional faces  $T \cap T'$  of neighboring simplices  $T, T' \in \mathcal{T}_H$ . In contrast, note that the exact solution  $u^* \in \mathcal{X}$  of (3) has vanishing jump of the normal component  $(\mathbf{A}\nabla u^* - \mathbf{f}) \cdot \mathbf{n}$  across all interior faces, where  $\mathbf{n}$  is a unit normal vector on  $T \cap T'$ . To measure inconsistency of any finite element function  $v_H \in \mathcal{X}_H$  in this respect, let

$$[(\mathbf{A}\nabla v_H - \mathbf{f}) \cdot \mathbf{n}]|_{T \cap T'} := ((\mathbf{A}\nabla v_H - \mathbf{f})|_T - (\mathbf{A}\nabla v_H - \mathbf{f})|_{T'}) \cdot \mathbf{n}$$

denote the normal jump as scalar-valued function on the interior face  $T \cap T'$  (with, e.g.,  $(\mathbf{A}\nabla v_H - \mathbf{f})|_T$  understood as the trace of a continuous function from  $T$  to  $T \cap T'$ ). For any discrete function  $v_H \in \mathcal{X}_H$ , the residual-based quantity

$$\eta_H(T, v_H)^2 := |T|^{2/d} \|f + \text{div}(\mathbf{A}\nabla v_H - \mathbf{f})\|_{L^2(T)}^2 + |T|^{1/d} \|[(\mathbf{A}\nabla v_H - \mathbf{f}) \cdot \mathbf{n}]\|_{L^2(\partial T \cap \Omega)}^2 \quad (10a)$$

is computable for all  $T \in \mathcal{T}_H$  (up to a quadrature error). Abbreviate any sum of the local contributions by

$$\eta_H(\mathcal{M}_H, v_H) := \left( \sum_{T \in \mathcal{M}_H} \eta_H(T, v_H)^2 \right)^{1/2} \quad \text{for all } \mathcal{M}_H \subseteq \mathcal{T}_H \quad (10b)$$

and set  $\eta_H(v_H) := \eta_H(\mathcal{T}_H, v_H)$ . The first summand in (10a) measures the volume residual of the finite element function  $v_H$  with respect to the strong form of the PDE (1). Note that any  $v_H \in \mathcal{X}_H$  satisfies the boundary conditions in (1) exactly so that no boundary residual is needed here. As noted above, the second summand in (10a) can be understood as a consistency error related to  $(\mathbf{A}\nabla v_H - \mathbf{f}) \notin H(\text{div}; \Omega)$ . Thus, (10) indicates, at least heuristically, which simplices have a large contribution to the discretization error  $\|u^* - u_H^*\|$ , allowing to steer the adaptive mesh refinement.

For further details on the construction and analysis of residual-based error estimators, the reader is referred, e.g., to the monographs [AO00; Ver13]. We emphasize that the a-posteriori error indicator (10) can be computed at overall linear cost  $\mathcal{O}(\#\mathcal{T}_H)$ .

The framework of the *axioms of adaptivity* from [CFPP14] summarizes the many contributions to the convergence analysis with rates. The following abstract conditions, that indeed hold for the residual a-posteriori error estimator (10), guarantee plain convergence (without rates) of the resulting adaptive algorithm. They involve generic constants  $C_{\text{stab}}, C_{\text{rel}}, C_{\text{drel}} > 0$  and  $0 < q_{\text{red}} < 1$ , where  $C_{\text{rel}}$  depends only on  $\gamma$ -shape regularity, while  $C_{\text{stab}}, C_{\text{drel}}$  depend additionally on the polynomial degree  $p$ , and  $q_{\text{red}} = 2^{-1/(2d)}$  for NVB refinement. For any  $\mathcal{T}_h \in \text{refine}(\mathcal{T}_H)$ , let  $u_H^*$  and  $u_h^*$  denote the corresponding exact discrete solutions that are never computed in practice, but are only used in the analysis.

- (A1) **stability:**  $|\eta_h(\mathcal{U}_H, v_h) - \eta_H(\mathcal{U}_H, v_H)| \leq C_{\text{stab}} \|v_h - v_H\|$  for all  $v_h \in \mathcal{X}_h, v_H \in \mathcal{X}_H$ , and any subset  $\mathcal{U}_H \subseteq \mathcal{T}_H \cap \mathcal{T}_h$  of unrefined simplices;
- (A2) **reduction:**  $\eta_h(\mathcal{T}_h \setminus \mathcal{T}_H, v_H) \leq q_{\text{red}} \eta_H(\mathcal{T}_H \setminus \mathcal{T}_h, v_H)$  for all  $v_H \in \mathcal{X}_H \subseteq \mathcal{X}_h$ ;
- (A3) **reliability:**  $\|u^* - u_H^*\| \leq C_{\text{rel}} \eta_H(u_H^*)$ ;
- (A4) **discrete reliability:**  $\|u_h^* - u_H^*\| \leq C_{\text{drel}} \eta_H(\mathcal{T}_H \setminus \mathcal{T}_h, u_H^*)$ .

Furthermore, the exact discrete solutions satisfy the following Galerkin orthogonality

$$a(u^* - u_H^*, v_H) = 0 \quad \text{for all } v_H \in \mathcal{X}_H, \quad (11)$$

leading, in particular, to the following Pythagorean identity

$$\|u^* - u_H^*\|^2 + \|u_H^* - v_H\|^2 = \|u^* - v_H\|^2 \quad \text{for all } v_H \in \mathcal{X}_H. \quad (12)$$

This immediately results in the Céa-type quasi-best approximation result

$$\|u^* - u_H^*\| \leq \|u^* - v_H\| \quad \text{for all } v_H \in \mathcal{X}_H. \quad (13)$$

Note that the residual a-posteriori error estimator in addition to reliability (A3) satisfies a so-called *efficiency* property

$$\eta_H(u_H^*) \lesssim \|u^* - u_H^*\| + \text{osc}_H(u_H^*), \quad (14)$$

with the latter term representing the *data oscillation*. It is defined as

$$\begin{aligned} \text{osc}_H(v_H)^2 := & \sum_{T \in \mathcal{T}_H} \left[ |T|^{2/d} \|(1 - \Pi_T^q)(f - \text{div } \mathbf{f} + \text{div } \mathbf{A}\nabla v_H)\|_{L^2(T)}^2 \right. \\ & \left. + \sum_{E \subset \partial T \setminus \Gamma} |T|^{1/d} \|(1 - \Pi_E^q)[(\mathbf{A}\nabla v_H - \mathbf{f}) \cdot \mathbf{n}]\|_{L^2(E)}^2 \right], \end{aligned} \quad (15)$$

where  $\Pi_T^q$  is the  $L^2(T)$ -orthogonal projection onto the space of polynomials of degree  $q = 2(p - 1)$  on the simplex  $T$  and, similarly,  $\Pi_E^q$  is the  $L^2(E)$ -orthogonal projection onto the polynomials of degree  $q$  on the interior face  $E$ . In particular, one can prove the generalized Céa-type estimate

$$\| \|u^* - u_H^* \| \| + \text{osc}_H(u_H^*) \lesssim \| \|u^* - v_H \| \| + \text{osc}_H(v_H) \quad \text{for all } v_H \in \mathcal{X}_H \quad (16)$$

which, together with reliability (A3) and efficiency (14), results in

$$\eta_H(u_H^*) \approx \inf_{v_H \in \mathcal{X}_H} (\| \|u^* - v_H \| \| + \text{osc}_H(v_H)). \quad (17)$$

However, since the convergence results in Subsection 2.7 focus on the estimator  $\eta_H(u_H^*)$  only, efficiency is not explicitly required in the analysis [CFPP14, Sect. 3.2]. For a-posteriori error analysis of data oscillation terms, we refer to, e.g., [KV21], see also references therein.

**2.4. Module MARK.** The a-posteriori estimator (10) for the discretization error is used within a marking strategy to indicate the error distribution among simplices and determine which ones should be refined. Preferably, a small set of simplices whose estimator contributions exceed a given percentage  $0 < \theta \leq 1$  of  $\eta_H(v_H)$  are marked. More precisely, the up-to-date numerical analysis employs the Dörfler criterion introduced in [Dör96] for reasons that are made precise below: Determine a set  $\mathcal{M}_H \subseteq \mathcal{T}_H$  of minimal cardinality such that

$$\theta \eta_H(u_H^k)^2 \leq \eta_H(\mathcal{M}_H, u_H^k)^2. \quad (18)$$

Note that small  $\theta \approx 0$  leads to few marked elements (and, hence, highly adapted meshes), whereas large  $\theta \approx 1$  essentially enforces uniform mesh refinement. A straight-forward implementation of the strategy (18) would rely on sorting the estimator contributions which would result in suboptimal  $\mathcal{O}(\#\mathcal{T}_H \log \#\mathcal{T}_H)$  complexity. However, a modification of the QuickSelect algorithm in [PP20] allows for linear complexity on average. Moreover, [Ste07] proposes a realization of (18) based on binning, which determines  $\mathcal{M}_H \subseteq \mathcal{T}_H$  satisfying (18) and containing, up to a factor 2, the minimal number of elements.

Having marked elements  $\mathcal{M}_H \subseteq \mathcal{T}_H$  for refinement, the refinement procedure generates a finer triangulation  $\mathcal{T}_h$  such that at least all marked simplices  $\mathcal{M}_H \subseteq \mathcal{T}_H \setminus \mathcal{T}_h$  with large estimator contributions are refined. The use of the Dörfler marking criterion (18) with arbitrary adaptivity parameter  $0 < \theta \leq 1$  guarantees the following estimator reduction property.

---

**Lemma 1 (perturbed reduction of the estimator for nested approximations).**

Let  $\mathcal{T}_H$  be a given triangulation with corresponding finite element space  $\mathcal{X}_H$ . Given  $u_H^k \in \mathcal{X}_H$  and  $0 < \theta < 1$ , let  $\mathcal{M}_H \subseteq \mathcal{T}_H$  be the elements marked for refinement by (18). Let  $\mathcal{T}_h = \text{refine}(\mathcal{T}_H, \mathcal{M}_H)$  with corresponding finite element space  $\mathcal{X}_h$  and set  $u_h^0 := u_H^k \in \mathcal{X}_H \subseteq \mathcal{X}_h$ . Then, the solver-generated iterates  $u_h^k \in \mathcal{X}_h$  with  $0 \leq k \leq \underline{k}$ , satisfy

---


$$\eta_h(u_h^k) \leq q_\theta \eta_H(u_H^k) + 2C_{\text{stab}} \| \|u_h^* - u_H^k \| \|, \quad \text{where } q_\theta := [1 - (1 - q_{\text{red}}^2)\theta]^{1/2} < 1. \quad (19)$$


---

*Proof.* Since all marked simplices are refined, the inclusion  $\mathcal{M}_H \subseteq \mathcal{T}_H \setminus \mathcal{T}_h$  holds and the Dörfler marking criterion (18) yields

$$-\eta_H(\mathcal{T}_H \setminus \mathcal{T}_h; u_H^k)^2 \leq -\eta_H(\mathcal{M}_H; u_H^k)^2 \stackrel{(18)}{\leq} -\theta \eta_H(u_H^k)^2.$$

This estimate, together with reduction (A2), leads to

$$\begin{aligned}
\eta_h(u_H^k)^2 &= \eta_h(\mathcal{T}_h \cap \mathcal{T}_H; u_H^k)^2 + \eta_h(\mathcal{T}_h \setminus \mathcal{T}_H; u_H^k)^2 \\
&\stackrel{(A2)}{\leq} \eta_H(\mathcal{T}_h \cap \mathcal{T}_H; u_H^k)^2 + q_{\text{red}}^2 \eta_H(\mathcal{T}_h \setminus \mathcal{T}_H; u_H^k)^2 \\
&= \eta_H(u_H^k)^2 - (1 - q_{\text{red}}^2) \eta_H(\mathcal{T}_h \setminus \mathcal{T}_H; u_H^k)^2 \\
&\leq [1 - (1 - q_{\text{red}}^2)\theta] \eta_H(u_H^k)^2 = q_\theta^2 \eta_H(u_H^k)^2.
\end{aligned} \tag{20}$$

Combining this with stability (A1), the estimate (9), and nested iteration  $u_h^0 = u_H^k$ , results in

$$\begin{aligned}
\eta_h(u_h^k) &\leq \eta_h(u_H^k) + C_{\text{stab}} \|u_h^k - u_H^k\| \leq q_\theta \eta_H(u_H^k) + C_{\text{stab}} \|u_h^k - u_H^k\| \\
&\leq q_\theta \eta_H(u_H^k) + 2C_{\text{stab}} \|u_h^* - u_H^k\|. \quad \square
\end{aligned}$$

**2.5. Algorithm 1: Adaptive FEM. Input:** Initial mesh  $\mathcal{T}_0$ , polynomial degree  $p \in \mathbb{N}$ , initial iterate  $u_0^0 := u_0^k := 0$ , marking parameter  $0 < \theta \leq 1$ , solver parameter  $\lambda_{\text{alg}} > 0$ .

**Adaptive loop:** For all  $\ell = 0, 1, 2, \dots$ , repeat the following steps (I)–(III):

- (I) **SOLVE & ESTIMATE.** For all  $k = 1, 2, 3, \dots$ , repeat the steps (a)–(b):
- (a) Compute  $u_\ell^k := \Psi_\ell(F; u_\ell^{k-1})$  and the corresponding refinement indicators  $\eta_\ell(T; u_\ell^k)$  for all  $T \in \mathcal{T}_\ell$ .
  - (b) Terminate  $k$ -loop and define  $\underline{k}[\ell] := k$  provided that

$$\|u_\ell^k - u_\ell^{k-1}\| \leq \lambda_{\text{alg}} \eta_\ell(u_\ell^k). \tag{21}$$

(II) **MARK.** Determine a set  $\mathcal{M}_\ell \subseteq \mathcal{T}_\ell$  that satisfies the Dörfler criterion (18).

(III) **REFINE.** Generate the new mesh  $\mathcal{T}_{\ell+1} := \text{refine}(\mathcal{T}_\ell, \mathcal{M}_\ell)$  by NVB and employ nested iteration  $u_{\ell+1}^0 := u_\ell^k$ .

**Output:** Sequences of successively refined triangulations  $\mathcal{T}_\ell$ , discrete approximations  $u_\ell^k$ , and corresponding error estimators  $\eta_\ell(u_\ell^k)$ .

---

**Remark 2.** Let us comment on the termination criterion (21) for the iterative solver used in Algorithm 1.

- (i) According to Lemma 3 below, the sum  $\|u_\ell^k - u_\ell^{k-1}\| + \eta_\ell(u_\ell^k)$  provides a computable upper bound for the error  $\|u^* - u_\ell^k\|$ . Stopping the iterative solver with the minimal index  $k \in \mathbb{N}$  such that (21) holds, can thus be understood as numerical equilibration of both summands.
  - (ii) Moreover, as seen in (7) above, the term  $\|u_\ell^k - u_\ell^{k-1}\|$  provides control on the algebraic error  $\|u_\ell^* - u_\ell^k\|$ , while  $\|u^* - u_\ell^*\| \lesssim \eta_\ell(u_\ell^*) \lesssim \eta_\ell(u_\ell^k) + \|u_\ell^* - u_\ell^k\|$  controls the discretization error. E.g., for  $\lambda_{\text{alg}} = 1/10$  and omitting other constants, the stopping criterion (21) may also be interpreted that the algebraic error should be below 10% of the discretization error.
  - (iii) An additional consequence of (21) is that  $\eta_\ell(u_\ell^k)$  provides a computable upper bound for the error  $\|u^* - u_\ell^k\|$  of each respective final iterate; see (24) below.
  - (iv) Finally, it can happen that the iterative solver does not terminate. In this case, it follows from Theorem 5 below that  $u^* = u_\ell^*$  and  $\eta_\ell(u_\ell^k) \rightarrow \eta_\ell(u_\ell^*) = 0$  as  $k \rightarrow \infty$ .
-

Since the numerical analysis below studies asymptotic behavior, this algorithm generates an infinite sequence  $(u_\ell^k)_{\ell \in \mathbb{N}_0}$ . However, a practical implementation may terminate when the estimated error is below a user-prescribed threshold  $\tau > 0$ , i.e.,

$$\| \|u_\ell^k - u_\ell^{k-1}\| \| + \eta_\ell(u_\ell^k) \leq \tau, \quad (22)$$

or after a maximal dimension  $\dim(\mathcal{X}_\ell)$  or runtime is reached. The following lemma shows that the left-hand side of (22) provides indeed a-posteriori error control on  $\| \|u^\star - u_\ell^k\| \|$  and that the stopping criterion (21) is designed in a way that it ensures reliability of  $\eta_\ell(u_\ell^k)$  for the a-posteriori error control of  $\| \|u^\star - u_\ell^k\| \|$ .

---

**Lemma 3 (a-posteriori control of the overall error).** *For  $\ell \in \mathbb{N}_0$  and  $k \geq 1$ , let  $u_\ell^k \in \mathcal{X}_\ell$  be computed by the adaptive loop of Algorithm 1. Then, there holds*

$$\| \|u^\star - u_\ell^k\| \| \lesssim \| \|u_\ell^k - u_\ell^{k-1}\| \| + \eta_\ell(u_\ell^k) \quad (23)$$

and for  $k = \underline{k}[\ell]$

$$\| \|u^\star - u_\ell^k\| \| \lesssim \eta_\ell(u_\ell^k). \quad (24)$$


---

*Proof.* The reliability (A3), the stability (A1), and a-posteriori control for the algebraic error (7) yield the result

$$\begin{aligned} \| \|u^\star - u_\ell^k\| \| &\leq \| \|u^\star - u_\ell^\star\| \| + \| \|u_\ell^\star - u_\ell^k\| \| \stackrel{(A3)}{\leq} C_{\text{rel}} \eta_\ell(u_\ell^\star) + \| \|u_\ell^\star - u_\ell^k\| \| \\ &\stackrel{(A1)}{\leq} C_{\text{rel}} \eta_\ell(u_\ell^k) + (C_{\text{rel}} C_{\text{stab}} + 1) \| \|u_\ell^\star - u_\ell^k\| \| \\ &\stackrel{(7)}{\leq} C_{\text{rel}} \eta_\ell(u_\ell^k) + (C_{\text{rel}} C_{\text{stab}} + 1) \frac{q_{\text{alg}}}{1 - q_{\text{alg}}} \| \|u_\ell^k - u_\ell^{k-1}\| \|. \end{aligned}$$

In particular, thanks to the stopping criterion (21), there holds

$$\| \|u^\star - u_\ell^k\| \| \leq [C_{\text{rel}} + (C_{\text{rel}} C_{\text{stab}} + 1) \frac{q_{\text{alg}}}{1 - q_{\text{alg}}} \lambda_{\text{alg}}] \eta_\ell(u_\ell^k). \quad \square$$

**2.6. Notions of quasi-errors and computational cost.** The sequential nature of Algorithm 1 motivates the countably infinite index set

$$\mathcal{Q} := \{(\ell, k) \in \mathbb{N}_0^2 : u_\ell^k \in \mathcal{X} \text{ is defined in Algorithm 1}\}.$$

The set  $\mathcal{Q}$  is equipped with the linear order

$$(\ell', k') \leq (\ell, k) : \iff u_{\ell'}^{k'} \text{ is used no later than } u_\ell^k \text{ in Algorithm 1}$$

and the total step counter

$$|\ell, k| := \#\{(\ell', k') \in \mathcal{Q} : (\ell', k') \leq (\ell, k)\} \in \mathbb{N}_0 \quad \text{for all } (\ell, k) \in \mathcal{Q}.$$

Consistently with the stopping indices in Algorithm 1, we define

$$\begin{aligned} \underline{\ell} &:= \sup\{\ell \in \mathbb{N}_0 : (\ell, 0) \in \mathcal{Q}\} \in \mathbb{N}_0 \cup \{\infty\}, \\ \underline{k}[\ell] &:= \sup\{k \in \mathbb{N}_0 : (\ell, k) \in \mathcal{Q}\} \in \mathbb{N} \cup \{\infty\}, \text{ whenever } (\ell, 0) \in \mathcal{Q}. \end{aligned}$$

To simplify notation, the dependency of indices is omitted whenever the relation is clear from the context, e.g.,  $\underline{k} := \underline{k}[\ell]$  in  $u_\ell^k = u_\ell^{k[\ell]}$  or  $(\ell, \underline{k}) = (\ell, \underline{k}[\ell])$ .

It is important to note that each of the modules in Subsections 2.1–2.4 above can be realized in linear complexity, i.e., for a given mesh  $\mathcal{T}_\ell$ , the number of arithmetic and logical operators is proportional to the number of elements  $\#\mathcal{T}_\ell$ , which in turn, for any fixed polynomial degree, is proportional to the number of degrees of freedom, i.e., the dimension of the discrete finite element space  $\mathcal{X}_\ell$ . Due to the nested nature of the adaptive

algorithm, the total computational cost (and, hence, empirical computational time) to compute  $u_\ell^k$  is thus proportional to

$$\text{cost}(\ell, k) := \sum_{\substack{(\ell', k') \in \mathcal{Q} \\ |\ell', k'| \leq |\ell, k|}} \#\mathcal{T}_{\ell'} \quad \text{for all } (\ell, k) \in \mathcal{Q}. \quad (25)$$

For the empirical comparison of the performance for various polynomial degrees  $p$ , a cost term is introduced using the dimension of the corresponding discrete spaces

$$\text{cost}_p(\ell, k) := \sum_{\substack{(\ell', k') \in \mathcal{Q} \\ |\ell', k'| \leq |\ell, k|}} \dim(\mathcal{X}_{\ell'}) \quad \text{for all } (\ell, k) \in \mathcal{Q}. \quad (26)$$

Note that the two cost terms (25) and (26) are equivalent with equivalence constants depending on the polynomial degree.

The following quasi-error is introduced to measure the algebraic and the discretization error

$$\mathbb{H}_\ell^k := \|\|u_\ell^\star - u_\ell^k\|\| + \eta_\ell(u_\ell^k) \quad \text{for all } (\ell, k) \in \mathcal{Q}. \quad (27)$$

Arguing as in the proof of Lemma 3 above, the following equivalences can be shown for the final iterates

$$\eta_\ell(u_\ell^k) \approx \mathbb{H}_\ell^k = \|\|u_\ell^\star - u_\ell^k\|\| + \eta_\ell(u_\ell^k) \approx \|\|u^\star - u_\ell^k\|\| + \eta_\ell(u_\ell^k),$$

linking the present quasi-error (27) with that of [CKNS08]. The contraction of the algebraic error ensures the following perturbed contraction of the weighted quasi-error.

---

**Lemma 4 (contraction of quasi-error of final iterates).** *Let  $\gamma \in (0, 1)$  such that  $\gamma < (1 - q_{\text{alg}})/(2C_{\text{stab}})$ . Consider the weighted quasi-error of the final iterates*

$$\mathbb{H}_\ell := \|\|u_\ell^\star - u_\ell^k\|\| + \gamma \eta_\ell(u_\ell^k) \quad \text{for all } (\ell, \underline{k}) \in \mathcal{Q}. \quad (28)$$

Then, there exists a constant  $0 < q_{\text{ctr}} < 1$  such that

$$\mathbb{H}_{\ell+1} \leq q_{\text{ctr}} \mathbb{H}_\ell + q_{\text{ctr}} \|\|u_{\ell+1}^\star - u_\ell^k\|\| \quad \text{for all } (\ell + 1, \underline{k}) \in \mathcal{Q}. \quad (29)$$


---

*Proof.* The solver contraction (C), nested iteration  $u_{\ell+1}^0 = u_\ell^k$ , and the estimator reduction (19) prove, for  $q_{\text{ctr}} := \max\{q_{\text{alg}} + 2C_{\text{stab}}\gamma, q_\theta\} \in (0, 1)$ ,

$$\begin{aligned} \|\|u_{\ell+1}^\star - u_{\ell+1}^k\|\| + \gamma \eta_{\ell+1}(u_{\ell+1}^k) &\stackrel{\text{(C)}}{\leq} q_{\text{alg}}^{k[\ell+1]} \|\|u_{\ell+1}^\star - u_\ell^k\|\| + \gamma \eta_{\ell+1}(u_{\ell+1}^k) \\ &\stackrel{\text{(19)}}{\leq} (q_{\text{alg}} + 2C_{\text{stab}}\gamma) \|\|u_{\ell+1}^\star - u_\ell^k\|\| + q_\theta \gamma \eta_\ell(u_\ell^k) \\ &\leq q_{\text{ctr}} [\|\|u_{\ell+1}^\star - u_\ell^k\|\| + \gamma \eta_\ell(u_\ell^k)]. \end{aligned}$$

The triangle inequality concludes the proof of (29).  $\square$

**2.7. Convergence and complexity.** The first main result asserts full R-linear convergence of the quasi-error  $\mathbb{H}_\ell^k$  introduced in (27). More precisely, estimate (30) below proves that independently of the algorithmic decision for either local mesh refinement or yet another solver step, Algorithm 1 essentially causes contraction of the quasi-error. In particular, we see that the Dörfler marking criterion (18) is sufficient to prove R-linear convergence of  $\mathbb{H}_\ell^k \approx \eta_\ell(u_\ell^k)$ .

---

**Theorem 5 (parameter-robust full R-linear convergence).** *Let  $0 < \theta \leq 1$  and  $\lambda_{\text{alg}} > 0$  be arbitrary. Then, Algorithm 1 guarantees the existence of constants  $C_{\text{lin}} > 0$  and  $0 < q_{\text{lin}} < 1$  such that*

$$\mathbb{H}_\ell^k \leq C_{\text{lin}} q_{\text{lin}}^{|\ell, k| - |\ell', k'|} \mathbb{H}_{\ell'}^{k'} \quad \text{for all } (\ell, k), (\ell', k') \in \mathcal{Q} \text{ with } |\ell, k| > |\ell', k'|. \quad (30)$$

*In particular, this yields parameter-robust convergence*

$$\|u^* - u_\ell^k\| \lesssim \mathbb{H}_\ell^k \leq C_{\text{lin}} q_{\text{lin}}^{|\ell, k|} \mathbb{H}_0^0 \rightarrow 0 \quad \text{as } |\ell, k| \rightarrow \infty. \quad (31)$$


---

The proof of Theorem 5 is given in Section 4.1 below. Theorem 5 guarantees convergence (without rates) for any choice of the parameters  $\theta$  and  $\lambda_{\text{alg}}$  in Algorithm 1.

The formal statement of optimal convergence rates employs the notion of nonlinear approximation classes [BDD04]. The computational effort for the solution of the discrete problem (5) on some mesh  $\mathcal{T}_H \in \mathbb{T}_N := \{\mathcal{T} \in \mathbb{T} : \#\mathcal{T} - \#\mathcal{T}_0 \leq N\}$  compared to the solution on the initial mesh  $\mathcal{T}_0$  is bounded (up to a multiplicative constant) by  $N \in \mathbb{N}_0$ . The value

$$e(u^*, \mathcal{T}_0, N) := \min_{\mathcal{T}_{\text{opt}} \in \mathbb{T}_N} \eta_{\text{opt}}(u_{\text{opt}}^*) \quad (32)$$

represents the best possible error measured by the estimator  $\eta_{\text{opt}}$  on the optimal (but not available) mesh  $\mathcal{T}_{\text{opt}}$  with at most  $N$  additional simplices compared to  $\mathcal{T}_0$ . Given  $s > 0$ , the approximation class  $\mathbb{A}_s$  consists of all  $u^*$  such that

$$\|u^*\|_{\mathbb{A}_s} := \sup_{N \in \mathbb{N}_0} (N + 1)^s e(u^*, \mathcal{T}_0, N) < \infty. \quad (33)$$

When the above expression is finite, the regularity parameter  $s > 0$  represents an achievable convergence rate: The best possible error  $e(u^*, \mathcal{T}_0, N)$  decreases at least at rate  $-s$  with respect to the number of additional elements  $N$  and thus the multiplicative terms in (33) counterbalance. A sequence of meshes  $\mathcal{T}_\ell \in \mathbb{T}$  is called *quasi-optimal*, if there holds

$$\sup_{\ell \in \mathbb{N}_0} (\#\mathcal{T}_\ell)^s \eta_\ell(u_\ell^*) \approx \|u^*\|_{\mathbb{A}_s} \quad \text{for all } s > 0,$$

i.e.,  $(\eta_\ell(u_\ell^*))_{\ell \in \mathbb{N}_0}$  converges with rate  $-s$  in the sense of

$$\eta_\ell(u_\ell^*) \lesssim \|u^*\|_{\mathbb{A}_s} (\#\mathcal{T}_\ell)^{-s} \quad \text{for all } \ell \in \mathbb{N}_0 \text{ and all } s > 0.$$

Since this estimate holds for all  $s > 0$  and since  $\|u^*\|_{\mathbb{A}_s}$  is finite if and only if the rate  $-s$  is possible, this constitutes the optimal convergence rate with respect to the number of elements and, hence, for fixed polynomial degree, with respect to the number of degrees of freedom. However, the rate with respect to the overall computational cost, equivalent to  $\text{cost}(\ell, k)$  from (25), is of more practical interest. In addition to the discretization error measured via  $\eta_\ell(u_\ell^*)$ , one has to include the algebraic error  $\|u_\ell^* - u_\ell^k\|$  as contribution to the quasi-error. Stability (A1) ensures  $\|u_\ell^* - u_\ell^k\| + \eta_\ell(u_\ell^*) \approx \|u_\ell^* - u_\ell^k\| + \eta_\ell(u_\ell^k) = \mathbb{H}_\ell^k$ , advocating for the quasi-error (27). This leads to the following notion of optimal complexity for sufficiently small adaptivity parameters  $\theta$  and  $\lambda_{\text{alg}}$ .

---

**Theorem 6 (optimal complexity).** *There exist upper bounds  $0 < \theta^* \leq 1$  and  $\lambda_{\text{alg}}^* > 0$  such that, for any  $0 < \theta < \theta^*$  and  $0 < \lambda_{\text{alg}} < \lambda_{\text{alg}}^*$ , the following holds: Algorithm 1 guarantees that*

$$\|u^*\|_{\mathbb{A}_s} \lesssim \sup_{(\ell, k) \in \mathcal{Q}} \text{cost}(\ell, k)^s \mathbb{H}_\ell^k \lesssim \max\{\|u^*\|_{\mathbb{A}_s}, \mathbb{H}_0^0\} \quad \text{for all } s > 0,$$

where the underlying constants depend on  $s$ . In particular,  $\|u^*\|_{\mathbb{A}_s} < \infty$  is equivalent to the quasi-error  $\mathbb{H}_\ell^k$  decaying with rate  $-s$  with respect to the overall computational cost, and, hence, time.

---

The proof of Theorem 6 is given in Section 4.2 below.

### 3. NUMERICAL EXPERIMENTS

This section provides numerical investigations underlining the theoretical results from Subsection 2.7. The experiments employ the MATLAB object-oriented code<sup>1</sup> from [IP23] and  $hp$ -robust geometric multigrid method from [IMPS24] for the arising linear systems.

Following [Kel74], we consider the benchmark problem (1) on the square domain  $\Omega := (-1, 1)^2$  with a strong jump in the piecewise constant scalar diffusion coefficient  $\mathbf{A}(x) := a(x) I_{2 \times 2} \in L^\infty(\Omega)$  for  $a(x) := 161.447\,638\,797\,588\,1$  if  $x_1 x_2 > 0$  and  $a(x) := 1$  if  $x_1 x_2 < 0$ . This setting models an interface problem. The exact weak solution in polar coordinates reads  $u^*(r, \phi) := r^\alpha \mu(\phi)$  with constants  $\alpha = 0.1$ ,  $\beta = -14.922\,565\,104\,551\,52$ ,  $\delta = \pi/4$ , and  $\mu(\phi)$  defined as

$$\mu(\phi) := \begin{cases} \cos((\pi/2 - \beta)\alpha) \cos((\phi - \pi/2 + \delta)\alpha) & \text{if } 0 \leq \phi < \pi/2, \\ \cos(\delta\alpha) \cos((\phi - \pi + \beta)\alpha) & \text{if } \pi/2 \leq \phi < \pi, \\ \cos(\beta\alpha) \cos((\phi - \pi - \delta)\alpha) & \text{if } \pi \leq \phi < 3\pi/2, \\ \cos((\pi/2 - \delta)\alpha) \cos((\phi - 3\pi/2 - \beta)\alpha) & \text{if } 3\pi/2 \leq \phi < 2\pi. \end{cases}$$

The solution determines the inhomogeneous Dirichlet boundary conditions  $u_D(x) := u^*(x)$  for  $x \in \partial\Omega$  and leads to  $f \equiv 0$  and  $\mathbf{f} \equiv 0$ . The parameter  $\alpha$  gives the regularity of the solution  $u \in H^{1+\alpha-\varepsilon}(\Omega)$  for all  $\varepsilon > 0$ , having a strong point singularity at the origin where the interfaces intersect. The boundary data  $u_D$  is approximated by nodal interpolation [MNS03; FPP14], leading to an additional boundary-data oscillation term (for sufficiently smooth  $u_D$ , see [FPP14] in 2D and [AFK+13] for arbitrary spatial dimension), in the error estimator

$$\begin{aligned} \eta_H(T, v_H)^2 &:= |T| \|\operatorname{div}(a \nabla v_H)\|_{L^2(T)}^2 + |T|^{1/2} \|[a \nabla v_H \cdot \mathbf{n}]\|_{L^2(\partial T \setminus \Gamma)}^2 \\ &\quad + \sum_{E \subset \partial T \cap \Gamma} |T|^{1/2} \|(1 - \Pi_E^{p-1}) \partial u_D / \partial s\|_{L^2(E)}, \end{aligned}$$

where  $\Pi_E^{p-1}$  is the  $L^2(E)$ -orthogonal projection onto the space of polynomials of degree  $p - 1$  on the boundary face  $E \subset \Gamma$  and  $\partial u_D / \partial s$  is the arc-length derivative of  $u_D$ .

Since the exact solution  $u^*$ , see Figure 4c, exhibits a strong singularity at the origin, Algorithm 1 aggressively refines the initial mesh from Figure 4a towards this point as displayed in Figure 4b. Figure 4d shows the corresponding discrete solution  $u_\ell^k$  on the level  $\ell = 15$ .

The notion of optimal convergence rates relates to some measure of computational costs. While the motivation for studying the number of degrees of freedom stems from the goal of using meshes as coarse as possible, the cumulative cost from (26) take into account all the work of computing a solution on an adaptive mesh. In practice, one is more interested in the cumulative runtime to compute a solution of a desired accuracy. All three notions of optimality are investigated in Figure 5. The timing results throughout this chapter display the median of the total runtime obtained from 5 identical runs. When the

---

<sup>1</sup>The MATLAB code for the reproduction of all the experiments is openly available under <https://www.tuwien.at/mg/asc/praetorius/software/mooafem>

adaptive algorithm is implemented in linear complexity, as in this case, the Figures 5a–5c exhibit the same optimal rate  $-p/2$  of estimator decrease for fixed polynomial degree  $p$ . We underline that the rates for adaptive refinement are significantly larger than the suboptimal rate of 0.1 attained with uniform refinement for any polynomial degree  $p$ .

Figure 6 confirms the linear complexity because, independently of  $p$ , the slope of total runtime versus the cumulative cost attains one. Moreover, already at  $10^4$  degrees of freedom, the runtime of the adaptive algorithm with the iterative algebraic solver is lower than with MATLAB’s highly optimized built-in direct solver `mldivide`. This showcases from a practical point of view why optimal iterative solvers are indispensable for linear complexity of Algorithm 1.

In Figure 7, we investigate full R-linear convergence of the quasi-error  $H_\ell^k$  from (27) as stated in Theorem 5. The quasi-error is reduced in each step of the adaptive algorithm only up to a multiplicative constant. Indeed,  $H_\ell^k$  slightly increases in algebraic solver steps, but this increase is limited and compensated by the reduction of the mesh refinement and Dörfler’s marking strategy, leading to overall optimal convergence.

While Theorem 6 ensures optimal complexity for sufficiently small adaptivity parameters, Figure 8 illustrates that also moderate values of  $\theta$  lead to optimal convergence rates. However, Figure 9 indicates that smaller values of  $\lambda_{\text{alg}}$  are required to achieve the optimal convergence rate as the rates decrease for large  $\lambda_{\text{alg}}$  at about  $\text{cost}(\ell, \underline{k}) \geq 10^5$ . This observation might be caused by the strong singularity in this benchmark problem and justifies the choice of  $\lambda_{\text{alg}} = 0.01$  in the remaining experiments. The joint influence of the adaptivity parameters  $\theta$  and  $\lambda_{\text{alg}}$  is investigated in Table 1, which displays the weighted cumulative runtime

$$\eta_\ell(u_\ell^k) \sum_{|\ell', k'| \leq |\ell, \underline{k}|} \text{time}(\ell', k') \quad (34)$$

with  $\eta_\ell(u_\ell^k)/\eta_\ell(u_0^0) < 10^{-2}$  as stopping criterion. The optimal choices with regard to this empirical balance of error estimator and computational runtime are moderate values  $0.5 \leq \theta \leq 0.7$  and  $0.5 \leq \lambda_{\text{alg}} = 0.9$ .

Figure 10 reveals that the use of nested iteration in Algorithm 1 is crucial to preserve a uniform number of algebraic solver iterations. Moreover, the plot illustrates how large parameters in the stopping criterion (21) lead to fewer algebraic iterations as the discretization error becomes the dominating error source.

## 4. CONVERGENCE ANALYSIS

**4.1. Proof of full R-Linear convergence (Theorem 5).** The following result, implicitly found in [CFPP14, Lemma 4.9], is the key tool for the characterization of R-linear convergence of adaptive algorithms. We refer to [BFM<sup>+</sup>23, Lemma 10] for the present statement.

---

**Lemma 7 (tail summability vs. R-linear convergence).** *Let  $(\alpha_k)_{k \in \mathbb{N}_0}$  with  $\alpha_k \in \mathbb{R}_{\geq 0}$  for all  $k \in \mathbb{N}_0$ . Then, the following statements are equivalent:*

- (i) Tail summability: *There exists  $C_{\text{sum}} > 0$  such that for all  $M, N \in \mathbb{N}_0$ ,*

$$\sum_{k=M+1}^{M+N} \alpha_k \leq C_{\text{sum}} \alpha_M. \quad (35)$$

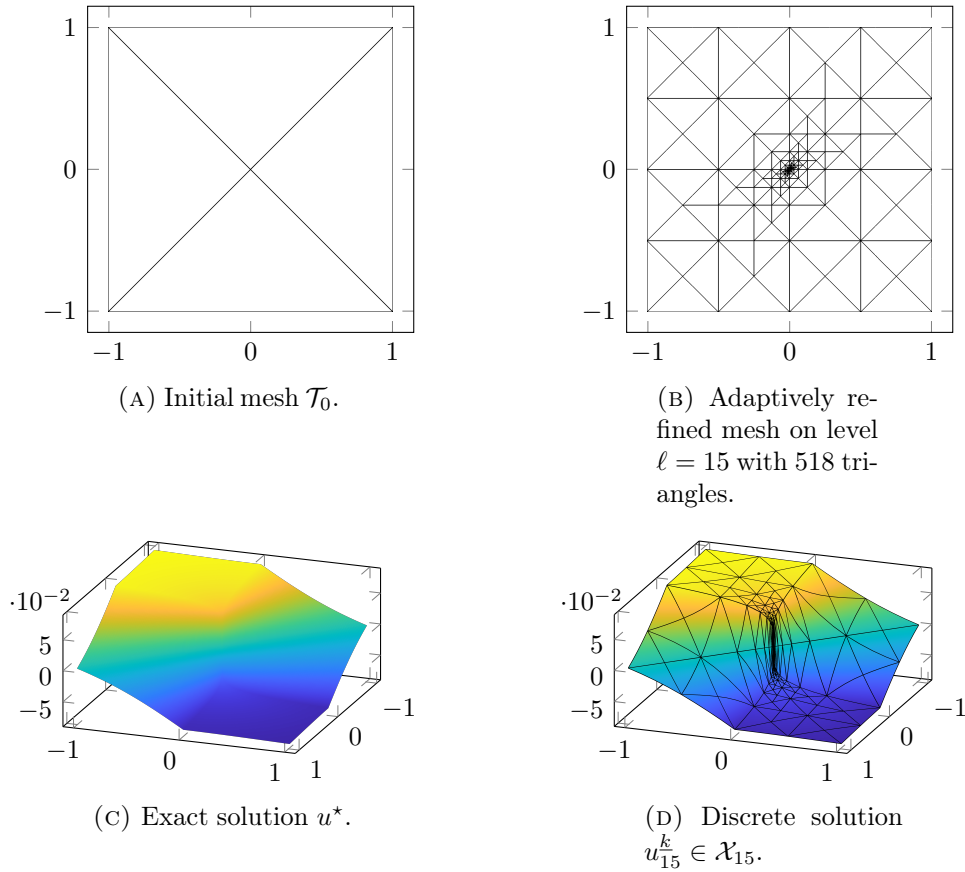


FIGURE 4. Initial mesh, adaptively refined mesh, exact solution  $u^*$ , and discrete solution  $u_{\ell}^k$  for the Kellogg benchmark problem from Subsection 3. The results are generated by Algorithm 1 with polynomial degree  $p = 2$ , bulk parameter  $\theta = 0.5$ , and stopping parameter  $\lambda_{\text{alg}} = 0.01$ .

$\lambda_{\text{alg}} \backslash \theta$	0.9	0.7	0.5	0.3	0.1
0.9	1.36	0.96	0.95	1.06	1.03
0.7	1.53	1.03	1.00	1.06	1.03
0.5	1.49	0.96	1.14	1.07	1.04
0.3	1.55	0.98	1.16	1.05	1.05
0.1	1.67	1.00	1.39	1.07	1.07

TABLE 1. Investigation of the influence of the adaptivity parameters  $\theta$  and  $\lambda_{\text{alg}}$  in Algorithm 1 to solve the Kellogg benchmark problem from Subsection 3. The polynomial degree is chosen as  $p = 2$ . The best choice per column is marked in yellow, per row in blue, and for both in green. For all  $\theta$ , the best performance is observed for  $\lambda_{\text{alg}} = 0.9$ , while overall best results are achieved for  $\theta \in \{0.5, 0.7\}$ .

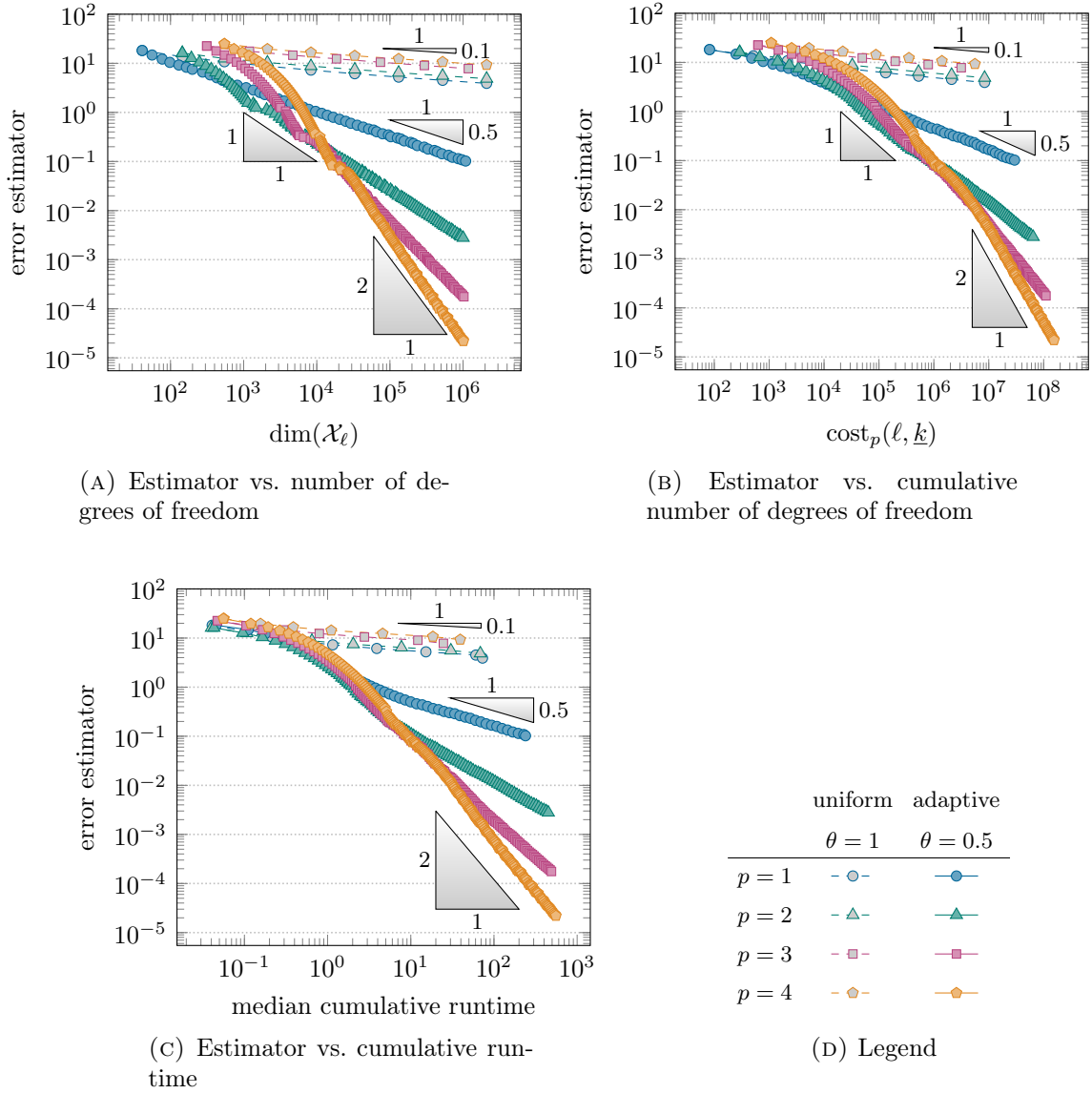


FIGURE 5. Convergence plot of Algorithm 1 to solve the Kellogg benchmark problem from Subsection 3 for various polynomial degrees. The adaptivity parameters read  $\theta = 0.5$  and  $\lambda_{\text{alg}} = 0.01$ . All graphs display values of the residual-based error estimator  $\eta_\ell(u_\ell^k)$  from (10).

(ii) R-linear convergence: *There exist  $0 < q_{\text{conv}} < 1$  and  $C_{\text{conv}} > 0$  such that for all  $M, N \in \mathbb{N}_0$*

$$\alpha_{M+N} \leq C_{\text{conv}} q_{\text{conv}}^N \alpha_M. \quad (36)$$

*Proof.* (i)  $\Rightarrow$  (ii): Note that for any  $M, N \in \mathbb{N}_0$ , tail summability (35) yields

$$(C_{\text{sum}}^{-1} + 1) \sum_{k=M+1}^{M+N} \alpha_k = C_{\text{sum}}^{-1} \sum_{k=M+1}^{M+N} \alpha_k + \sum_{k=M+1}^{M+N} \alpha_k \leq \alpha_M + \sum_{k=M+1}^{M+N} \alpha_k = \sum_{k=M}^{M+N} \alpha_k.$$

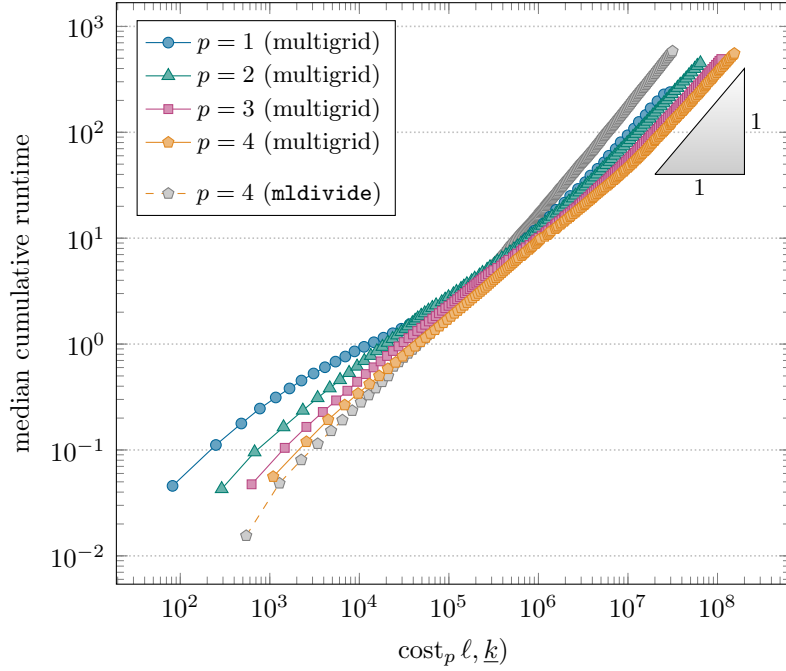


FIGURE 6. Plot of the cumulative runtime in Algorithm 1 with `mldivide` and iterative algebraic solvers versus the cumulative number of degrees of freedom to solve the benchmark problem from Subsection 3 for various polynomial degrees. The chosen adaptivity parameters read  $\theta = 0.5$  and  $\lambda_{\text{alg}} = 0.01$ . The plot displays the runtime of one out of five identical runs chosen by the median of the total runtime.

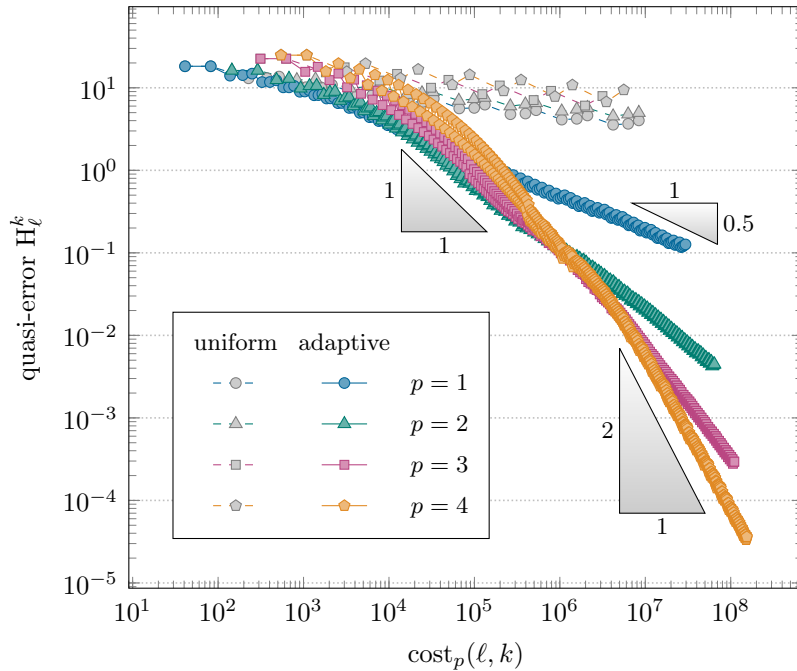


FIGURE 7. Convergence plot of Algorithm 1 for various polynomial degrees. The chosen adaptivity parameters read  $\theta = 0.5$  and  $\lambda_{\text{alg}} = 0.01$ . The graphs display the values of the quasi-error  $H_\ell^k$  from (27) in each algebraic iteration step.

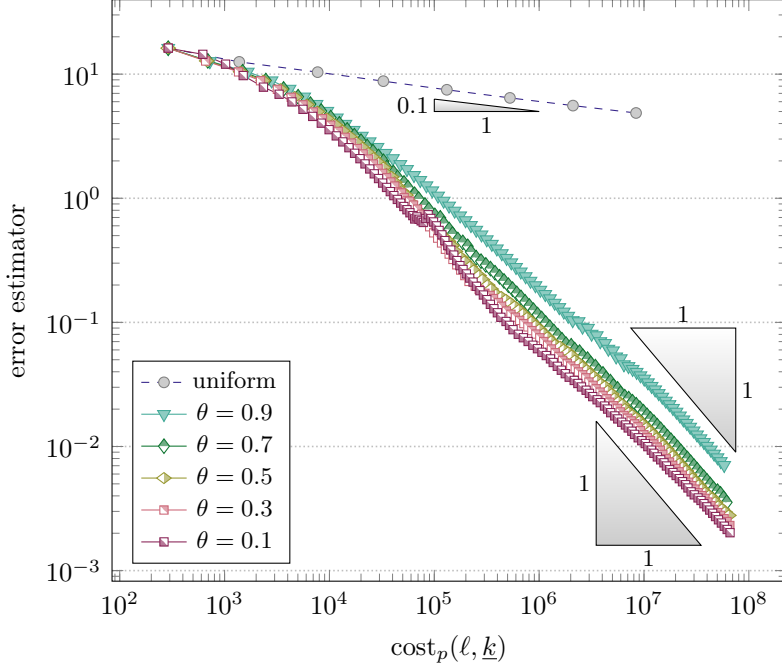


FIGURE 8. Convergence plot of Algorithm 1 to solve the Kellogg benchmark problem from Subsection 3 for various choices of the bulk parameter  $\theta$ . The remaining adaptivity parameter is chosen as  $\lambda_{\text{alg}} = 0.01$  and the polynomial degree as  $p = 2$ . The graphs display the values of the residual-based error estimator  $\eta_\ell(u_\ell^k)$  from (10).

Repeat this estimate inductively and use tail summability (35) to obtain

$$\begin{aligned} \alpha_{M+N} &= \sum_{k=M+N}^{M+N} \alpha_k \leq (C_{\text{sum}}^{-1} + 1)^{-1} \sum_{k=M+N-1}^{M+N} \alpha_k \leq \dots \\ &\leq (C_{\text{sum}}^{-1} + 1)^{-N} \sum_{k=M}^{M+N} \alpha_k \leq (C_{\text{sum}} + 1)(C_{\text{sum}}^{-1} + 1)^{-N} \alpha_M. \end{aligned}$$

This proves the claim for  $q_{\text{conv}} = (C_{\text{sum}}^{-1} + 1)^{-1} \in (0, 1)$  and  $C_{\text{conv}} = C_{\text{sum}} + 1$ .

(ii)  $\Rightarrow$  (i): Using R-linear convergence (36) for each term of the sum and the geometric series, we derive

$$\sum_{k=M+1}^{M+N} \alpha_k = \sum_{i=1}^N \alpha_{M+i} \leq C_{\text{conv}} \sum_{i=1}^N q_{\text{conv}}^i \alpha_M \leq \frac{C_{\text{conv}} q_{\text{conv}}}{1 - q_{\text{conv}}} \alpha_M.$$

This proves the claim for  $C_{\text{sum}} = C_{\text{conv}} q_{\text{conv}} (1 - q_{\text{conv}})^{-1}$ .  $\square$

*Proof of Theorem 5.* The proof consists of five steps.

*Step 1* (contraction up to tail summable remainder). Fix  $0 < \mu < (1 - q_{\text{ctr}}^2) q_{\text{ctr}}^{-2}$  so that  $q_\mu := (1 + \mu) q_{\text{ctr}}^2 < 1$  and  $C_\mu := (1 + \mu^{-1}) q_{\text{ctr}}^2 > 0$ . Then, the quasi-error contraction (29) and the Young inequality prove, for all  $(\ell + 1, \underline{k}) \in \mathcal{Q}$ , that

$$(\mathbb{H}_{\ell+1})^2 \leq q_\mu (\mathbb{H}_\ell)^2 + C_\mu \|u_{\ell+1}^* - u_\ell^*\|^2. \quad (37)$$

*Step 2* (tail summability with respect to  $\ell$ ). For all  $(\ell', \underline{k}) \in \mathcal{Q}$  with  $\ell' < \underline{\ell} - 1$ , the Galerkin orthogonality in the form (12), the telescoping sum, reliability (A3), and

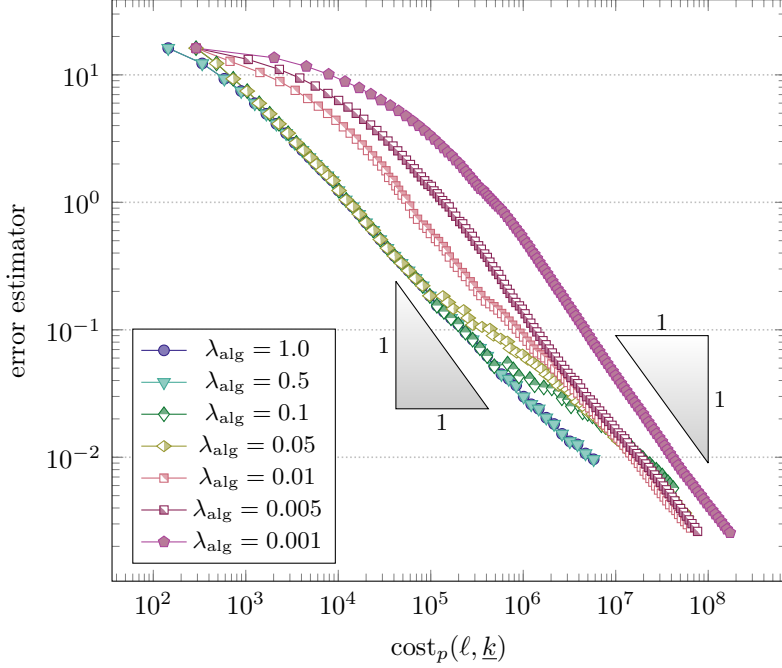


FIGURE 9. Convergence plot of Algorithm 1 to solve the Kellogg benchmark problem from Subsection 3 for various choices of the stopping parameter  $\lambda_{\text{alg}}$ . The remaining adaptivity parameter is chosen as  $\theta = 0.3$  and the polynomial degree as  $p = 2$ . The graphs display the values of the residual-based error estimator  $\eta_\ell(u_\ell^k)$  from (10).

stability (A1), prove that

$$\begin{aligned} \sum_{\ell=\ell'}^{\underline{\ell}-1} \|u_{\ell+1}^* - u_\ell^*\|^2 &\stackrel{(12)}{=} \sum_{\ell=\ell'}^{\underline{\ell}-1} [\|u^* - u_\ell^*\|^2 - \|u^* - u_{\ell+1}^*\|^2] \leq \|u^* - u_{\ell'}^*\|^2 \\ &\stackrel{(A3)}{\lesssim} \eta_{\ell'}(u_{\ell'}^*)^2 \stackrel{(A1)}{\lesssim} \eta_{\ell'}(u_{\ell'}^k)^2 + \|u_{\ell'}^* - u_{\ell'}^k\|^2 \stackrel{(28)}{\approx} (H_{\ell'})^2. \end{aligned}$$

The combination with Step 1 and the geometric series results in *quadratic tail summability* of the form, for all  $(\ell', \underline{k}) \in \mathcal{Q}$  with  $\ell' < \underline{\ell} - 1$ ,

$$\sum_{\ell=\ell'+1}^{\underline{\ell}-1} (H_\ell)^2 \stackrel{(37)}{\leq} (H_{\ell'})^2 \sum_{\ell=\ell'}^{\underline{\ell}-2} q_{\mu\delta}^{\ell-\ell'} + C_\mu \sum_{\ell=\ell'}^{\underline{\ell}-2} \|u_{\ell+1}^* - u_\ell^*\|^2 \lesssim (H_{\ell'})^2.$$

According to Lemma 7, this quadratic tail summability is equivalent to R-linear convergence, i.e., there exist  $C_1 > 0$  and  $0 < q_1 < 1$  such that

$$(H_\ell)^2 \leq C_1 q_1^{\ell-\ell'} (H_{\ell'})^2 \quad \text{for all } (\ell, \underline{k}), (\ell', \underline{k}) \in \mathcal{Q} \text{ with } 0 \leq \ell' \leq \ell.$$

Taking the square-root of this quasi-contraction estimate and another application of Lemma 7 result in *linear tail summability*

$$\sum_{\ell=\ell'+1}^{\underline{\ell}-1} H_\ell \lesssim H_{\ell'} \quad \text{for all } (\ell', \underline{k}) \in \mathcal{Q}. \quad (38)$$

This proves tail summability of the final iterates  $(\ell, \underline{k}) \in \mathcal{Q}$  with respect to  $\ell$ . It remains to prove summability with respect to the algebraic solver step index  $k$ .

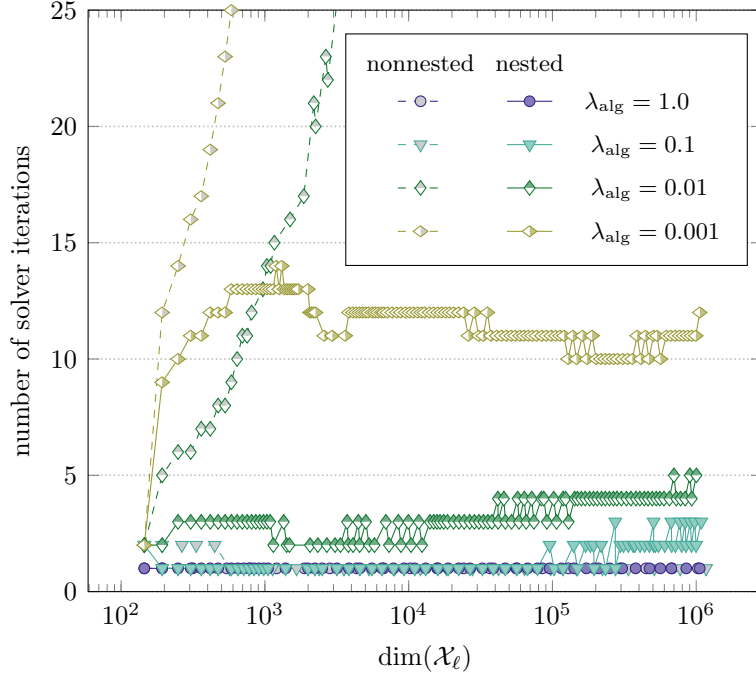


FIGURE 10. Number of iteration steps of algebraic solver for the Kellogg benchmark problem from Subsection 3 with nested (i.e.,  $u_{\ell+1}^0 := u_{\ell}^k$ ) and non-nested (i.e.,  $u_{\ell+1}^0 := 0$ ) iteration for various stopping parameters  $\lambda_{\text{alg}}$ . The chosen polynomial degree reads  $p = 2$  and the adaptivity parameter  $\theta = 0.5$ .

*Step 3* (quasi-contraction of quasi-error for every iterate). Recall the quasi-error with respect to every iterate  $H_{\ell}^k = \|||u_{\ell}^* - u_{\ell}^k\||| + \eta_{\ell}(u_{\ell}^k)$  for all  $(\ell, k) \in \mathcal{Q}$  from (27) and note that

$$H_{\ell}^k \approx H_{\ell}, \quad (39)$$

where the hidden equivalence constants depend only on  $\gamma$ . The contraction (C) of the algebraic solver in estimate (7) establishes, for all  $1 \leq k \leq \underline{k}$ ,

$$\|||u_{\ell}^k - u_{\ell}^{k-1}\||| \stackrel{(7)}{\leq} (1 + q_{\text{alg}}) \|||u_{\ell}^* - u_{\ell}^{k-1}\||| \leq 2 \|||u_{\ell}^* - u_{\ell}^{k-1}\|||. \quad (40)$$

For all  $(\ell, \underline{k}) \in \mathcal{Q}$ , this leads to

$$\begin{aligned} H_{\ell}^k &= \|||u_{\ell}^* - u_{\ell}^k\||| + \eta_{\ell}(u_{\ell}^k) \stackrel{(A1)}{\lesssim} \|||u_{\ell}^* - u_{\ell}^k\||| + \|||u_{\ell}^k - u_{\ell}^{k-1}\||| + \eta_{\ell}(u_{\ell}^{k-1}) \\ &\stackrel{(27)}{\leq} H_{\ell}^{k-1} + 2 \|||u_{\ell}^k - u_{\ell}^{k-1}\||| \stackrel{(40)}{\leq} 5 H_{\ell}^{k-1}. \end{aligned} \quad (41)$$

For the iterates with  $0 \leq k' < k < \underline{k}[\ell]$ , the failure of the stopping criterion (21) for the algebraic solver in Algorithm 1 (I.b) guarantees

$$\begin{aligned} H_{\ell}^k &= \|||u_{\ell}^* - u_{\ell}^k\||| + \eta_{\ell}(u_{\ell}^k) \stackrel{(21)}{<} \|||u_{\ell}^* - u_{\ell}^k\||| + \lambda_{\text{alg}}^{-1} \|||u_{\ell}^k - u_{\ell}^{k-1}\||| \\ &\stackrel{(40)}{\leq} \|||u_{\ell}^* - u_{\ell}^k\||| + 2 \lambda_{\text{alg}}^{-1} \|||u_{\ell}^* - u_{\ell}^{k-1}\||| \stackrel{(C)}{\leq} (q_{\text{alg}} + 2 \lambda_{\text{alg}}^{-1}) \|||u_{\ell}^* - u_{\ell}^{k-1}\||| \\ &\stackrel{(C)}{\leq} \frac{q_{\text{alg}} + 2 \lambda_{\text{alg}}^{-1}}{q_{\text{alg}}} q_{\text{alg}}^{k-k'} \|||u_{\ell}^* - u_{\ell}^{k'}\|||. \end{aligned} \quad (42)$$

For  $0 \leq k' < k = \underline{k}[\ell]$ , the combination of (41)–(42) results in

$$\mathbb{H}_\ell^k \stackrel{(41)}{\lesssim} \mathbb{H}_\ell^{k-1} \stackrel{(42)}{\lesssim} q_{\text{alg}}^{(k-1)-k'} \|\|u_\ell^\star - u_\ell^{k'}\|\| = \frac{1}{q_{\text{alg}}} q_{\text{alg}}^{k-k'} \|\|u_\ell^\star - u_\ell^{k'}\|\|. \quad (43)$$

Since  $\|\|u_\ell^\star - u_\ell^{k'}\|\| \leq \mathbb{H}_\ell^{k'}$ , the estimates (42)–(43) prove

$$\mathbb{H}_\ell^k \lesssim q_{\text{alg}}^{k-k'} \mathbb{H}_\ell^{k'} \quad \text{for all } (\ell, k) \in \mathcal{Q} \text{ with } 0 \leq k' \leq k \leq \underline{k}[\ell]. \quad (44)$$

In the remaining case of  $k = 0$ , Céa-type estimate (13), reliability (A3), and stability (A1) imply

$$\begin{aligned} \|\|u_\ell^\star - u_{\ell-1}^\star\|\| &\leq \|\|u_\ell^\star - u^\star\|\| + \|\|u^\star - u_{\ell-1}^\star\|\| \stackrel{(13)}{\lesssim} \|\|u^\star - u_{\ell-1}^\star\|\| \stackrel{(A3)}{\lesssim} \eta_{\ell-1}(u_{\ell-1}^\star) \\ &\stackrel{(A1)}{\lesssim} \eta_{\ell-1}(u_{\ell-1}^k) + \|\|u_{\ell-1}^\star - u_{\ell-1}^k\|\| = \mathbb{H}_{\ell-1}^k \stackrel{(39)}{\approx} \mathbb{H}_{\ell-1}. \end{aligned}$$

This and nested iteration  $u_\ell^0 = u_{\ell-1}^k$  yield

$$\begin{aligned} \mathbb{H}_\ell^0 &\stackrel{(27)}{=} \|\|u_\ell^\star - u_{\ell-1}^k\|\| + \eta_\ell(u_{\ell-1}^k) \stackrel{(20)}{\lesssim} \|\|u_\ell^\star - u_{\ell-1}^k\|\| + \eta_{\ell-1}(u_{\ell-1}^k) \\ &\leq \|\|u_\ell^\star - u_{\ell-1}^\star\|\| + \mathbb{H}_{\ell-1}^k \stackrel{(39)}{\lesssim} \mathbb{H}_{\ell-1} \quad \text{for all } (\ell, 0) \in \mathcal{Q} \text{ with } \ell > 0. \end{aligned} \quad (45)$$

*Step 4* (tail summability with respect to  $\ell$  and  $k$ ). Let  $(\ell', k') \in \mathcal{Q}$ . The quasi-contraction estimates from Step 3 and the geometric series prove that

$$\begin{aligned} \sum_{\substack{(\ell, k) \in \mathcal{Q} \\ |\ell, k| > |\ell', k'|}} \mathbb{H}_\ell^k &= \sum_{k=k'+1}^{\underline{k}[\ell']} \mathbb{H}_\ell^k + \sum_{\ell=\ell'+1}^{\ell} \sum_{k=0}^{\underline{k}[\ell]} \mathbb{H}_\ell^k \stackrel{(44)}{\lesssim} \mathbb{H}_{\ell'}^{k'} + \sum_{\ell=\ell'+1}^{\ell} \mathbb{H}_\ell^0 \\ &\stackrel{(45)}{\lesssim} \mathbb{H}_{\ell'}^{k'} + \sum_{\ell=\ell'}^{\ell-1} \mathbb{H}_\ell \stackrel{(38)}{\lesssim} \mathbb{H}_{\ell'}^{k'} + \mathbb{H}_{\ell'} \stackrel{(39)}{\approx} \mathbb{H}_{\ell'}^{k'} + \mathbb{H}_{\ell'}^k \stackrel{(44)}{\lesssim} \mathbb{H}_{\ell'}^{k'}. \end{aligned} \quad (46)$$

*Step 5* (full R-linear convergence). Since the index set  $\mathcal{Q}$  is linearly ordered with respect to the total step counter  $|\cdot, \cdot|$ , the tail summability (46) and Lemma 7 conclude the proof, i.e., there exist  $C_2 > 0$  and  $0 < q_2 < 1$  such that

$$\mathbb{H}_\ell^k \leq C_2 q_2^{|\ell, k| - |\ell', k'|} \mathbb{H}_{\ell'}^{k'} \quad \text{for all } (\ell', k'), (\ell, k) \in \mathcal{Q} \text{ with } |\ell, k| \geq |\ell', k'|.$$

Finally, we show the upper bound on the overall error by the quasi-error in (31) yielding parameter-robust convergence. Using reliability (A3) and stability (A1), there holds

$$\begin{aligned} \|\|u^\star - u_\ell^k\|\| &\leq \|\|u^\star - u_\ell^\star\|\| + \|\|u_\ell^\star - u_\ell^k\|\| \stackrel{(A3)}{\lesssim} \eta_\ell(u_\ell^\star) + \|\|u_\ell^\star - u_\ell^k\|\| \\ &\stackrel{(A1)}{\lesssim} \eta_\ell(u_\ell^k) + \|\|u_\ell^\star - u_\ell^k\|\| = \mathbb{H}_\ell^k. \end{aligned} \quad \square$$

**4.2. Proof of optimal complexity (Theorem 6).** The following corollary asserts that full R-linear convergence from Theorem 5 implies the coincidence of the convergence rates of the quasi-error from (27) with respect to the number of degrees of freedom and with respect to the total computational work. Thus, full R-linear convergence is a key argument to prove optimal complexity of Algorithm 1.

---

**Corollary 8 ([BFM<sup>+</sup>23, Corollary 11]).** For  $s > 0$ , abbreviate

$$M(s) := \sup_{(\ell, k) \in \mathcal{Q}} (\#\mathcal{T}_\ell)^s \mathbf{H}_\ell^k. \quad (47)$$

Suppose that the assumptions of Theorem 5 hold. Then, Algorithm 1 guarantees the equivalence

$$M(s) \leq \sup_{(\ell, k) \in \mathcal{Q}} \text{cost}(\ell, k)^s \mathbf{H}_\ell^k \leq \frac{C_{\text{lin}}}{[1 - q_{\text{lin}}^{1/s}]^s} M(s). \quad (48)$$


---

*Proof.* Recall from (25) that

$$\text{cost}(\ell, k) = \sum_{\substack{(\ell', k') \in \mathcal{Q} \\ |\ell', k'| \leq |\ell, k|}} \#\mathcal{T}_{\ell'}.$$

The first estimate in (48) is thus immediate as it suffices to bound the sum of positive terms from below by one of its components. Next, note that for all  $(\ell', k') \in \mathcal{Q}$ , the definition (47) provides

$$\#\mathcal{T}_{\ell'} \leq M(s)^{1/s} (\mathbf{H}_{\ell'}^{k'})^{-1/s}.$$

Summing and using the full R-linear convergence (30) together with the geometric series gives

$$\begin{aligned} \text{cost}(\ell, k) &= \sum_{\substack{(\ell', k') \in \mathcal{Q} \\ |\ell', k'| \leq |\ell, k|}} \#\mathcal{T}_{\ell'} \leq M(s)^{1/s} \sum_{\substack{(\ell', k') \in \mathcal{Q} \\ |\ell', k'| \leq |\ell, k|}} (\mathbf{H}_{\ell'}^{k'})^{-1/s} \\ &\stackrel{(30)}{\leq} M(s)^{1/s} C_{\text{lin}}^{1/s} \sum_{\substack{(\ell', k') \in \mathcal{Q} \\ |\ell', k'| \leq |\ell, k|}} (q_{\text{lin}}^{1/s})^{|\ell, k| - |\ell', k'|} (\mathbf{H}_{\ell'}^{k'})^{-1/s} \\ &\leq M(s)^{1/s} \frac{C_{\text{lin}}^{1/s}}{1 - q_{\text{lin}}^{1/s}} (\mathbf{H}_\ell^k)^{-1/s}. \end{aligned}$$

Rearranging the terms and taking the supremum over  $(\ell, k) \in \mathcal{Q}$  proves the second estimate in (48).  $\square$

The following result relates the error estimator for the final algebraic iterates to the one for the exact solution. It imposes a restriction on the algebraic stopping parameter  $\lambda_{\text{alg}}$  to ensure that the final iterate is *sufficiently close* to the exact solution.

---

**Lemma 9 (estimator equivalence).** *There exists  $\lambda_{\text{alg}}^* := (1 - q_{\text{alg}})/(C_{\text{stab}} q_{\text{alg}}) > 0$  such that every  $0 < \theta \leq 1$  and  $0 < \lambda_{\text{alg}} < \lambda_{\text{alg}}^*$  guarantee*

$$(1 - \lambda_{\text{alg}}/\lambda_{\text{alg}}^*) \eta_\ell(u_\ell^k) \leq \eta_\ell(u_\ell^*) \leq (1 + \lambda_{\text{alg}}/\lambda_{\text{alg}}^*) \eta_\ell(u_\ell^k). \quad (49)$$


---

*Proof.* The a-posteriori error control in (7) and the stopping criterion (21) establish

$$C_{\text{stab}} \|\| u_\ell^* - u_\ell^k \|\| \leq \frac{C_{\text{stab}} q_{\text{alg}}}{1 - q_{\text{alg}}} \|\| u_\ell^k - u_\ell^{k-1} \|\| \leq \frac{\lambda_{\text{alg}}}{\lambda_{\text{alg}}^*} \eta_\ell(u_\ell^k). \quad (50)$$

For any  $\lambda_{\text{alg}} > 0$ , this and stability (A1) prove the upper bound

$$\eta_\ell(u_\ell^*) \leq \eta_\ell(u_\ell^k) + C_{\text{stab}} \|\| u_\ell^* - u_\ell^k \|\| \leq (1 + \lambda_{\text{alg}}/\lambda_{\text{alg}}^*) \eta_\ell(u_\ell^k).$$

Analogously, we prove

$$\eta_\ell(u_\ell^k) \leq \eta_\ell(u_\ell^*) + C_{\text{stab}} \|u_\ell^* - u_\ell^k\| \leq \eta_\ell(u_\ell^*) + \frac{\lambda_{\text{alg}}}{\lambda_{\text{alg}}^*} \eta_\ell(u_\ell^k).$$

Rearrangement yields, for all  $0 < \lambda_{\text{alg}} < \lambda_{\text{alg}}^*$ , that

$$(1 - \lambda_{\text{alg}}/\lambda_{\text{alg}}^*) \eta_\ell(u_\ell^k) \leq \eta_\ell(u_\ell^*). \quad \square$$

Given a particular triangulation  $\mathcal{T}_\ell$ , the following lemma provides the existence of an optimal set for refinement satisfying the Dörfler criterion for a sufficiently small bulk parameter  $\theta_{\text{mark}}$ . In the subsequent proof of optimal complexity of Algorithm 1, this allows to relate the actual marked set with these theoretical optimal sets of refined elements.

**Lemma 10 (equivalence with optimal-practical refinement).** *Given  $\lambda_{\text{alg}}^* > 0$  from Lemma 9, choose  $0 < \theta^* \leq 1$  sufficiently small to ensure that the parameters  $0 < \theta < \theta^*$  and  $0 < \lambda_{\text{alg}} < \lambda_{\text{alg}}^*$  satisfy*

$$0 < \theta_{\text{mark}} := (\theta^{1/2} + \lambda_{\text{alg}}/\lambda_{\text{alg}}^*)^2 / (1 - \lambda_{\text{alg}}/\lambda_{\text{alg}}^*)^2 < (1 + C_{\text{stab}}^2 C_{\text{drel}}^2)^{-1}.$$

Then, there exists a set  $\mathcal{R}_\ell \subseteq \mathcal{T}_\ell$  such that

$$\#\mathcal{R}_\ell \lesssim \|u^*\|_{\mathbb{A}_s}^{1/s} \eta_\ell(u_\ell^*)^{-1/s} \quad \text{and} \quad \theta_{\text{mark}} \eta_\ell(u_\ell^*)^2 \leq \eta_\ell(\mathcal{R}_\ell, u_\ell^*)^2. \quad (51)$$

Moreover, the above Dörfler marking (51) for  $(\theta_{\text{mark}}, u_\ell^*)$  implies that  $\mathcal{R}_\ell$  also satisfies the Dörfler marking (18) for  $(\theta, u_\ell^k)$ , meaning that

$$\theta \eta_\ell(u_\ell^k)^2 \leq \eta_\ell(\mathcal{R}_\ell, u_\ell^k)^2. \quad (52)$$

*Proof.* The existence of the set  $\mathcal{R}_\ell$  satisfying (51) follows from [CFPP14, Lem. 4.14], because  $\theta_{\text{mark}} < (1 + C_{\text{stab}}^2 C_{\text{drel}}^2)^{-1}$  is guaranteed by the choice of the parameters. To show (52), we use the estimator equivalence from Lemma 9 and the marking criterion (51) to obtain

$$(1 - \lambda_{\text{alg}}/\lambda_{\text{alg}}^*) \theta_{\text{mark}}^{1/2} \eta_\ell(u_\ell^k) \stackrel{(49)}{\leq} \theta_{\text{mark}}^{1/2} \eta_\ell(u_\ell^*) \stackrel{(51)}{\leq} \eta_\ell(\mathcal{R}_\ell, u_\ell^*).$$

Next, using stability (A1), a-posteriori control (7), and the stopping criterion (21), we deduce

$$\begin{aligned} \eta_\ell(\mathcal{R}_\ell, u_\ell^*) &\stackrel{(A1)}{\leq} \eta_\ell(\mathcal{R}_\ell, u_\ell^k) + C_{\text{stab}} \|u_\ell^* - u_\ell^k\| \\ &\stackrel{(7)}{\leq} \eta_\ell(\mathcal{R}_\ell, u_\ell^k) + C_{\text{stab}} \frac{q_{\text{alg}}}{1 - q_{\text{alg}}} \|u_\ell^k - u_\ell^{k-1}\| \\ &\stackrel{(21)}{\leq} \eta_\ell(\mathcal{R}_\ell, u_\ell^k) + \lambda_{\text{alg}}/\lambda_{\text{alg}}^* \eta_\ell(u_\ell^k). \end{aligned}$$

The combination of the two previous estimates with the definition of  $\theta_{\text{mark}}$  yields

$$(1 - \lambda_{\text{alg}}/\lambda_{\text{alg}}^*) \theta_{\text{mark}}^{1/2} \eta_\ell(u_\ell^k) \leq \eta_\ell(\mathcal{R}_\ell, u_\ell^k) + [\theta_{\text{mark}}^{1/2} (1 - \lambda_{\text{alg}}/\lambda_{\text{alg}}^*) - \theta^{1/2}] \eta_\ell(u_\ell^k).$$

Rearranging the terms gives the practical marking criterion (52).  $\square$

**Remark 11 (optimality of Dörfler marking).** *Though the details on the set  $\mathcal{R}_\ell$  satisfying (51) are not fully discussed in the previous proof, note that this provides a central argument for using Dörfler marking criterion (18) in adaptive FEMs. Indeed, referring to, e.g., [CFPP14, Lem. 4.14] and the seminal paper [Ste07], let us suppose that, for a given sequence of successively refined triangulations  $(\mathcal{T}_\ell)_{\ell \in \mathbb{N}_0}$ , we compute the exact*

discrete solutions  $u_\ell^*$  and that there holds linear convergence  $\eta_{\ell+n}(u_{\ell+n}^*) \leq Cq_{\text{lin}}^n \eta_\ell(u_\ell^*)$  for all  $\ell, n \in \mathbb{N}_0$ , where  $C > 0$  and  $0 < q_{\text{lin}} < 1$  are  $\ell$ -independent. Then, there exists  $0 < \theta_* \leq 1$  such that, for any  $0 < \theta < \theta_*$ , the set  $\mathcal{R}_\ell := \mathcal{T}_\ell \setminus \mathcal{T}_{\ell+1}$  satisfies the Dörfler marking

$$\theta \eta_\ell(u_\ell^*)^2 \leq \eta_\ell(\mathcal{R}_\ell, u_\ell^*)^2 \quad \text{for all } \ell \in \mathbb{N}_0. \quad (53)$$

Independently of how the marked elements are chosen, Dörfler marking is thus satisfied along the sequence of refined elements if there holds R-linear convergence. In this sense, Dörfler marking is not only sufficient for (full) R-linear convergence, but also necessary.

*Proof of Theorem 6.* By Corollary 8, it suffices to prove, for every  $s > 0$ ,

$$\sup_{(\ell, k) \in \mathcal{Q}} (\#\mathcal{T}_\ell)^s \mathbf{H}_\ell^k \lesssim \max\{\|u^*\|_{\mathbb{A}_s}, \mathbf{H}_0^0\}.$$

Let  $s > 0$  and assume that the right-hand side of the previous estimate is finite, because otherwise the claim is trivial. The proof consists of three steps.

*Step 1.* For all  $0 \leq \ell' < \underline{\ell}$ , Lemma 10 guarantees existence of a set  $\mathcal{R}_{\ell'} \subseteq \mathcal{T}_{\ell'}$  satisfying (51) for  $\ell'$  replacing  $\ell$ . This, the estimate (45), a-posteriori control of the algebraic error (7), the stopping criterion (21), and the estimator equivalence from Lemma 9 imply

$$\mathbf{H}_{\ell'+1}^0 \stackrel{(45)}{\lesssim} \mathbf{H}_{\ell'} \stackrel{(7)}{\lesssim} \| \|u_{\ell'}^k - u_{\ell'}^{k-1} \| \| + \eta_{\ell'}(u_{\ell'}^k) \stackrel{(21)}{\lesssim} \eta_{\ell'}(u_{\ell'}^k) \stackrel{(49)}{\approx} \eta_{\ell'}(u_{\ell'}^*).$$

The combination with (51) proves

$$\#\mathcal{R}_{\ell'} \lesssim \|u^*\|_{\mathbb{A}_s}^{1/s} (\mathbf{H}_{\ell'+1}^0)^{-1/s}.$$

*Step 2.* Since  $\mathcal{R}_{\ell'} \subseteq \mathcal{T}_{\ell'}$ , the quasi-minimality of  $\mathcal{M}_{\ell'}$  implies  $\#\mathcal{M}_{\ell'} \lesssim \#\mathcal{R}_{\ell'}$  due to the comparison of optimal and practical marking (52). This and the mesh-closure estimate (R3) show

$$\#\mathcal{T}_\ell - \#\mathcal{T}_0 \lesssim \sum_{\ell'=0}^{\ell} \#\mathcal{M}_{\ell'} \lesssim \sum_{\ell'=0}^{\ell} \#\mathcal{R}_{\ell'}.$$

*Step 3.* Full R-linear convergence (30) proves

$$\sum_{\ell'=0}^{\ell-1} (\mathbf{H}_{\ell'+1}^0)^{-1/s} \leq \sum_{\substack{(\ell', k') \in \mathcal{Q} \\ |\ell', k'| \leq |\ell, k|}} (\mathbf{H}_{\ell'}^{k'})^{-1/s} \lesssim (\mathbf{H}_\ell^k)^{-1/s} \sum_{\substack{(\ell', k') \in \mathcal{Q} \\ |\ell', k'| \leq |\ell, k|}} (q_{\text{lin}})^{|\ell, k| - |\ell', k'|} \lesssim \|u^*\|_{\mathbb{A}_s}^{1/s} (\mathbf{H}_\ell^k)^{-1/s}.$$

The combination of this with the Steps 1–2 reads

$$\#\mathcal{T}_\ell - \#\mathcal{T}_0 \lesssim \|u^*\|_{\mathbb{A}_s}^{1/s} (\mathbf{H}_\ell^k)^{-1/s}.$$

For  $\ell > 0$ , the lower bound  $1 \leq \#\mathcal{T}_\ell - \#\mathcal{T}_0$  implies  $\#\mathcal{T}_\ell - \#\mathcal{T}_0 + 1 \leq 2(\#\mathcal{T}_\ell - \#\mathcal{T}_0)$  and thus

$$(\#\mathcal{T}_\ell - \#\mathcal{T}_0 + 1)^s \mathbf{H}_\ell^k \lesssim \|u^*\|_{\mathbb{A}_s}.$$

For  $\ell = 0$ , full R-linear convergence (30) yields

$$(\#\mathcal{T}_0 - \#\mathcal{T}_0 + 1)^s \mathbf{H}_0^k \lesssim \mathbf{H}_0^0.$$

The combination with the elementary estimate  $\#\mathcal{T}_\ell \leq \#\mathcal{T}_0(\#\mathcal{T}_\ell - \#\mathcal{T}_0 + 1)$  from [BHP17, Lemma 22] concludes the proof

$$(\#\mathcal{T}_\ell)^s \mathbf{H}_\ell^k \lesssim \max\{\|u^*\|_{\mathbb{A}_s}, \mathbf{H}_0^0\} \quad \text{for all } (\ell, k) \in \mathcal{Q}. \quad \square$$

## 5. EXTENSION 1: GOAL-ORIENTED ADAPTIVITY

The Algorithm 1 from Subsection 2.5 aims at the efficient approximation of the solution  $u^*$  with respect to the energy norm  $\|\cdot\|$ . In many applications, one rather looks for a particular quantity of interest  $G(u^*)$  in terms of a linear goal functional  $G : \mathcal{X} \rightarrow \mathbb{R}$ . A non-standard marking procedure allows to approximate the goal functional with the doubled optimal convergence rate. In this section, we present some results from [BGIP23] on cost-optimal goal-oriented adaptivity with inexact solver.

**5.1. Adaptive FEM with linear goal functional.** Let  $u^* \in H_0^1(\Omega)$  be the weak solution to (3). Given  $g \in L^2(\Omega)$  and  $\mathbf{g} \in [L^2(\Omega)]^d$ , we consider the linear functional

$$G(u^*) := \int_{\Omega} (g u^* - \mathbf{g} \cdot \nabla u^*) \, dx. \quad (54)$$

The goal-oriented adaptive finite element method (GOAFEM) seeks for an efficient approximation of  $G(u^*)$  using an (approximate) solution  $u_H \in \mathcal{X}_H$  to the discrete formulation (5).

A duality approach from [GS02] employs the solution  $z^* \in \mathcal{X}$  to the so-called dual problem

$$a(v, z^*) = G(v) \quad \text{for all } v \in \mathcal{X}. \quad (55)$$

While  $\eta_H(u_H^*)$  from (10) controls the energy error of the primal variable  $u_H^* \approx u^*$ , GOAFEM requires another a-posteriori error estimator for the discrete dual problem with solution  $z_H^* \in \mathcal{X}_H$  to the problem

$$a(v_H, z_H^*) = G(v_H) \quad \text{for all } v_H \in \mathcal{X}_H. \quad (56)$$

To this end, note that (55) corresponds to the elliptic PDE

$$-\operatorname{div}(\mathbf{A}\nabla z^*) = g - \operatorname{div} \mathbf{g} \text{ in } \Omega \quad \text{and} \quad z^* = 0 \text{ on } \partial\Omega.$$

For  $z_H \in \mathcal{X}_H$ , we thus define  $\zeta_H(z_H) := \left( \sum_{T \in \mathcal{T}_H} \zeta_H(T, z_H)^2 \right)^{1/2}$  by

$$\zeta_H(T, z_H)^2 := |T|^{2/d} \|g + \operatorname{div}(\mathbf{A}\nabla z_H - \mathbf{g})\|_{L^2(T)}^2 + |T|^{1/d} \|[(\mathbf{A}\nabla z_H - \mathbf{g}) \cdot \mathbf{n}]\|_{L^2(\partial T \cap \Omega)}^2$$

and employ the same abbreviation  $\zeta_H(z_H)$  for the global values analogously to the primal estimator with (10b). It is well-known that  $\zeta_H$  satisfies (A1)–(A4) with  $\eta_H$  replaced by  $\zeta_H$  and all primal variables replaced by their dual counterparts [FPZ16]. Hence, the dual estimator  $\zeta_H(z_H)$  allows for a quasi-optimal adaptive resolution of the dual solution  $z^*$ . Using the linearity of the goal functional  $G$  and the dual problem (56), for any  $u_H, z_H \in \mathcal{X}_H$ , recall from [GS02] that there holds

$$\begin{aligned} G(u^*) - G(u_H) &= G(u^* - u_H) = a(u^* - u_H, z^*) = a(u^* - u_H, z^* - z_H) + a(u^* - u_H, z_H) \\ &= a(u^* - u_H, z^* - z_H) + [F(z_H) - a(u_H, z_H)]. \end{aligned}$$

This motivates the definition of the discrete goal functional

$$G_H(u_H, z_H) := G(u_H) + [F(z_H) - a(u_H, z_H)] \quad (57)$$

and ensures the estimate

$$|G(u^*) - G_H(u_H, z_H)| \leq |a(u^* - u_H, z^* - z_H)| \leq \|u^* - u_H\| \|z^* - z_H\|$$

for the  $a(\cdot, \cdot)$ -induced energy norm. Consequently, for sufficiently good approximations  $u_H$  to  $u^*$  and  $z_H$  to  $z^*$ , the discrete goal value  $G_H(u_H, z_H)$  converges to  $G(u^*)$  with the

sum of the convergence rates for the primal and the dual problem. The reliability (A3) of the primal and the dual estimator result in

$$|G(u^*) - G_H(u_H^*, z_H^*)| \lesssim \eta_H(u_H^*) \zeta_H(z_H^*). \quad (58)$$

This reveals that GOAFEM needs to ensure optimal convergence of the product of the primal and the dual estimator. To this end, [FPZ16] introduces the marking strategy in step (III) of Algorithm 2 below that avoids over-refinement for both primal and dual solutions. Since the bilinear form  $a(\cdot, \cdot)$  is symmetric, the iterative solver  $\Psi$  from Section 2.2 may be also applied for the solution of the discrete dual problem (56).

**5.2. Algorithm 2: Goal-oriented adaptive FEM. Input:** Initial mesh  $\mathcal{T}_0$ , polynomial degree  $p \in \mathbb{N}$ , initial iterates  $u_0^0 := u_0^m := z_0^0 := z_0^\mu := 0$ , marking parameter  $0 < \theta \leq 1$ , solver parameter  $\lambda_{\text{alg}} > 0$ .

**Adaptive loop:** For all  $\ell = 0, 1, 2, \dots$ , repeat the following steps (I)–(IV):

(I) **SOLVE & ESTIMATE (PRIMAL)**. For all  $m = 1, 2, 3, \dots$ , repeat (a)–(b):

- (a) Compute  $u_\ell^m := \Psi_\ell(F; u_\ell^{m-1})$  and the corresponding refinement indicators  $\eta_\ell(T; u_\ell^m)$  for all  $T \in \mathcal{T}_\ell$ .
- (b) Terminate  $m$ -loop and define  $\underline{m}[\ell] := m$  provided that

$$\| \| u_\ell^m - u_\ell^{m-1} \| \| \leq \lambda_{\text{alg}} \eta_\ell(u_\ell^m).$$

(II) **SOLVE & ESTIMATE (DUAL)**. For all  $\mu = 1, 2, 3, \dots$ , repeat (a)–(b):

- (a) Compute  $z_\ell^\mu := \Psi_\ell(G; z_\ell^{\mu-1})$  and the corresponding refinement indicators  $\zeta_\ell(T; z_\ell^\mu)$  for all  $T \in \mathcal{T}_\ell$ .
- (b) Terminate  $\mu$ -loop and define  $\underline{\mu}[\ell] := \mu$  provided that

$$\| \| z_\ell^\mu - z_\ell^{\mu-1} \| \| \leq \lambda_{\text{alg}} \zeta_\ell(z_\ell^\mu).$$

(III) **COMBINED MARK**. Determine sets  $\overline{\mathcal{M}}_\ell^u, \overline{\mathcal{M}}_\ell^z \subseteq \mathcal{T}_\ell$  of minimal cardinality that satisfy the Dörfler marking criteria

$$\theta \eta_\ell(u_\ell^{\underline{m}})^2 \leq \eta_\ell(\overline{\mathcal{M}}_\ell^u, u_\ell^{\underline{m}})^2 \quad \text{and} \quad \theta \zeta_\ell(z_\ell^{\underline{\mu}})^2 \leq \zeta_\ell(\overline{\mathcal{M}}_\ell^z, z_\ell^{\underline{\mu}})^2.$$

Following [FPZ16], let the marked elements  $\mathcal{M}_\ell := \mathcal{M}_\ell^u \cup \mathcal{M}_\ell^z$  consist of subsets  $\mathcal{M}_\ell^u \subseteq \overline{\mathcal{M}}_\ell^u$  and  $\mathcal{M}_\ell^z \subseteq \overline{\mathcal{M}}_\ell^z$  of same cardinality  $\#\mathcal{M}_\ell^u = \#\mathcal{M}_\ell^z = \min\{\#\overline{\mathcal{M}}_\ell^u, \#\overline{\mathcal{M}}_\ell^z\}$ .

(IV) **REFINE**. Generate the new mesh  $\mathcal{T}_{\ell+1} := \text{refine}(\mathcal{T}_\ell, \mathcal{M}_\ell)$  by NVB and employ nested iteration  $u_{\ell+1}^0 := u_\ell^{\underline{m}}$  and  $z_{\ell+1}^0 := z_\ell^{\underline{\mu}}$ .

**Output:** Sequences of successively refined triangulations  $\mathcal{T}_\ell$ , discrete approximations  $u_\ell^m$ ,  $z_\ell^\mu$ , and corresponding error estimators  $\eta_\ell(u_\ell^k)$ ,  $\zeta_\ell(z_\ell^k)$ .

Note that, in practice, the primal (I) and dual (II) iterations can be performed in parallel: The underlying matrix is indeed the same, one just needs to accommodate the implementation for two different right-hand sides. Algorithm 2 essentially goes back to [MS09] for the Poisson model problem, while the analysis for general second-order elliptic PDEs is given in [FPZ16]. While the earlier work [MS09] employed the combined marking strategy with  $\mathcal{M}_\ell \in \{\overline{\mathcal{M}}_\ell^u, \overline{\mathcal{M}}_\ell^z\}$  such that  $\#\mathcal{M}_\ell = \min\{\#\overline{\mathcal{M}}_\ell^u, \#\overline{\mathcal{M}}_\ell^z\}$ , it empirically turned out that the marking strategy (III) from [FPZ16] is computationally more efficient. Note, however, that [MS09; FPZ16] employ the exact computation of the primal and the dual solutions, while the extension to inexact solutions is done in [BGIP23] for symmetric PDEs.

The simultaneous consideration of primal and dual solution requires an adaptation of the countably infinite index set which reads, for the function  $v \in \{u, z\}$ ,

$$\mathcal{Q}^v := \{(\ell, k) \in \mathbb{N}_0^2 : v_\ell^k \text{ is defined in Algorithm 2}\}.$$

The following definitions of the final indices coincide with those defined in Algorithm 2

$$\begin{aligned} \underline{\ell} &:= \sup\{\ell \in \mathbb{N}_0 : (\ell, 0) \in \mathcal{Q}^u \text{ or } (\ell, 0) \in \mathcal{Q}^z\} \in \mathbb{N}_0 \cup \{\infty\}, \\ \underline{m}[\ell] &:= \sup\{m \in \mathbb{N} : (\ell, m) \in \mathcal{Q}^u\}, \quad \underline{\mu}[\ell] := \sup\{\mu \in \mathbb{N} : (\ell, \mu) \in \mathcal{Q}^z\}. \end{aligned}$$

In addition to the quasi-error  $H_\ell^k$  and  $H_\ell$  from (27)–(28) for the primal problem, the corresponding quasi-errors for the dual problem read

$$\begin{aligned} Z_\ell^k &:= \|\|z_\ell^* - z_\ell^k\|\| + \zeta_\ell(z_\ell^k) \quad \text{for all } (\ell, k) \in \mathcal{Q}^z, \\ Z_\ell &:= \|\|z_\ell^* - z_\ell^k\|\| + \gamma \zeta_\ell(z_\ell^k) \quad \text{for all } (\ell, k) \in \mathcal{Q}^z. \end{aligned}$$

The quasi-errors naturally extend to the full index set  $(\ell, k) \in \mathcal{Q} := \mathcal{Q}^u \cup \mathcal{Q}^z$  with the maximum  $\underline{k}[\ell] := \max\{\underline{m}[\ell], \underline{\mu}[\ell]\}$  via

$$H_\ell^k := H_\ell^m \text{ if } (\ell, k) \notin \mathcal{Q}^u \quad \text{and} \quad Z_\ell^k := Z_\ell^\mu \text{ if } (\ell, k) \notin \mathcal{Q}^z.$$

Arguing as for Lemma 3, one obtains the following a-posteriori control on the goal-error, which can be used to terminate Algorithm 2.

---

**Lemma 12.** *For  $\ell \in \mathbb{N}_0$  and  $m, \mu \geq 1$ , let  $u_\ell^m, z_\ell^\mu \in \mathcal{X}_\ell$  be computed by the adaptive loop of Algorithm 2. Then, there holds*

$$|G(u^*) - G_H(u_\ell^m, z_\ell^\mu)| \lesssim [\|\|u_\ell^m - u_\ell^{m-1}\|\| + \eta_\ell(u_\ell^m)] [\|\|z_\ell^\mu - z_\ell^{\mu-1}\|\| + \zeta_\ell(z_\ell^\mu)]$$

and, for  $m = \underline{m}[\ell]$ ,  $\mu = \underline{\mu}[\ell]$ ,

$$|G(u^*) - G_H(u_\ell^m, z_\ell^\mu)| \lesssim \eta_\ell(u_\ell^m) \zeta_\ell(z_\ell^\mu). \quad \square \quad (59)$$


---

**5.3. Convergence and complexity.** Algorithm 2 satisfies the following convergence results from [BGIP23] generalizing the statements from Subsection 2.7 to goal-oriented adaptivity. The proof of full R-linear convergence follows the summability-based proof given for Theorem 5 above. Additional difficulties arise from the inherent nonlinear product structure of  $H_\ell^k Z_\ell^k$ , when compared to the linear quasi-error  $H_\ell^k$  for standard AFEM.

---

**Theorem 13 (parameter-robust full R-linear convergence [BGIP23, Thm. 6]).** *Let  $0 < \theta \leq 1$  and  $\lambda_{\text{alg}} > 0$ . Then, Algorithm 2 guarantees the existence of constants  $C_{\text{lin}} > 0$  and  $0 < q_{\text{lin}} < 1$  such that*

$$H_\ell^k Z_\ell^k \leq C_{\text{lin}} q_{\text{lin}}^{|\ell, k| - |\ell', k'|} H_{\ell'}^{k'} Z_{\ell'}^{k'} \quad \text{for all } (\ell, k), (\ell', k') \in \mathcal{Q} \text{ with } |\ell, k| > |\ell', k'|.$$

In particular, this yields parameter-robust convergence

$$|G(u^*) - G_\ell(u_\ell^k, z_\ell^k)| \lesssim H_\ell^k Z_\ell^k \leq C_{\text{lin}} q_{\text{lin}}^{|\ell, k|} H_0^0 Z_0^0 \rightarrow 0 \text{ as } |\ell, k| \rightarrow \infty. \quad \square$$


---

The proof of optimal complexity follows as for standard AFEM. The only new ingredient is the comparison lemma (see Lemma 10 for standard AFEM), which needs to be adapted to the product structure of GOAFEM.

---

**Theorem 14 (optimal complexity [BGIP23, Thm. 8]).** *There exist upper bounds  $0 < \theta^* \leq 1$  and  $\lambda_{\text{alg}}^* > 0$  such that, for sufficiently small  $0 < \theta < \theta^*$  and  $0 < \lambda_{\text{alg}} < \lambda_{\text{alg}}^*$ , the following holds: Algorithm 2 guarantees that*

$$\sup_{(\ell, k) \in \mathcal{Q}} \text{cost}(\ell, k)^{s+t} \mathbb{H}_\ell^k Z_\ell^k \lesssim \max\{\|u^*\|_{\mathbb{A}_s}, \|z^*\|_{\mathbb{A}_t}, \mathbb{H}_0^0 Z_0^0\} \text{ for all } s, t > 0. \quad \square$$


---

**5.4. Numerical example.** For the empirical investigation of Algorithm 2, consider the Z-shaped domain  $\Omega := (-1, 1)^2 \setminus \text{conv}\{(0, 0), (-1, 0), (-1, -1)\} \subset \mathbb{R}^2$  with the Dirichlet boundary  $\Gamma_D := \text{conv}\{(-1, 0), (0, 0)\} \cup \text{conv}\{(-1, -1), (0, 0)\}$  and the Neumann boundary  $\Gamma_N := \partial\Omega \setminus \Gamma_D$ . The benchmark problem seeks  $u^* \in H^1(\Omega)$  such that

$$-\Delta u^* = 1 \text{ in } \Omega \quad \text{with} \quad u^* = 0 \text{ on } \Gamma_D \text{ and } \partial u / \partial n = 0 \text{ on } \Gamma_N.$$

Given the subdomain  $S := (-0.5, 0.5)^2 \cap \Omega$ , the goal functional is determined by  $g := 0$  and  $\mathbf{g} := \chi_S(1, 1)^\top$  and reads

$$G(u^*) = \int_S (\partial_1 u^* + \partial_2 u^*) dx \approx 1.015559272415834. \quad (60)$$

The exact goal value (60) is approximated by a reference solution with sextic polynomial functions with adaptive mesh refinement until  $\dim(\mathcal{X}_\ell)$  exceeds  $5 \times 10^6$ .

Some discrete primal and dual solutions are depicted in Figure 11. The corresponding adaptively generated mesh exhibits increased refinement at the reentrant corner (singularity of  $u^*$ ) as well as at the vertices of the support  $S$  of  $\mathbf{g}$  (singularities of  $z^*$ ). This adaptive refinement ensures the (doubled) optimal convergence rates for the primal and dual estimator product in Figure 12. The approximated goal error with respect to the extrapolated goal value from (60) in Figure 13 confirms these convergence rates.

## 6. EXTENSION 2: NON-SYMMETRIC PROBLEMS

While iterative algebraic solvers for non-symmetric problems are widely used in practice (e.g., GMRES, BiCGStab), obtaining a uniform contraction property (C) in the energy norm remains an open question. As a remedy, and inspired by the state-of-the-art proof of the famous Lax–Milgram lemma, [BHI<sup>+</sup>23; BIM<sup>+</sup>24] introduced an additional Zarantonello iteration for the symmetrization of the discrete equation. This allows for the application of the previously used optimal iterative solvers within Algorithm 1 for symmetric linear systems to compute the inexact Zarantonello update. This section addresses the generalization of the adaptive algorithm to non-symmetric problems by using such a two-fold nested iteration with a symmetrization step.

**6.1. General second-order linear elliptic model problem.** The (non-symmetric) second-order linear elliptic problem seeks a solution  $u^* \in \mathcal{X}$  with

$$-\text{div}(\mathbf{A}\nabla u^*) + \mathbf{b} \cdot \nabla u^* + cu^* = f - \text{div} \mathbf{f} \text{ in } \Omega \quad \text{and} \quad u^* = 0 \text{ on } \partial\Omega, \quad (61)$$

where  $\mathbf{b} \in [L^\infty(\Omega)]^d$  is the convection coefficient and  $c \in L^\infty(\Omega)$  the reaction coefficient, in addition to the diffusion matrix  $\mathbf{A}$  and the right-hand sides  $f$  and  $\mathbf{f}$  from Subsection 1.2. Using the bilinear form  $a(\cdot, \cdot)$  from (3), the weak formulation of (61) seeks  $u^* \in \mathcal{X}$  such that

$$b(u^*, v) := a(u^*, v) + \int_\Omega (\mathbf{b} \cdot \nabla u^* + cu^*) v dx = F(v) \quad \text{for all } v \in \mathcal{X}. \quad (62)$$

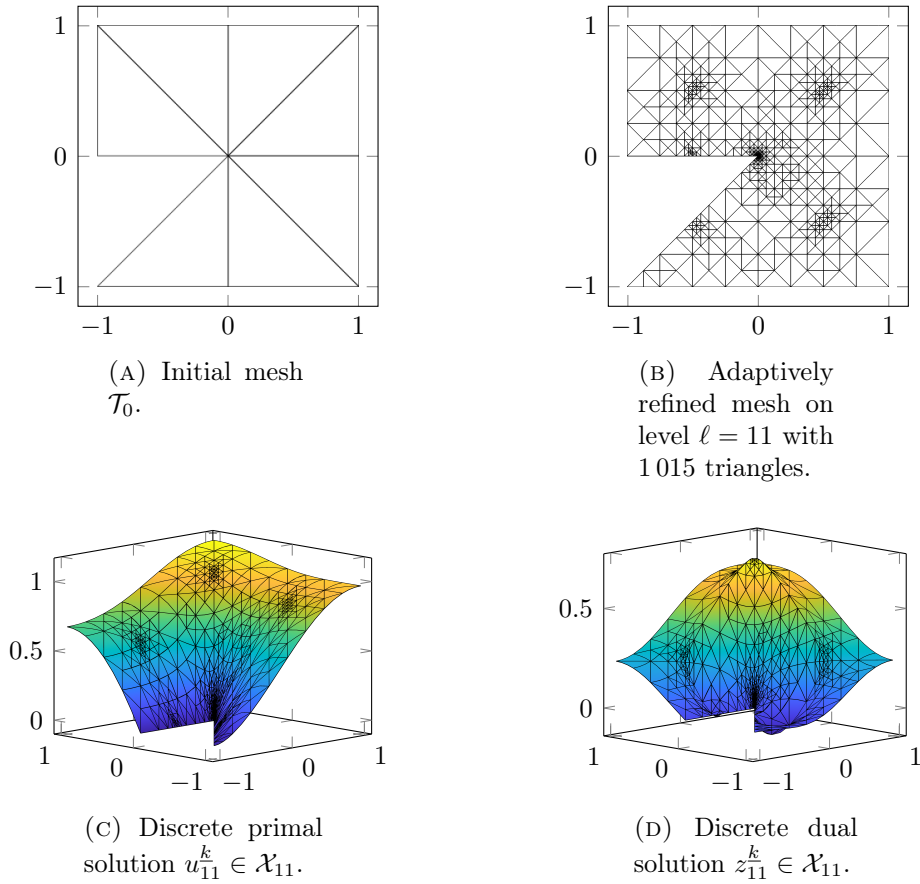


FIGURE 11. Mesh and corresponding discrete primal and dual solution for the benchmark problem from Subsection 5.4. The results are generated by Algorithm 2 with polynomial degree  $p = 2$ , bulk parameter  $\theta = 0.3$ , and stopping parameter  $\lambda_{\text{alg}} = 0.7$ .

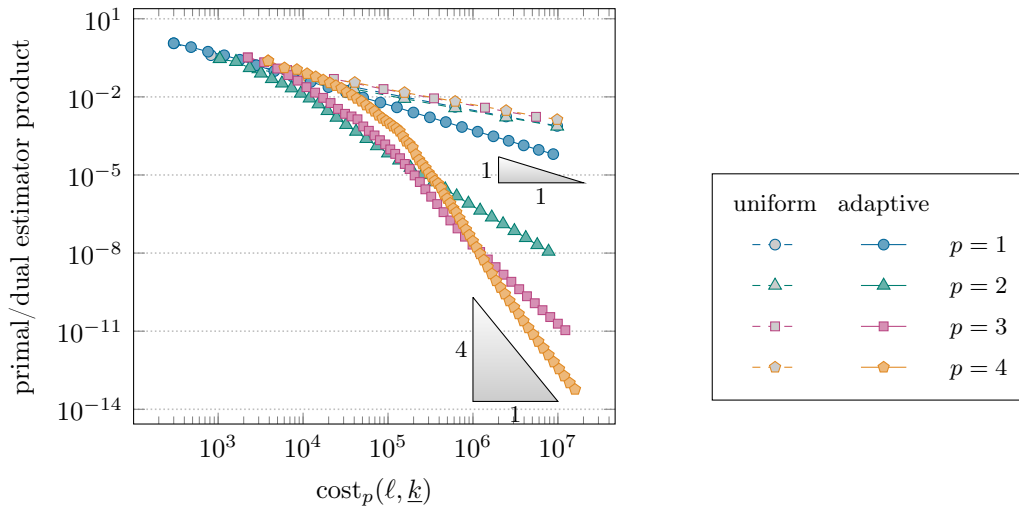


FIGURE 12. Convergence plot of the adaptive Algorithm 2 to solve the benchmark problem from Subsection 5.4 for various polynomial degrees. The adaptivity parameters read  $\theta = 0.3$  and  $\lambda_{\text{alg}} = 0.7$ . All graphs display values of the residual-based error estimator product  $\eta_\ell(u_\ell^m) \zeta_\ell(z_\ell^\mu)$  from (59).

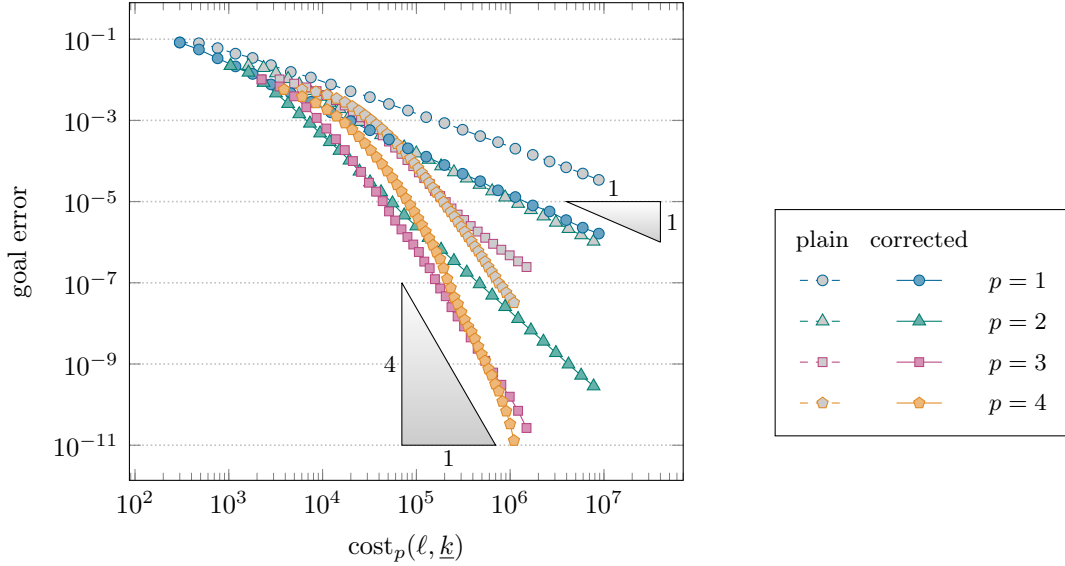


FIGURE 13. Convergence plot of the goal error for the adaptive Algorithm 2 to solve the benchmark problem from Subsection 5.4 for various polynomial degrees. The adaptivity parameters read  $\theta = 0.3$  and  $\lambda_{\text{alg}} = 0.7$ . The graphs display the error of the discrete goal value  $G(u_\ell^m)$  from (54) using only the primal problem (plain) and the discrete goal value  $G_H(u_\ell^m, z_\ell^\mu)$  from (57) using the duality technique to double the convergence rates (corrected). The error is computed with respect to the reference goal value from (60). The reference value only allowed reasonable results up to error values of about  $10^{-11}$  and thus the remaining results of the graphs are omitted.

We suppose that  $b(\cdot, \cdot)$  is elliptic with respect to the  $a(\cdot, \cdot)$ -induced norm  $\|\cdot\|$  in the sense of

$$b(v, v) \gtrsim \|v\|^2 \quad \text{for all } v \in \mathcal{X}. \quad (63)$$

For instance, this is satisfied if  $-\frac{1}{2} \operatorname{div} \mathbf{b} + c \geq 0$ . Under the assumption (63), the Lax–Milgram lemma applies and indeed proves existence and uniqueness of the weak solution  $u^* \in \mathcal{X}$  to (62) and likewise that of the discrete solution  $u_H^* \in \mathcal{X}_H$  to

$$b(u_H^*, v_H) = F(v_H) \quad \text{for all } v_H \in \mathcal{X}_H.$$

Moreover, the corresponding residual-based error estimator reads

$$\begin{aligned} \eta_H(T, v_H)^2 &:= |T|^{2/d} \|f + \operatorname{div}(\mathbf{A}\nabla u^* - \mathbf{f}) - \mathbf{b} \cdot \nabla u^* - cu^*\|_{L^2(T)}^2 \\ &\quad + |T|^{1/d} \|[(\mathbf{A}\nabla u^* - \mathbf{f}) \cdot \mathbf{n}]\|_{L^2(\partial T \cap \Omega)}^2. \end{aligned} \quad (64)$$

It is well-known from, e.g., [CFPP14, Sect. 6] that  $\eta_H$  satisfies the axioms of adaptivity (A1)–(A4).

Standard iterative solvers for non-symmetric linear systems lack the contraction property (C) in the energy norm. This prevents the straight-forward application of the full R-linear convergence proof from Subsection 4.1 to problem (61) and motivated the use of the additional Zarantonello iteration [Zar60] for the symmetrization of the discrete equation in [BHI<sup>+</sup>23]. For a given damping parameter  $\delta > 0$  and the current iterate  $u_H \in \mathcal{X}_H$ , the Zarantonello mapping  $\Phi_H(\delta; \cdot) : \mathcal{X}_H \rightarrow \mathcal{X}_H$  is defined by

$$a(\Phi_H(\delta; u_H), v_H) = a(u_H, v_H) + \delta[F(v_H) - b(u_H, v_H)] \quad \text{for all } v_H \in \mathcal{X}_H. \quad (65)$$

Since  $a(\cdot, \cdot)$  is a scalar product, the Riesz–Fischer theorem guarantees well-definedness of  $\Phi_H(\delta; u_H) \in \mathcal{X}_H$ . For sufficiently small  $\delta > 0$ , the mapping  $\Phi_H(\delta; \cdot)$  is a contraction [HW20a; HW20b], i.e., there exists  $0 < q_{\text{sym}}^* < 1$  such that

$$\| \|u_H^* - \Phi_H(\delta; u_H)\| \| \leq q_{\text{sym}}^* \| \|u_H^* - u_H\| \| \quad \text{for all } u_H \in \mathcal{X}_H. \quad (66)$$

As in Subsection 2.2, the linear SPD system (65) can be treated using the algebraic solver  $\Psi_H : \mathcal{X}^* \times \mathcal{X}_H \rightarrow \mathcal{X}_H$  from Subsection 2.2 with the contraction property (C). In case of a complicated right-hand side as in (65), the first argument of  $\Psi_H$  is replaced by the exact Riesz representative  $\Phi_H(\delta; u_H)$  of the right-hand side to shorten the notation. Importantly, the solution  $\Phi_H(\delta; u_H)$  of (65) will never be computed in practice, but only approximated via this iterative solver.

Overall, a nested solver iteration is necessary and thus a triple index  $(\ell, k, j)$  will be used in the adaptive algorithm: The index  $\ell \in \mathbb{N}_0$  denotes the mesh-level,  $k \in \mathbb{N}_0$  denotes the Zarantonello step, and  $j \in \mathbb{N}_0$  denotes the step of the algebraic solver, i.e.,

$$u_\ell^{k,j} = \Psi_\ell(u_\ell^{k,*}, u_\ell^{k,j-1}) \approx u_\ell^{k,*} := \Phi_\ell(\delta; u_\ell^{k-1,j}) \approx u_\ell^*,$$

where neither  $u_\ell^{k,*}$  nor  $u_\ell^*$  are computed, but only  $u_\ell^{k,j}$ .

**6.2. Algorithm 3: Adaptive iteratively symmetrized FEM. Input:** Initial mesh  $\mathcal{T}_0$ , polynomial degree  $p \in \mathbb{N}$ , initial iterate  $u_0^{0,0} := u_0^{0,j} := 0$ , the Zarantonello damping parameter  $\delta > 0$ , marking parameter  $0 < \theta \leq 1$ , stopping parameters  $\lambda_{\text{sym}}, \lambda_{\text{alg}} > 0$ .

**Adaptive loop:** For all  $\ell = 0, 1, 2, \dots$ , repeat the steps (I)–(III):

(I) **SOLVE & ESTIMATE.** For all  $k = 1, 2, 3, \dots$ , repeat the steps (a)–(b):

(a) **Algebraic solver loop:** For all  $j = 1, 2, 3, \dots$ , repeat the steps (i)–(ii):

(i) Compute  $u_\ell^{k,j} := \Psi_\ell(u_\ell^{k,*}, u_\ell^{k,j-1})$  (for the approximation of the theoretical quantity  $u_\ell^{k,*} := \Phi_\ell(\delta; u_\ell^{k-1,j}) \in \mathcal{X}_\ell$  solving (65) with  $u_H = u_\ell^{k-1,j}$ ) and refinement indicators  $\eta_\ell(T, u_\ell^{k,j})$  for all  $T \in \mathcal{T}_\ell$ .

(ii) Terminate  $j$ -loop with  $\underline{j}[\ell, k] := j$  and employ nested iteration  $u_\ell^{k,0} := u_\ell^{k-1,\underline{j}}$  provided that

$$\| \|u_\ell^{k,j} - u_\ell^{k,j-1}\| \| \leq \lambda_{\text{alg}} [\lambda_{\text{sym}} \eta_\ell(u_\ell^{k,j}) + \| \|u_\ell^{k,j} - u_\ell^{k-1,\underline{j}}\| \|]. \quad (67)$$

(b) Terminate  $k$ -loop and define  $\underline{k}[\ell] := k$  provided that

$$\| \|u_\ell^{k,\underline{j}} - u_\ell^{k-1,\underline{j}}\| \| \leq \lambda_{\text{sym}} \eta_\ell(u_\ell^{k,\underline{j}}). \quad (68)$$

(II) **MARK.** Determine a set  $\mathcal{M}_\ell \subseteq \mathcal{T}_\ell$  of minimal cardinality that satisfies the Dörfler marking criterion

$$\theta \eta_\ell(u_\ell^{k,\underline{j}})^2 \leq \eta_\ell(\mathcal{M}_\ell, u_\ell^{k,\underline{j}})^2.$$

(III) **REFINE.** Generate the new mesh  $\mathcal{T}_{\ell+1} := \text{refine}(\mathcal{T}_\ell, \mathcal{M}_\ell)$  by NVB and define  $u_{\ell+1}^{0,0} := u_{\ell+1}^{0,\underline{j}} := u_\ell^{k,\underline{j}}$  (nested iteration).

**Output:** Sequences of successively refined triangulations  $\mathcal{T}_\ell$ , discrete approximations  $u_\ell^{k,j}$ , and corresponding error estimators  $\eta_\ell(u_\ell^{k,j})$ .

---

**Remark 15.** *Let us comment on the stopping criteria (67)–(68) of Algorithm 3.*

- (i) Since the algebraic solver is contractive, the term  $\|u_\ell^{k,j} - u_\ell^{k,j-1}\|$  in (67) provides computable a-posteriori error control on the algebraic error  $\|u_\ell^{k,*} - u_\ell^{k,j}\|$ . With the interpretation that  $\eta_\ell(u_\ell^{k,j}) \approx \eta_\ell(u_\ell^*)$  measures the discretization error and  $\|u_\ell^{k,j} - u_\ell^{k-1,j}\| \approx \|u_\ell^{k,*} - u_\ell^{k,j}\|$  measures the symmetrization error, the stopping criterion (67) can be interpreted as numerical equilibration of the algebraic error with the sum of discretization and symmetrization error.
- (ii) With the same understanding, the stopping criterion (68) for the symmetrization can be interpreted as numerical equilibration of symmetrization and discretization error.
- (iii) These interpretations can be made rigorous with the help of Lemma 18 below. Moreover, Lemma 17 below proves that the full error  $\|u^* - u_\ell^{k,j}\|$  is indeed controlled by the sum of the terms in (67). An additional consequence of (67)–(68) is that  $\eta_\ell(u_\ell^{k,j})$  provides a computable upper bound for the error  $\|u^* - u_\ell^{k,j}\|$ .
- (iv) The innermost  $j$ -loop of the algebraic solver indeed turns out to be finite; see Lemma 16 below. The  $k$ -loop of the symmetrization can formally fail to terminate. In this case, Theorem 20 below proves that  $u^* = u_\ell^*$  and  $\eta_\ell(u_\ell^{k,j}) \rightarrow \eta_\ell(u_\ell^*) = 0$  as  $k \rightarrow \infty$ .

Analogous notation to Subsection 2.6 applies for the index set

$$\mathcal{Q} := \{(\ell, k, j) \in \mathbb{N}_0^3 : u_\ell^{k,j} \text{ is defined in Algorithm 3}\},$$

the lexicographic ordering on  $\mathcal{Q}$

$$(\ell', k', j') \leq (\ell, k, j) : \iff u_{\ell'}^{k',j'} \text{ is defined no later than } u_\ell^{k,j} \text{ in Algorithm 3,}$$

the stopping indices

$$\begin{aligned} \underline{\ell} &:= \sup\{\ell \in \mathbb{N}_0 : (\ell, 0, 0) \in \mathcal{Q}\} \in \mathbb{N}_0 \cup \{\infty\}, \\ \underline{k}[\ell] &:= \sup\{k \in \mathbb{N}_0 : (\ell, k, 0) \in \mathcal{Q}\} \in \mathbb{N}_0 \cup \{\infty\} \text{ for } (\ell, 0, 0) \in \mathcal{Q}, \\ \underline{j}[\ell, k] &:= \sup\{j \in \mathbb{N}_0 : (\ell, k, j) \in \mathcal{Q}\} \in \mathbb{N}_0 \cup \{\infty\} \text{ for } (\ell, k, 0) \in \mathcal{Q}, \end{aligned}$$

the total step counter

$$|\ell, k, j| := \#\{(\ell', k', j') \in \mathcal{Q} : (\ell', k', j') \leq (\ell, k, j)\} \in \mathbb{N}_0 \text{ for all } (\ell, k, j) \in \mathcal{Q},$$

and the computational cost, for all  $(\ell, k, j) \in \mathcal{Q}$

$$\text{cost}(\ell, k, j) := \sum_{\substack{(\ell', k', j') \in \mathcal{Q} \\ |\ell', k', j'| \leq |\ell, k, j|}} \#\mathcal{T}_\ell \quad \text{and} \quad \text{cost}_p(\ell, k, j) := \sum_{\substack{(\ell', k', j') \in \mathcal{Q} \\ |\ell', k', j'| \leq |\ell, k, j|}} \dim(\mathcal{X}_\ell).$$

Moreover, the quasi-error is modified to include the additional error related to the symmetrization: Indeed, the first term is the error between exact discrete solution and its inexactly symmetrized approximation

$$H_\ell^{k,j} := \|u_\ell^* - u_\ell^{k,j}\| + \|u_\ell^{k,*} - u_\ell^{k,j}\| + \eta_\ell(u_\ell^{k,j}).$$

Importantly, the following result states that the innermost  $j$ -loop is known to terminate.

**Lemma 16 (bounded number of algebraic solvers steps [BHI<sup>+</sup>23, Lem. 3.2]).** Consider arbitrary parameters  $0 < \theta \leq 1$ ,  $0 < \lambda_{\text{lin}}$ ,  $0 < \lambda_{\text{alg}}$ . Then, Algorithm 3 guarantees that  $\underline{j}[\ell, k] < \infty$  for all  $(\ell, k, 0) \in \mathcal{Q}$ , i.e., the number of algebraic solver steps is finite.  $\square$

Note that there holds a-posteriori error control at each step of the adaptive algorithm, which can again be used to terminate Algorithm 3.

---

**Lemma 17 (a-posteriori error control [BHI<sup>+</sup>23, Prop. 3.5]).** *For any  $(\ell, k, j) \in \mathcal{Q}$  with  $k \geq 1$  and  $j \geq 1$ , it holds that*

$$\| \| u^\star - u_\ell^{k,j} \| \| \lesssim [\eta_\ell(u_\ell^{k,j}) + \| \| u_\ell^{k,j} - u_\ell^{k-1,j} \| \| + \| \| u_\ell^{k,j} - u_\ell^{k,j-1} \| \|], \quad (69)$$

and for  $k = \underline{k}[\ell]$ ,  $j = \underline{j}[\ell, \underline{k}]$

$$\| \| u^\star - u_\ell^{\underline{k}, \underline{j}} \| \| \lesssim \eta_\ell(u_\ell^{\underline{k}, \underline{j}}). \quad (70)$$


---

**6.3. Convergence and complexity.** Algorithm 3 does not compute the exact Zaranonello iterates with contraction (66). Nevertheless, the following lemma establishes that the contraction property also holds for the inexact symmetrization in order to replace Lemma 4.

---

**Lemma 18 (contraction of inexact Zaranonello iteration [BFM<sup>+</sup>23, Lem. 5.1]).**

*There exists  $0 < \lambda_{\text{alg}}^\star$  and  $0 < q_{\text{sym}} < 1$  such that, for all  $0 < \lambda_{\text{alg}} < \lambda_{\text{alg}}^\star$ , it holds*

$$\begin{aligned} \| \| u_\ell^\star - u_\ell^{\underline{k}, \underline{j}} \| \| &\leq q_{\text{sym}} \| \| u_\ell^\star - u_\ell^{k-1, j} \| \| \quad \text{for all } (\ell, k, j) \in \mathcal{Q} \text{ with } 1 \leq k < \underline{k}[\ell], \\ \| \| u_\ell^\star - u_\ell^{\underline{k}, \underline{j}} \| \| &\leq q_{\text{sym}}^\star \| \| u_\ell^\star - u_\ell^{k-1, j} \| \| + \frac{2q_{\text{alg}}}{1 - q_{\text{alg}}} \lambda_{\text{alg}} \lambda_{\text{sym}} \eta_\ell(u_\ell^{\underline{k}, \underline{j}}) \quad \text{for all } (\ell, \underline{k}, \underline{j}) \in \mathcal{Q}. \end{aligned}$$


---

Since the non-symmetric problem (61) ensures the Galerkin orthogonality (11) for  $b(\cdot, \cdot)$ , but not for its symmetric part  $a(\cdot, \cdot)$ , the Pythagorean identity (12) is replaced by the quasi-orthogonality introduced as additional axiom in [CFPP14]. The following generalization from [Fei22] has been applied in the optimal-complexity analysis in [BFM<sup>+</sup>23].

---

**Lemma 19 (quasi-orthogonality [BFM<sup>+</sup>23, Prop. 2]).** *There exists  $0 < \alpha \leq 1$  such that the following holds: For any sequence  $\mathcal{X}_\ell \subseteq \mathcal{X}_{\ell+1} \subset \mathcal{X}$  of nested subspaces, the corresponding exact Galerkin solutions  $u_\ell^\star \in \mathcal{X}_\ell$  to (62) satisfy*

$$\sum_{\ell'=\ell}^{\ell+N} \| \| u_{\ell'}^\star - u_\ell^\star \| \| ^2 \lesssim (N+1)^{1-\alpha} \| \| u^\star - u_\ell^\star \| \| ^2 \quad \text{for all } \ell, N \in \mathbb{N}_0. \quad (71)$$


---

The two previous lemmas allow for the following generalization of the convergence results from Subsection 2.7. Note that, in contrast to Theorem 5 and Theorem 13, full R-linear convergence is subject to some requirements on the stopping parameter  $\lambda_{\text{alg}}$  stemming from Lemma 18. In this sense, the following theorem fails to state parameter-robust convergence. Finally, we note that the present formulation is proved in [BFM<sup>+</sup>23], while an earlier result [BHI<sup>+</sup>23] had even more severe restrictions on  $\lambda_{\text{alg}}$  and  $\lambda_{\text{sym}}$ .

---

**Theorem 20 (full R-linear convergence of Algorithm 3, [BFM<sup>+</sup>23, Thm. 14]).**

*Let  $0 < \theta \leq 1$  and  $0 < \lambda_{\text{sym}} \leq 1$  be arbitrary. Let  $\delta > 0$  be sufficiently small to guarantee contraction (66) of the exact Zaranonello iteration. Recall  $\lambda_{\text{alg}}^\star$  from Lemma 18. Then, there exists an upper bound  $\lambda^\star > 0$  such that, for all  $0 < \lambda_{\text{alg}} < \lambda_{\text{alg}}^\star$  with  $\lambda_{\text{alg}} \lambda_{\text{sym}} < \lambda^\star$ , the following holds: Algorithm 3 guarantees the existence of  $C_{\text{lin}} > 0$  and  $0 < q_{\text{lin}} < 1$  such that*

$$H_\ell^{k,j} \lesssim q_{\text{lin}}^{|\ell, k, j| - |\ell', k', j'|} H_{\ell'}^{k', j'} \quad \text{for all } (\ell, k, j), (\ell', k', j') \in \mathcal{Q} \text{ with } |\ell, k, j| > |\ell', k', j'|. \quad (72)$$

In particular, this yields convergence

$$\|u^* - u_\ell^{k,j}\| \lesssim H_\ell^{k,j} \leq C_{\text{lin}} q_{\text{lin}}^{|\ell,k,j|} H_0^{0,0} \rightarrow 0 \quad \text{as } |\ell, k, j| \rightarrow \infty. \quad \square$$

With validity of linear convergence (72), one can follow the lines of the proof of Theorem 14 to conclude optimal complexity.

**Theorem 21 (optimal computational complexity [BFM<sup>+</sup>23; BHI<sup>+</sup>23]).** *Under the assumptions of Theorem 20, there exist additional upper bounds  $\theta^*, \lambda_{\text{sym}}^* > 0$  such that, for all  $0 < \theta < \theta^*$ ,  $0 < \lambda_{\text{sym}} < \lambda_{\text{sym}}^*$ , and  $0 < \lambda_{\text{alg}} < \lambda_{\text{alg}}^*$ , with  $\lambda_{\text{alg}} \lambda_{\text{sym}} < \lambda^*$ , the following holds: Algorithm 3 guarantees, for all  $s > 0$ , that*

$$\|u^*\|_{\mathbb{A}_s} \lesssim \sup_{(\ell,k,j) \in \mathcal{Q}} \text{cost}(\ell, k, j)^s H_\ell^{k,j} \lesssim \max\{\|u^*\|_{\mathbb{A}_s}, H_0^{0,0}\}. \quad (73)$$

Based on the ideas from Section 5, one can extend the results in the Theorems 20–21 for general second-order linear elliptic PDEs from standard AFEM to GOAFEM. Details are found in the recent work [BBPS23].

**6.4. Numerical example.** The performance of Algorithm 3 is tested using a benchmark example on the L-shaped domain  $\Omega := (-1, 1)^2 \setminus [0, 1)^2$  with dominating convection  $\mathbf{b} := (-10, -10)^\top$  and  $c = 0$ . It seeks  $u^* \in H^1(\Omega)$  satisfying

$$-\Delta u^* + \begin{pmatrix} -10 \\ -10 \end{pmatrix} \cdot \nabla u^* = 1 \text{ in } \Omega \quad \text{with} \quad u^* = 0 \text{ on } \partial\Omega.$$

In addition to increased refinement due to the singularity at the reentrant corner, the strong convection term causes additional refinement at the lower and left boundary layer; see Figure 14a. This is due to the large gradients of the discrete solution as shown in Figure 14b. Therewith, the adaptive algorithm recovers optimal convergence rates of the residual-based error estimator for several polynomial degrees in Figure 15. A closer investigation of the involved stopping parameters  $\lambda_{\text{sym}}$  and  $\lambda_{\text{alg}}$  in Table 2 in the fashion of Table 1 in Section 3 supports the choice of a comparably small value  $\lambda_{\text{sym}} = 0.1$  for an optimal performance independently of the parameters  $\theta$  and  $\lambda_{\text{alg}}$ . In the present case of a dominating convection term, the choice of the damping parameter  $\delta$  is crucial. A large norm of  $\mathbf{b}$  results in a strong deviation from the symmetric bilinear form  $a(\cdot, \cdot)$  and, thus, the Zarantonello iteration requires a small  $\delta \ll 1$  to ensure the contraction property (66). However, a small  $\delta$  leads to a slow convergence. Figure 16 displays the convergence of the error estimator for various damping parameters. For all larger values of  $\delta$ , no significant convergence could be achieved. This justifies the choice of  $\delta = 0.1$  in the remaining experiments of this section.

## 7. EXTENSION 3: NON-LINEAR PROBLEMS

The Zarantonello iteration from Subsection 6 is one possible choice for the linearization of non-linear problems. This leads to an analogous adaptive algorithm to Algorithm 3, where the Zarantonello symmetrization (65) is replaced by a suitable linearization scheme with non-linear residual. The convergence results from Theorems 20–21 apply verbatim in this setting. For further details, the reader is referred to [BFM<sup>+</sup>23] and [HPSV21]. Instead, this section presents a novel energy-based approach from [MPS24] that allows for a parameter-robust alternative.

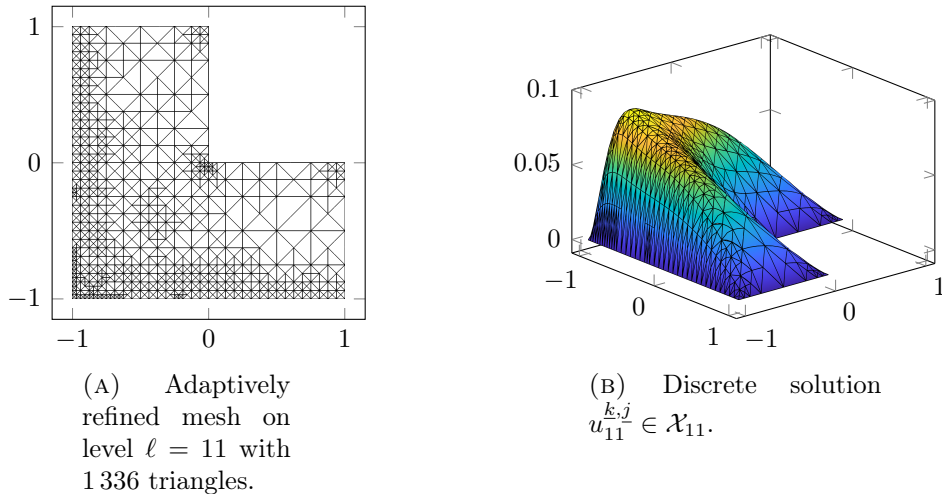


FIGURE 14. Mesh and corresponding discrete solution for the benchmark problem from Subsection 6.4. The results are generated by Algorithm 3 with polynomial degree  $p = 2$ , damping parameter  $\delta = 0.1$ , bulk parameter  $\theta = 0.3$ , and stopping parameters  $\lambda_{\text{sym}} = \lambda_{\text{alg}} = 0.1$ .

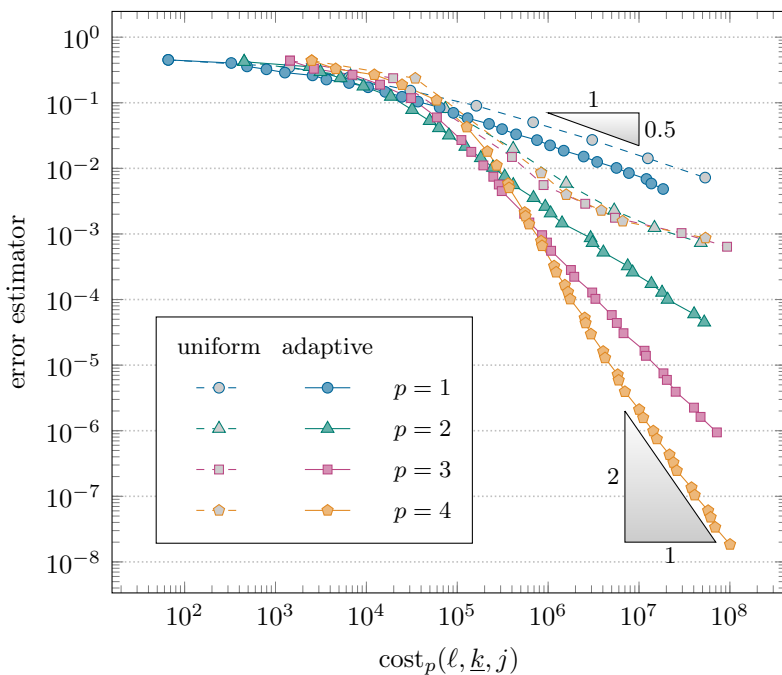


FIGURE 15. Convergence plot of the adaptive Algorithm 3 to solve the benchmark problem from Subsection 6.4 for various polynomial degrees. The damping parameter reads  $\delta = 0.1$  and the adaptivity parameters  $\theta = 0.3$  and  $\lambda_{\text{sym}} = \lambda_{\text{alg}} = 0.1$ . All graphs display values of the residual-based error estimator  $\eta_\ell^{k,j}(u_\ell^{k,j})$  from (64) for the final iterates on the level  $\ell \in \mathbb{N}_0$ .

**7.1. Strongly monotone model problem.** Throughout this subsection, consider a non-linear mapping  $\mathbf{A} : \mathbb{R}^d \rightarrow \mathbb{R}^d$  in the non-linear elliptic PDE

$$-\operatorname{div}(\mathbf{A}(\nabla u^*)) = f - \operatorname{div} \mathbf{f} \text{ in } \Omega \quad \text{and} \quad u^* = 0 \text{ on } \partial\Omega. \quad (74)$$

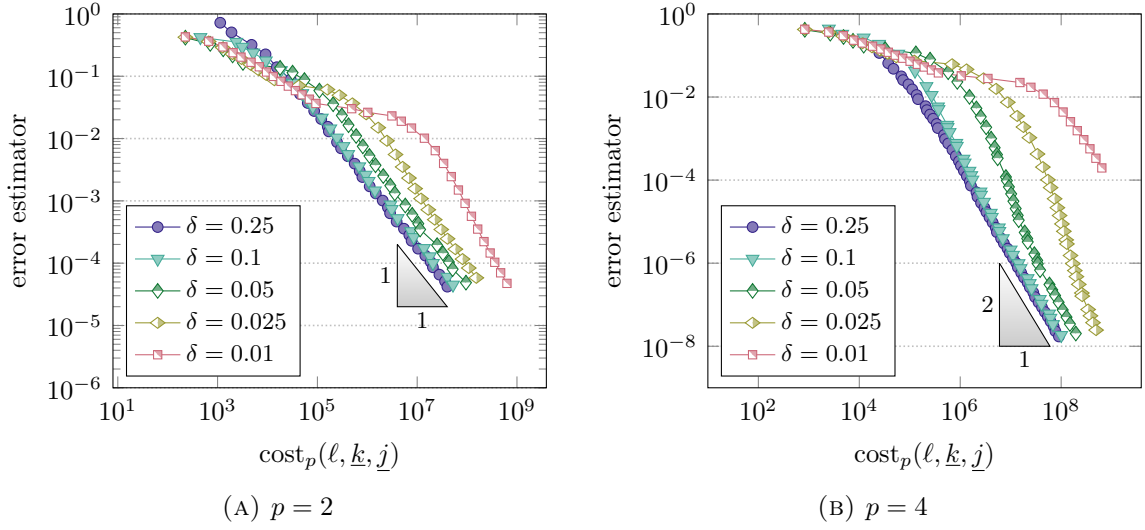


FIGURE 16. Convergence plot of the adaptive Algorithm 3 to solve the benchmark problem from Subsection 6.4 for various damping parameters  $\delta$  and polynomial degrees  $p$ . The adaptivity parameters read  $\theta = 0.3$ , and  $\lambda_{\text{sym}} = \lambda_{\text{alg}} = 0.1$ . All graphs display values of the residual-based error estimator  $\eta_\ell^{k,j}(u_\ell^{k,j})$  from (64) for the final iterates on the level  $\ell \in \mathbb{N}_0$ .

The analysis in [MPS24] is based on an energy-minimization setting and, thus, is restricted to scalar non-linearities of the form  $\mathbf{A}(\xi) := \mu(|\xi|^2)\xi$  for some continuous  $\mu : \mathbb{R}_{\geq 0} \rightarrow \mathbb{R}_{\geq 0}$ . The weak formulation of (74) seeks  $u^* \in \mathcal{X}$  such that

$$\langle \mathcal{A}(u^*), v \rangle = F(v) \quad \text{for all } v \in \mathcal{X}, \quad (75)$$

where  $\mathcal{A} : \mathcal{X} \rightarrow \mathcal{X}^*$  denotes the non-linear operator defined by

$$\mathcal{A}(u) := \langle \mathbf{A}(\nabla u), \nabla(\cdot) \rangle_{L^2(\Omega)} := \int_{\Omega} \mathbf{A}(\nabla u) \cdot \nabla(\cdot) \, dx.$$

The non-linear coefficient  $\mu$  is assumed to satisfy a linear growth condition, i.e., there exist  $0 < \alpha \leq L$  such that

$$\alpha(t - s) \leq \mu(t^2)t - \mu(s^2)s \leq \frac{L}{3}(t - s) \quad \text{for all } t \geq s \geq 0, \quad (76)$$

which is, for instance, satisfied for typical non-linearities in the context of magnetostatics. This condition ensures that  $\mathcal{A}$  is strongly monotone and Lipschitz continuous, i.e., for all  $u, v, w \in \mathcal{X}$ , there holds

$$\alpha \| \|u - v\| \|^2 \leq \langle \mathcal{A}(u) - \mathcal{A}(v), u - v \rangle \text{ and } \langle \mathcal{A}(u) - \mathcal{A}(v), w \rangle \leq L \| \|u - v\| \| \|w\|.$$

This provides existence and uniqueness of the solution  $u^* \in \mathcal{X}$  of the weak formulation (75); see [Zei90, Sect. 25.4].

The discretization uses piecewise affine functions since stability (A1) is only known for this case [GMZ12, Rem. 6.2], while empirically also larger  $p > 1$  works in practice. The discrete formulation seeks  $u_H^* \in \mathcal{X}_H$  with

$$\langle \mathcal{A}(u_H^*), v_h \rangle = F(v_h) \quad \text{for all } v_h \in \mathcal{X}_H. \quad (77)$$

Existence and uniqueness of  $u_H^* \in \mathcal{X}_H$  follow from the abstract arguments that also apply to the weak formulation (75). The corresponding residual-based a-posteriori error

$\lambda_{\text{alg}} \backslash \lambda_{\text{sym}}$	0.1	0.3	0.5	0.7	0.9
0.1	$2.37 \cdot 10^{-2}$	$2.47 \cdot 10^{-2}$	$3.13 \cdot 10^{-2}$	$3.67 \cdot 10^{-2}$	$4.79 \cdot 10^{-2}$
0.3	$1.90 \cdot 10^{-2}$	$2.15 \cdot 10^{-2}$	$2.87 \cdot 10^{-2}$	$4.32 \cdot 10^{-2}$	$5.17 \cdot 10^{-2}$
0.5	$1.90 \cdot 10^{-2}$	$2.50 \cdot 10^{-2}$	$3.21 \cdot 10^{-2}$	$4.42 \cdot 10^{-2}$	$5.33 \cdot 10^{-2}$
0.7	$1.90 \cdot 10^{-2}$	$2.39 \cdot 10^{-2}$	$2.99 \cdot 10^{-2}$	$4.00 \cdot 10^{-2}$	$5.45 \cdot 10^{-2}$
0.9	$2.03 \cdot 10^{-2}$	$2.34 \cdot 10^{-2}$	$2.92 \cdot 10^{-2}$	$4.38 \cdot 10^{-2}$	$5.46 \cdot 10^{-2}$

(A)  $\theta = 0.3$ 

$\lambda_{\text{alg}} \backslash \lambda_{\text{sym}}$	0.1	0.3	0.5	0.7	0.9
0.1	$2.05 \cdot 10^{-2}$	$2.25 \cdot 10^{-2}$	$3.29 \cdot 10^{-2}$	$3.36 \cdot 10^{-2}$	$4.89 \cdot 10^{-2}$
0.3	$1.78 \cdot 10^{-2}$	$2.51 \cdot 10^{-2}$	$3.52 \cdot 10^{-2}$	$4.04 \cdot 10^{-2}$	$5.25 \cdot 10^{-2}$
0.5	$1.79 \cdot 10^{-2}$	$1.89 \cdot 10^{-2}$	$3.44 \cdot 10^{-2}$	$4.22 \cdot 10^{-2}$	$6.26 \cdot 10^{-2}$
0.7	$1.78 \cdot 10^{-2}$	$1.97 \cdot 10^{-2}$	$3.48 \cdot 10^{-2}$	$4.07 \cdot 10^{-2}$	$5.80 \cdot 10^{-2}$
0.9	$1.78 \cdot 10^{-2}$	$1.92 \cdot 10^{-2}$	$3.49 \cdot 10^{-2}$	$4.26 \cdot 10^{-2}$	$5.92 \cdot 10^{-2}$

(B)  $\theta = 0.5$ 

$\lambda_{\text{alg}} \backslash \lambda_{\text{sym}}$	0.1	0.3	0.5	0.7	0.9
0.1	$2.31 \cdot 10^{-2}$	$2.32 \cdot 10^{-2}$	$3.28 \cdot 10^{-2}$	$4.35 \cdot 10^{-2}$	$4.39 \cdot 10^{-2}$
0.3	$1.68 \cdot 10^{-2}$	$2.53 \cdot 10^{-2}$	$3.14 \cdot 10^{-2}$	$5.28 \cdot 10^{-2}$	$6.53 \cdot 10^{-2}$
0.5	$1.66 \cdot 10^{-2}$	$2.57 \cdot 10^{-2}$	$3.35 \cdot 10^{-2}$	$5.37 \cdot 10^{-2}$	$6.71 \cdot 10^{-2}$
0.7	$1.65 \cdot 10^{-2}$	$2.66 \cdot 10^{-2}$	$3.37 \cdot 10^{-2}$	$5.58 \cdot 10^{-2}$	$6.70 \cdot 10^{-2}$
0.9	$1.70 \cdot 10^{-2}$	$2.58 \cdot 10^{-2}$	$3.45 \cdot 10^{-2}$	$5.54 \cdot 10^{-2}$	$6.56 \cdot 10^{-2}$

(C)  $\theta = 0.7$ 

TABLE 2. Investigation of the influence of the adaptivity parameters  $\lambda_{\text{sym}}$  and  $\lambda_{\text{alg}}$  on the performance of Algorithm 3 to solve the benchmark problem from Subsection 6.4 for various polynomial degrees. The damping parameter reads  $\delta = 0.1$  and the polynomial degree  $p = 2$ . The best choice per column is marked in yellow, per row in blue, and for both in green. In either case  $\theta \in \{0.3, 0.5, 0.7\}$ , the best choice is  $\lambda_{\text{sym}} = 0.1$  and  $\lambda_{\text{alg}} = 0.7$ .

estimator reads  $\eta_H(u_H)^2 := \sum_{T \in \mathcal{T}_H} \eta_H(T, u_H)^2$  with the local contributions

$$\begin{aligned} \eta_H(T, u_H)^2 := & |T|^{2/d} \|f + \operatorname{div}(\mu(|\nabla u_H|^2) \nabla u_H - \mathbf{f})\|_{L^2(T)}^2 \\ & + |T|^{1/d} \|[(\mu(|\nabla u_H|^2) \nabla u_H - \mathbf{f}) \cdot \mathbf{n}]\|_{L^2(\partial T \cap \Omega)}^2. \end{aligned} \quad (78)$$

It is well-known from [CFPP14, Section 10.1] that  $\eta_H$  satisfies (A1)–(A4).

The (non-linear) discrete problem (77), could be treated with the Zangwill iteration or alternatively a damped Newton method. However, in the present setting we employ the Kačanov linearization [Kač59], see also [HPW21], which does not rely on the choice of appropriate additional damping parameters, thus guaranteeing parameter-robust full R-linear convergence. Instead, the Kačanov linearization exploits the multiplicative structure of the non-linearity  $\mathbf{A}(\nabla u_H) = \mu(|\nabla u_H|^2) \nabla u_H$ . The corresponding iteration mapping  $\Phi_H: \mathcal{X}_H \rightarrow \mathcal{X}_H$  is determined via

$$\langle \mu(|\nabla u_H|^2) \nabla \Phi_H(u_H), \nabla v_H \rangle_{L^2(\Omega)} = F(v_H) \quad \text{for all } u_H, v_H \in \mathcal{X}_H. \quad (79)$$

Since  $\alpha \leq \mu(|\nabla u_H|^2) \leq L/3$  from (76) with  $s = 0$ , this discrete linear system is well-posed and admits a unique solution  $\Phi_H(u_H) \in \mathcal{X}_H$  so that  $\Phi_H$  is indeed well-defined. Moreover, (79) takes the form of the linear system from Section 1.2 and can thus be solved using the appropriate iterative algebraic solver  $\Psi_H: \mathcal{X}^* \times \mathcal{X}_H \rightarrow \mathcal{X}_H$  from Subsection 2.2. Further details are omitted here and the reader is referred to [MPS24, Sect. 2.3]. As in Section 6, the adaptive algorithm will thus require a triple index  $(\ell, k, j)$ : The index  $\ell \in \mathbb{N}_0$  denotes the mesh-level, the index  $k \in \mathbb{N}_0$  denotes the Kačanov step, and the index  $j \in \mathbb{N}_0$  denotes the step of the algebraic solver, i.e.,

$$u_\ell^{k,j} = \Psi_\ell(u_\ell^{k,*}, u_\ell^{k,j-1}) \approx u_\ell^{k,*} := \Phi_\ell(u_\ell^{k-1,j}) \approx u_\ell^*,$$

where neither  $u_\ell^{k,*}$  nor  $u_\ell^*$  are computed, but only  $u_\ell^{k,j}$ .

Solving the weak problem (75) (resp. the discrete problem (77)) can indeed be seen as minimizing the energy  $\mathcal{E}$

$$\mathcal{E}(v) := \frac{1}{2} \int_\Omega \int_0^{|\nabla v|^2} \mu(t) \, dt \, dx - F(v) \quad \text{for all } v \in \mathcal{X} \quad (80)$$

over  $v \in \mathcal{X}$  with unique minimizer  $u^* \in \mathcal{X}$  (resp. over  $v_H \in \mathcal{X}_H$  with unique minimizer  $u_H^* \in \mathcal{X}_H$ ); see, e.g., [MPS24]. The corresponding energy difference

$$\mathbf{d}^2(v, w) := \mathcal{E}(w) - \mathcal{E}(v) \quad \text{for all } v, w \in \mathcal{X}$$

satisfies

$$\frac{\alpha}{2} \| \|v_H - u_H^* \| \|^2 \leq \mathbf{d}^2(u_H^*, v_H) \leq \frac{L}{2} \| \|v_H - u_H^* \| \|^2 \quad \text{for all } v_H \in \mathcal{X}_H;$$

see, e.g., [GHPS18, Lemma 5.1]. Since the Kačanov linearization can be proved to be contractive in the energy difference, we employ  $\mathbf{d}^2(\cdot, \cdot)$  in a novel stopping criterion for the adaptive algorithm in [MPS24].

---

**Remark 22.** *The reader is also referred to [BBI<sup>+</sup>22; BBI<sup>+</sup>23; BPS24] for results addressing locally Lipschitz semi-linear problems, where linearization is based on the Zangwill iteration from Section 6.*

---

**7.2. Algorithm 4: Adaptive iteratively linearized FEM. Input:** Initial mesh  $\mathcal{T}_0$ , polynomial degree  $p \in \mathbb{N}$ , initial iterate  $u_0^{0,0} := u_0^{0,j} := 0$ , marking parameter  $0 < \theta \leq 1$ , stopping parameter  $\lambda_{\text{lin}} > 0$ , and algebraic solver parameter  $0 < \rho < 1$ . Moreover, initialize  $\alpha_{\text{min}} > 0$ ,  $J_{\text{max}} \in \mathbb{N}$  with arbitrary values.

**Adaptive loop:** For all  $\ell = 0, 1, 2, \dots$ , repeat the steps (I)–(III):

(I) **SOLVE & ESTIMATE.** For all  $k = 1, 2, 3, \dots$ , repeat the steps (a)–(c):

(a) **Algebraic solver loop:** For all  $j = 1, 2, 3, \dots$ , repeat the steps (i)–(ii):

- (i) Compute  $u_\ell^{k,j} := \Psi_\ell(u_\ell^{k,\star}, u_\ell^{k,j-1})$  (for the approximation of the theoretical quantity  $u_\ell^{k,\star} := \Phi_\ell(u_\ell^{k-1,\underline{j}}) \in \mathcal{X}_\ell$  solving (79) for  $u_H = u_\ell^{k-1,\underline{j}}$ ), refinement indicators  $\eta_\ell(T, u_\ell^{k,j})$  for all  $T \in \mathcal{T}_\ell$ , and the energy difference  $\mathbf{d}^2(u_\ell^{k,j}, u_\ell^{k-1,\underline{j}})$ .
- (ii) Compute  $\alpha_\ell^{k,j} := \mathbf{d}^2(u_\ell^{k,j}, u_\ell^{k-1,\underline{j}}) / \|\|u_\ell^{k,j} - u_\ell^{k-1,\underline{j}}\|\|^2$ .
- (iii) Terminate  $j$ -loop with  $\underline{j}[\ell, k] := j$  and employ nested iteration  $u_\ell^{k,0} := u_\ell^{k-1,\underline{j}}$  provided that either

$$\alpha_\ell^{k,j} \geq \alpha_{\min} \quad \text{or} \quad u_\ell^{k,j} = u_\ell^{k-1,\underline{j}} \quad \text{or} \quad [\alpha_\ell^{k,j} > 0 \ \& \ j > J_{\max}]$$

- (b) If  $\underline{j}[\ell, k] > J_{\max}$ , then update  $J_{\max} := \underline{j}[\ell, k]$  and  $\alpha_{\min} := \rho \alpha_{\min}$ .
- (c) Terminate  $k$ -loop and define  $\underline{k}[\ell] := k$  provided that

$$\mathbf{d}^2(u_\ell^{k,j}, u_\ell^{k-1,\underline{j}}) \leq \lambda_{\min} \eta_\ell(u_\ell^{k,j})^2. \quad (81)$$

- (II) **MARK**. Determine a set  $\mathcal{M}_\ell \subseteq \mathcal{T}_\ell$  of minimal cardinality that satisfies the Dörfler marking criterion

$$\theta \eta_\ell(u_\ell^{k,j})^2 \leq \eta_\ell(\mathcal{M}_\ell, u_\ell^{k,j})^2.$$

- (III) **REFINE**. Generate the new mesh  $\mathcal{T}_{\ell+1} := \text{refine}(\mathcal{T}_\ell, \mathcal{M}_\ell)$  by NVB and define  $u_{\ell+1}^{0,0} := u_{\ell+1}^{0,\underline{j}} := u_\ell^{k,j}$  (nested iteration).

In practice, Algorithm 4 will be stopped after finite time if the number of degrees of freedom exceeds a given threshold or if the computational time has reached a maximum or if the approximation is sufficiently accurate.

This algorithm coincides with Algorithm 3 except for the novel stopping condition in step (I.a.iii) for the algebraic solver loop and in step (I.c) for the linearization loop that exploits the inherent energy structure of the PDE (74).

---

**Remark 23.** *Let us comment on the stopping criteria in Algorithm 4 for the Kačanov linearization and the algebraic solver.*

- (i) *Note the novel and parameter-free stopping criterion for the algebraic solver loop in step (I.a.iii) of Algorithm 4 when compared to Algorithm 3. It is motivated by the fact that the Kačanov linearization guarantees existence of a constant  $C_{nrg}^\star > 0$  such that*

$$\alpha := \mathbf{d}^2(u_\ell^{k,\star}, u_\ell^{k-1,\underline{j}}) / \|\|u_\ell^{k,\star} - u_\ell^{k-1,\underline{j}}\|\|^2 \geq C_{nrg}^\star > 0; \quad (82)$$

*see, e.g., [HPW21]. Since this holds analytically for  $u_\ell^{k,\star}$ , the algebraic solver should iterate until this condition is satisfied for the computed approximation  $u_\ell^{k,j}$ . Indeed, the estimate (82) ensures that the nested linearization with algebraic solver is contractive in energy, i.e.,*

$$\mathbf{d}^2(u_\ell^\star, u_\ell^{k,j}) \leq q_{\text{lin}} \mathbf{d}^2(u_\ell^\star, u_\ell^{k-1,\underline{j}}),$$

*where  $0 < q_{\text{lin}} < 1$  is independent of  $\ell$  and  $k$ . The latter contraction is the crucial ingredient in proving full  $R$ -linear convergence for the adaptive algorithm, where the proof follows the above lines essentially replacing  $\|\|\cdot\|\|^2$  by the energy difference  $\mathbf{d}^2(\cdot, \cdot)$ .*

- (ii) With this understanding, the stopping criterion (81) for the linearization has the same interpretation as for Algorithm 1. We numerically equilibrate the linearization error  $\mathbf{d}^2(u_\ell^*, u_\ell^{k,j})^{1/2} \lesssim \mathbf{d}^2(u_\ell^{k,j}, u_\ell^{k-1,j})^{1/2}$  with the discretization error  $\|u^* - u_\ell^*\| \lesssim \eta_\ell(u_\ell^*)$  measured in terms of  $\eta_\ell(u_\ell^{k,j})$ .
- (iii) While the innermost  $j$ -loop of the algebraic solver is known to terminate (see Lemma 24 below), the  $k$ -loop of the linearization can fail. However, in this case Theorem 26 predicts  $u^* = u_\ell^*$  and  $\eta_\ell(u_\ell^{k,j}) \rightarrow \eta_\ell(u_\ell^*) = 0$  as  $k \rightarrow \infty$ .

An analogous notation applies for the totally ordered index set  $\mathcal{Q} \subset \mathbb{N}_0^3$  as in Subsection 6.2. The corresponding quasi-error reads

$$H_\ell^{k,j} := \|u_\ell^* - u_\ell^{k,j}\| + \|u_\ell^{k,*} - u_\ell^{k,j}\| + \eta_\ell(u_\ell^{k,j}). \quad (83)$$

A first important observation is that the innermost  $j$ -loop is known to terminate. Unlike Algorithm 3 (see Lemma 16), the energy structure exploited by the novel stopping criterion of Algorithm 4 even allows to conclude that the number of algebraic solver steps per linearization step is uniformly bounded.

**Lemma 24 (uniform bound on number of algebraic solvers steps [MPS24, Prop. 4]).** Consider arbitrary parameters  $0 < \theta \leq 1$ ,  $0 < \lambda_{\text{lin}}$ ,  $0 < \rho < 1$ ,  $\alpha_{\text{min}} > 0$ ,  $J_{\text{max}} \in \mathbb{N}$ . Then, Algorithm 4 guarantees the existence of  $j_0 \in \mathbb{N}$  such that  $j[\ell, k] \leq j_0$  for all  $(\ell, k, 0) \in \mathcal{Q}$ , i.e., the number of algebraic solver steps is finite and even uniformly bounded.  $\square$

The following proposition provides a-posteriori error control at each step of the adaptive algorithm, which can again be used to terminate Algorithm 4.

**Lemma 25 (a-posteriori error control [MPS24, Prop. 5]).** For any  $(\ell, k, j) \in \mathcal{Q}$  with  $k \geq 1$  and  $j \geq 1$ , it holds that

$$\|u^* - u_\ell^{k,j}\| \lesssim [\eta_\ell(u_\ell^{k,j}) + \|u_\ell^{k,j} - u_\ell^{k-1,j}\| + \|u_\ell^{k,j} - u_\ell^{k,j-1}\|] \quad (84)$$

and for  $k = \underline{k}[\ell]$ ,  $j = \underline{j}[\ell, k]$

$$\|u^* - u_\ell^{k,j}\| \lesssim \eta_\ell(u_\ell^{k,j}). \quad \square$$

**7.3. Convergence and complexity.** By definition, the energy difference from (83) satisfies

$$\mathbf{d}^2(u_\ell^{k,j}, u_\ell^{k-1,j}) = \mathbf{d}^2(u_\ell^*, u_\ell^{k-1,j}) - \mathbf{d}^2(u_\ell^*, u_\ell^{k,j}),$$

where all terms are guaranteed to be non-negative. This replaces the role of the Pythagorean identity (12) in the energy-based proof in [MPS24] to establish the following convergence results for Algorithm 4. Importantly, the theorems state parameter robust full R-linear convergence and, for sufficiently small adaptivity parameters, optimal complexity of the adaptive algorithm.

**Theorem 26 (parameter-robust full R-linear convergence [MPS24, Thm. 6]).** Consider arbitrary parameters  $0 < \theta \leq 1$ ,  $0 < \lambda_{\text{lin}}$ , and  $0 < \rho < 1$  as well as initialization values  $\alpha_{\text{min}} > 0$ ,  $J_{\text{max}} \in \mathbb{N}$ . Then, Algorithm 4 guarantees the existence of constants  $0 < q_{\text{lin}} < 1$  and  $C_{\text{lin}} > 0$  such that

$$H_\ell^{k,j} \leq C_{\text{lin}} q_{\text{lin}}^{|\ell, k, j| - |\ell', k', j'|} H_{\ell'}^{k', j'} \quad \text{for all } (\ell, k, j), (\ell', k', j') \in \mathcal{Q} \text{ with } |\ell, k, j| > |\ell', k', j'|.$$

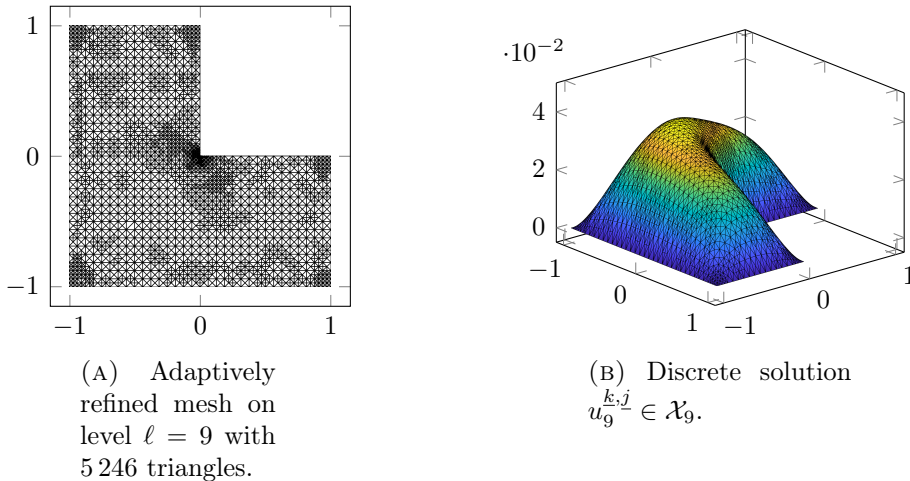


FIGURE 17. Mesh and corresponding discrete solution for the benchmark problem from Subsection 7.4. The results are generated by Algorithm 4 with polynomial degree  $p = 1$ , bulk parameter  $\theta = 0.3$ , and stopping parameter  $\lambda_{\text{lin}} = 0.7$ .

In particular, this yields parameter-robust convergence

$$\|u^* - u_\ell^{k,j}\| \lesssim H_\ell^{k,j} \leq C_{\text{lin}} q_{\text{lin}}^{|\ell,k,j|} H_0^{0,0} \rightarrow 0 \quad \text{as } |\ell, k, j| \rightarrow \infty. \quad \square$$

---

**Theorem 27 (optimal complexity [MPS24, Thm. 10]).** *There exist upper bounds  $0 < \theta^* \leq 1$  and  $\lambda_{\text{lin}}^* > 0$  such that, for all  $0 < \theta \leq \theta^*$  and  $0 < \lambda_{\text{lin}} \leq \lambda_{\text{lin}}^*$ , the following holds: Algorithm 4 guarantees that*

$$\|u^*\|_{\mathbb{A}_s} \lesssim \sup_{(\ell,k,j) \in \mathcal{Q}} \text{cost}(\ell, k, j)^s H_\ell^{k,j} \lesssim \max\{\|u^*\|_{\mathbb{A}_s}, H_0^{0,0}\} \quad \text{for all } s > 0. \quad \square$$


---

**7.4. Numerical example.** Consider the benchmark problem (75) on the L-shaped domain  $\Omega := (-1, 1)^2 \setminus [0, 1]^2$  with scalar non-linear coefficient  $\mu(t) := 2 + (1 + t)^{-2}$ . The adaptive algorithm creates meshes with increased resolution of the reentrant corner where the exact solution exhibits a singularity. This is illustrated in Figure 17. Consequently, Figure 18 demonstrates that the adaptive algorithm converges with the optimal rate for the error estimator and the energy difference. The computation with the Zarantonello linearization employs an algorithm analogous to Algorithm 3 whereas the Kačanov linearization is utilized in Algorithm 4. Due to the nested structure of the algorithm and the  $h$ -robustness of the iterative algebraic solver, the number of algebraic solver steps (accumulated over each level  $\ell$ ) is uniformly bounded as depicted in Figures 19. It turns out that the novel stopping criterion in Algorithm 4 appears more robust with respect to a disadvantageous choice of the initial iterate for the algebraic solver.

## 8. FURTHER GENERALIZATIONS AND COMMENTS

We comment that the results on adaptive algorithms treated in this chapter are not restricted to a specific linear or non-linear model problem but are rather formulated in an abstract setting that covers a wide range of problems. The only requirements are the properties of the a-posteriori error estimator as established in [CFPP14] and presented by (A1)–(A4) on page 8, a contraction property as (C) on page 6 for the integrated

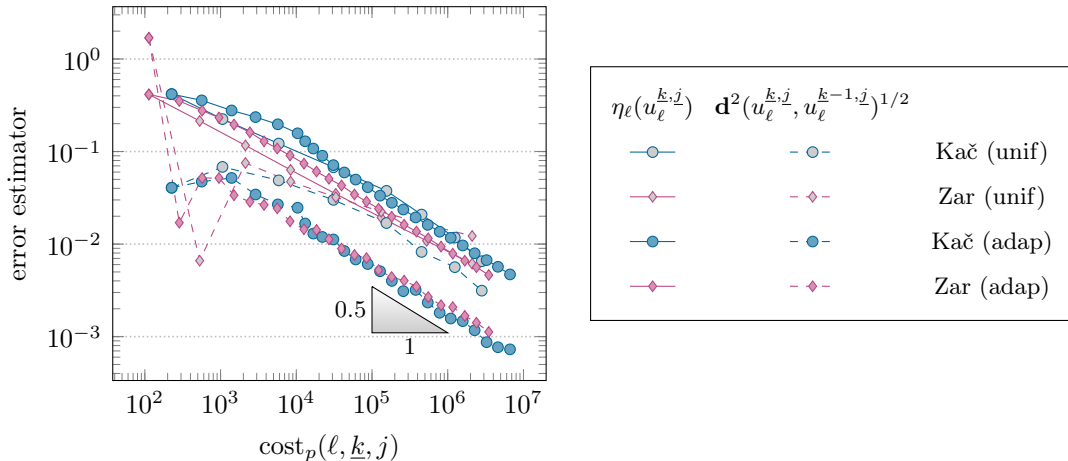


FIGURE 18. Convergence plot of the adaptive Algorithm 3 with Zaranonello linearization and the adaptive Algorithm 4 with Kačanov linearization, with polynomial degree  $p = 1$ , to solve the benchmark problem from Subsection 7.4 for two different linearizations. The damping parameter of the Zaranonello iteration reads  $\delta = 1/3$  and the adaptivity parameters  $\theta = 0.3$  and  $\lambda_{\text{lin}} = \lambda_{\text{alg}} = 0.7$ , whereas Kačanov linearization uses initial parameters  $\alpha_{\text{min}} = 100$  and  $J_{\text{max}} = 1$ . The graphs display values of the residual-based error estimator  $\eta_\ell(u_\ell^{\underline{k}, \underline{j}})$  from (78) for the final iterates on the level  $\ell \in \mathbb{N}_0$  and the energy differences  $\mathbf{d}^2(u_\ell^{\underline{k}, \underline{j}}, u_\ell^{\underline{k}-1, \underline{j}})^{1/2}$ .

iterative solver, as well as the quasi-orthogonality (71) on page 34. The latter is satisfied for any well-posed saddle-point problem [Fei22], but as exemplified in Section 7 can be proved for certain energy minimization problems [GHPS21b; HPW21; BFM+23]. In the following, we briefly comment on potential generalizations.

**More general problems.** Note that adaptivity has been successfully applied to a variety of problems, in particular, to variational problems, such as the obstacle problem; see, e.g., [PP13] for linear convergence as well as [CH15] for optimal convergence rates with respect to the dimension of the underlying discrete space, provided that the variational inequality is solved exactly. In practice, the iterative solution of variational inequalities typically employs a semi-smooth Newton method as formulated in [HIK02]. However, the super-linear convergence result in [HIK02] holds only for initial iterates sufficiently close to the exact solution and thus the required contraction property is only guaranteed locally. Consequently, the application within our framework of optimal complexity is subject to future research.

**Boundary conditions.** While the treatment of Robin or Neumann boundary conditions is rather immediate, see, e.g., [CFPP14], the treatment of inhomogeneous Dirichlet boundary conditions needs more careful consideration. Available results rely on the discretization of the Dirichlet data followed by the solution of the discrete weak formulation; see, e.g., [BCD04; AFK+13; CFPP14]. In two dimensions, the nodal interpolation of the boundary data suffices to ensure optimal convergence rates; see, e.g., [FPP14] for the lowest-order case  $p = 1$  and [BC17] for a generalization to arbitrary order  $p \geq 1$ . It turned out that, in any dimension, each  $H^{1/2}$ -stable operator such as the Scott-Zhang quasi-interpolation is an admissible choice for the approximation of the Dirichlet boundary data [AFK+13]; see also [CFPP14]. Alternatively, the  $L^2$  projection

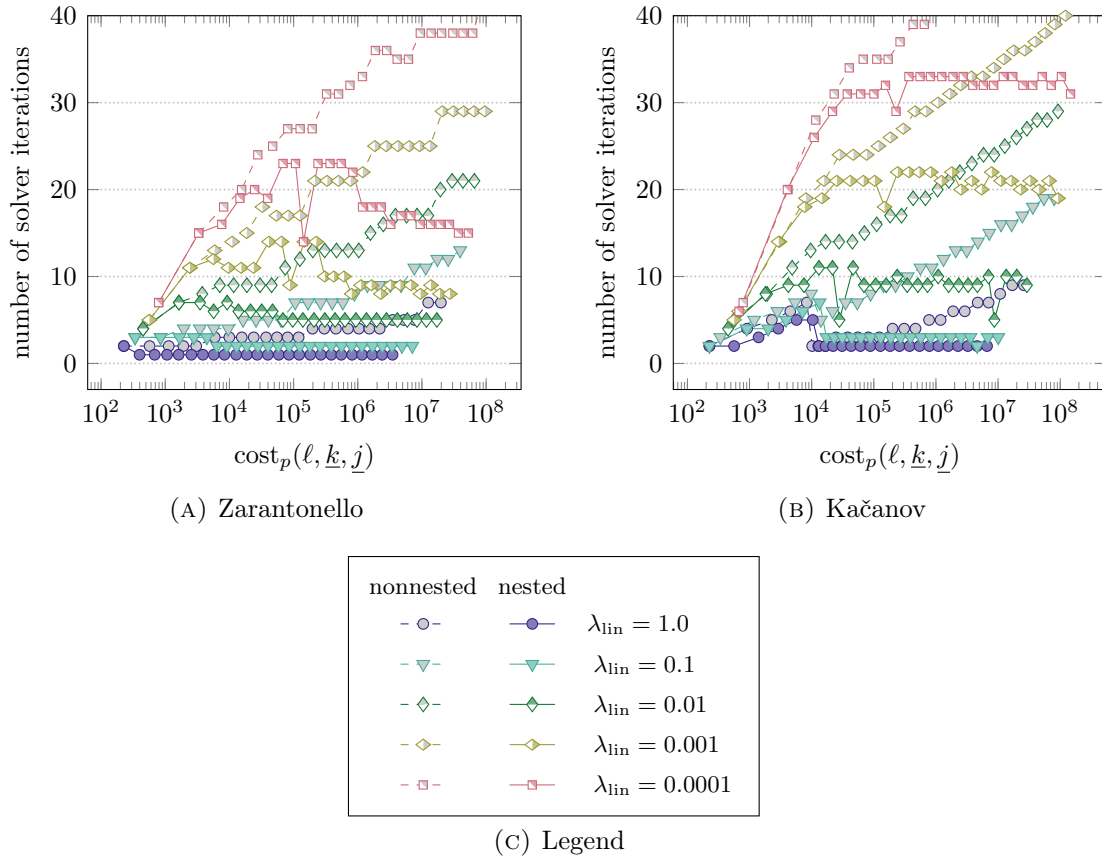


FIGURE 19. Number of iteration steps of algebraic iteration for the benchmark problem from Subsection 7.4 with nested and non-nested iteration for various stopping parameters  $\lambda_{\text{lin}}$ . The damping parameter of the Zarantonello iteration reads  $\delta = 1/3$  and the adaptivity parameters  $\theta = 0.3$  and  $\lambda_{\text{alg}} = 0.7$ , whereas Kačanov linearization additionally uses initial parameters  $\alpha_{\text{min}} = 100$  and  $J_{\text{max}} = 1$ .

can be used [BCD04]. However, beyond the 2D case [FPP14; BC17] or the Scott-Zhang quasi-interpolation for  $d \geq 2$  [CFPP14], the state-of-the-art analysis requires an extended marking strategy to equilibrate the approximation error of the Dirichlet data and the discretization error of the weak form [AFK<sup>+</sup>13].

**Equivalent estimators.** Finally let us comment on other a-posteriori error estimators which were applied in the context of adaptive mesh refinement. The work [KS11] considers a variety of a-posteriori error estimators (including equilibrated fluxes [Vej04; BS08a]) for the Poisson model problem and proves linear convergence with optimal convergence rates for an adaptive algorithm with exact solver. The technical constraint that not only the marked elements but also all their neighbors must be refined, has been removed in [CFPP14, Sect. 8], where the standard adaptive algorithm with exact solver (exemplified for Zienkiewicz-Zhu-type estimators [ZZ87]) is considered and analyzed: The key idea (for linear elliptic PDEs) is the observation that the usual estimators are locally equivalent, i.e., the use of Dörfler marking for one of the usual a-posteriori error estimators also yields implicitly the Dörfler marking for the standard residual a-posteriori error estimator (with a different marking parameter though). Then the usual analysis for the residual a-posteriori error estimator applies and proves linear convergence with optimal rates [KS11;

[CFPP14](#)]. For linear PDEs, this idea extends to the adaptive algorithm with contractive solver, while the extension to non-linear PDEs remains for future work.

## REFERENCES

- [AFK<sup>+</sup>13] M. Aurada, M. Feischl, J. Kemetmüller, M. Page, and D. Praetorius. Each  $H^{1/2}$ -stable projection yields convergence and quasi-optimality of adaptive FEM with inhomogeneous Dirichlet data in  $\mathbb{R}^d$ . *ESAIM Math. Model. Numer. Anal.*, 47(4):1207–1235, 2013.
- [AO00] M. Ainsworth and J. T. Oden. *A posteriori error estimation in finite element analysis*. Wiley, New York, 2000.
- [BBCO24] R. Becker, S. P. A. Bordas, F. Chouly, and P. Omnes. A short perspective on a posteriori error control and adaptive discretizations. In F. Chouly, S. P. Bordas, R. becker, and P. Omnes, editors, *Error Control, Adaptive Discretizations, and Applications, Part 1, ISBN: 9780443294488*. Volume 58. Elsevier, 2024.
- [BBI<sup>+</sup>22] R. Becker, M. Brunner, M. Innerberger, J. M. Melenk, and D. Praetorius. Rate-optimal goal-oriented adaptive FEM for semilinear elliptic PDEs. *Comput. Math. Appl.*, 118:18–35, 2022.
- [BBI<sup>+</sup>23] R. Becker, M. Brunner, M. Innerberger, J. M. Melenk, and D. Praetorius. Cost-optimal adaptive iterative linearized FEM for semilinear elliptic PDEs. *ESAIM Math. Model. Numer. Anal.*, 57(4):2193–2225, 2023.
- [BBPS23] P. Bringmann, M. Brunner, D. Praetorius, and J. Streitberger. Optimal complexity of goal-oriented adaptive FEM for nonsymmetric linear elliptic PDEs, 2023. arXiv: [2312.00489](#).
- [BC17] P. Bringmann and C. Carstensen.  $h$ -adaptive least-squares finite element methods for the 2D Stokes equations of any order with optimal convergence rates. *Comput. Math. Appl.*, 74(8):1923–1939, 2017.
- [BCD04] S. Bartels, C. Carstensen, and G. Dolzmann. Inhomogeneous Dirichlet conditions in a priori and a posteriori finite element error analysis. *Numer. Math.*, 99(1):1–24, 2004.
- [BDD04] P. Binev, W. Dahmen, and R. DeVore. Adaptive finite element methods with convergence rates. *Numer. Math.*, 97(2):219–268, 2004.
- [BFM<sup>+</sup>23] P. Bringmann, M. Feischl, A. Miraçi, D. Praetorius, and J. Streitberger. On full linear convergence and optimal complexity of adaptive FEM with inexact solver, 2023. arXiv: [2311.15738](#).
- [BGIP23] R. Becker, G. Gantner, M. Innerberger, and D. Praetorius. Goal-oriented adaptive finite element methods with optimal computational complexity. *Numer. Math.*, 153(1):111–140, 2023.
- [BHI<sup>+</sup>23] M. Brunner, P. Heid, M. Innerberger, A. Miraçi, D. Praetorius, and J. Streitberger. Adaptive FEM with quasi-optimal overall cost for nonsymmetric linear elliptic PDEs. *IMA J. Numer. Anal.*, in print, 2023.
- [BHP17] A. Bespalov, A. Haberl, and D. Praetorius. Adaptive FEM with coarse initial mesh guarantees optimal convergence rates for compactly perturbed elliptic problems. *Comput. Methods Appl. Mech. Engrg.*, 317:318–340, 2017.
- [BIM<sup>+</sup>24] M. Brunner, M. Innerberger, A. Miraçi, D. Praetorius, J. Streitberger, and P. Heid. Corrigendum to: Adaptive FEM with quasi-optimal overall cost for nonsymmetric linear elliptic PDEs. *IMA J. Numer. Anal.*, in print, 2024.

- [BN10] A. Bonito and R. H. Nochetto. Quasi-optimal convergence rate of an adaptive discontinuous Galerkin method. *SIAM J. Numer. Anal.*, 48(2):734–771, 2010.
- [BPS24] M. Brunner, D. Praetorius, and J. Streitberger. Cost-optimal adaptive FEM with linearization and algebraic solver for semilinear elliptic PDEs. 2024.
- [BR78] I. Babuška and W. C. Rheinboldt. Error estimates for adaptive finite element computations. *SIAM J. Numer. Anal.*, 15(4):736–754, 1978.
- [BS08a] D. Braess and J. Schöberl. Equilibrated residual error estimator for edge elements. *Math. Comp.*, 77(262):651–672, 2008.
- [BS08b] S. C. Brenner and L. R. Scott. *The mathematical theory of finite element methods*. Springer, New York, third edition, 2008.
- [BV84] I. Babuška and M. Vogelius. Feedback and adaptive finite element solution of one-dimensional boundary value problems. *Numer. Math.*, 44(1):75–102, 1984.
- [CFPP14] C. Carstensen, M. Feischl, M. Page, and D. Praetorius. Axioms of adaptivity. *Comput. Math. Appl.*, 67(6):1195–1253, 2014.
- [CH15] C. Carstensen and J. Hu. An optimal adaptive finite element method for an obstacle problem. *Comput. Methods Appl. Math.*, 15(3):259–277, 2015.
- [CKNS08] J. M. Cascón, C. Kreuzer, R. H. Nochetto, and K. G. Siebert. Quasi-optimal convergence rate for an adaptive finite element method. *SIAM J. Numer. Anal.*, 46(5):2524–2550, 2008.
- [CNX12] L. Chen, R. H. Nochetto, and J. Xu. Optimal multilevel methods for graded bisection grids. *Numer. Math.*, 120(1):1–34, 2012.
- [DGS23] L. Dening, L. Gehring, and J. Storn. Adaptive Mesh Refinement for arbitrary initial Triangulations, 2023. arXiv: [2306.02674](https://arxiv.org/abs/2306.02674).
- [Dör96] W. Dörfler. A convergent adaptive algorithm for Poisson’s equation. *SIAM J. Numer. Anal.*, 33(3):1106–1124, 1996.
- [EG21] A. Ern and J.-L. Guermond. *Finite elements II—Galerkin approximation, elliptic and mixed PDEs*. Springer, Cham, 2021.
- [EV13] A. Ern and M. Vohralík. Adaptive inexact Newton methods with a posteriori stopping criteria for nonlinear diffusion PDEs. *SIAM J. Sci. Comput.*, 35(4):A1761–A1791, 2013.
- [Eva98] L. C. Evans. *Partial differential equations*. American Mathematical Society, Providence, RI, 1998.
- [Fei22] M. Feischl. Inf-sup stability implies quasi-orthogonality. *Math. Comp.*, 91(337):2059–2094, 2022.
- [FPP14] M. Feischl, M. Page, and D. Praetorius. Convergence and quasi-optimality of adaptive FEM with inhomogeneous Dirichlet data. *J. Comput. Appl. Math.*, 255:481–501, 2014.
- [FPZ16] M. Feischl, D. Praetorius, and K. G. van der Zee. An abstract analysis of optimal goal-oriented adaptivity. *SIAM J. Numer. Anal.*, 54(3):1423–1448, 2016.
- [GHPS18] G. Gantner, A. Haberl, D. Praetorius, and B. Stiftner. Rate optimal adaptive FEM with inexact solver for nonlinear operators. *IMA J. Numer. Anal.*, 38(4):1797–1831, 2018.
- [GHPS21a] G. Gantner, A. Haberl, D. Praetorius, and S. Schimanko. Rate optimality of adaptive finite element methods with respect to overall computational costs. *Math. Comp.*, 90(331):2011–2040, 2021.

- [GHPS21b] G. Gantner, A. Haberl, D. Praetorius, and S. Schimanko. Rate optimality of adaptive finite element methods with respect to overall computational costs. *Math. Comp.*, 90(331):2011–2040, 2021.
- [GKZB83] J. P. d. S. R. Gago, D. W. Kelly, O. C. Zienkiewicz, and I. Babuška. A posteriori error analysis and adaptive processes in the finite element method. II. Adaptive mesh refinement. *Internat. J. Numer. Methods Engrg.*, 19(11):1621–1656, 1983.
- [GMZ12] E. Garau, P. Morin, and C. Zuppa. Quasi-Optimal Convergence Rate of an AFEM for Quasi-Linear Problems of Monotone Type. *Numer. Math: Theory, Meth. Appl.*, 5(2):131–156, 2012.
- [GS02] M. B. Giles and E. Süli. Adjoint methods for PDEs: a posteriori error analysis and postprocessing by duality. *Acta Numer.*, 11:145–236, 2002.
- [GSS14] D. Gallistl, M. Schedensack, and R. P. Stevenson. A remark on newest vertex bisection in any space dimension. *Comput. Methods Appl. Math.*, 14(3):317–320, 2014.
- [HIK02] M. Hintermüller, K. Ito, and K. Kunisch. The primal-dual active set strategy as a semismooth Newton method. *SIAM J. Optim.*, 13(3):865–888, 2002.
- [HPSV21] A. Haberl, D. Praetorius, S. Schimanko, and M. Vohralík. Convergence and quasi-optimal cost of adaptive algorithms for nonlinear operators including iterative linearization and algebraic solver. *Numer. Math.*, 147(3):679–725, 2021.
- [HPW21] P. Heid, D. Praetorius, and T. P. Wihler. Energy contraction and optimal convergence of adaptive iterative linearized finite element methods. *Comput. Methods Appl. Math.*, 21(2):407–422, 2021.
- [HW20a] P. Heid and T. P. Wihler. Adaptive iterative linearization Galerkin methods for nonlinear problems. *Math. Comp.*, 89:2707–2734, 2020.
- [HW20b] P. Heid and T. P. Wihler. On the convergence of adaptive iterative linearized Galerkin methods. *Calcolo*, 57:24, 2020.
- [IMPS24] M. Innerberger, A. Miraçi, D. Praetorius, and J. Streitberger. *hp*-robust multigrid solver on locally refined meshes for FEM discretizations of symmetric elliptic PDEs. *ESAIM Math. Model. Numer. Anal.*, 58(1):247–272, 2024.
- [IP23] M. Innerberger and D. Praetorius. MooAFEM: An object oriented Matlab code for higher-order adaptive FEM for (nonlinear) elliptic PDEs. *Appl. Math. Comput.*, 442:127731, 2023.
- [Kač59] L. Kačanov. Variational methods of solution of plasticity problems. *J. Appl. Math. Mech.*, 23:880–883, 1959.
- [Kel74] R. B. Kellogg. On the Poisson equation with intersecting interfaces. *Applicable Anal.*, 4:101–129, 1974.
- [KPP13] M. Karkulik, D. Pavlicek, and D. Praetorius. On 2D newest vertex bisection: optimality of mesh-closure and  $H^1$ -stability of  $L_2$ -projection. *Constr. Approx.*, 38(2):213–234, 2013.
- [KS11] C. Kreuzer and K. G. Siebert. Decay rates of adaptive finite elements with Dörfler marking. *Numer. Math.*, 117(4):679–716, 2011.
- [KV21] C. Kreuzer and A. Veese. Oscillation in a posteriori error estimation. *Numer. Math.*, 148(1):43–78, 2021.
- [Mit91] W. F. Mitchell. Adaptive refinement for arbitrary finite-element spaces with hierarchical bases. *J. Comput. Appl. Math.*, 36(1):65–78, 1991.

- [MNS00] P. Morin, R. H. Nochetto, and K. G. Siebert. Data oscillation and convergence of adaptive FEM. *SIAM J. Numer. Anal.*, 38(2):466–488, 2000.
- [MNS03] P. Morin, R. H. Nochetto, and K. G. Siebert. Local problems on stars: a posteriori error estimators, convergence, and performance. *Math. Comp.*, 72(243):1067–1097, 2003.
- [MPS24] A. Miraçi, D. Praetorius, and J. Streitberger. Parameter-robust full linear convergence and optimal complexity of adaptive iteratively linearized FEM for nonlinear PDEs. 2024.
- [MS09] M. S. Mommer and R. Stevenson. A goal-oriented adaptive finite element method with convergence rates. *SIAM J. Numer. Anal.*, 47(2):861–886, 2009.
- [PP13] M. Page and D. Praetorius. Convergence of adaptive FEM for some elliptic obstacle problem. *Appl. Anal.*, 92(3):595–615, 2013.
- [PP20] C.-M. Pfeiler and D. Praetorius. Dörfler marking with minimal cardinality is a linear complexity problem. *Math. Comp.*, 89(326):2735–2752, 2020.
- [SMPZ08] J. Schöberl, J. M. Melenk, C. Pechstein, and S. Zaglmayr. Additive Schwarz preconditioning for  $p$ -version triangular and tetrahedral finite elements. *IMA J. Numer. Anal.*, 28(1):1–24, 2008.
- [Ste07] R. Stevenson. Optimality of a standard adaptive finite element method. *Found. Comput. Math.*, 7(2):245–269, 2007.
- [Ste08] R. Stevenson. The completion of locally refined simplicial partitions created by bisection. *Math. Comp.*, 77(261):227–241, 2008.
- [Vej04] T. Vejchodský. Local a posteriori error estimator based on the hypercircle method. In *Proc. of the European Congress on Computational Methods in Applied Sciences and Engineering (ECCOMAS 2004), Jyväskylä, Finland, 2004*.
- [Ver13] R. Verfürth. *A posteriori error estimation techniques for finite element methods*. Oxford University Press, Oxford, 2013.
- [WZ17] J. Wu and H. Zheng. Uniform Convergence of Multigrid Methods for Adaptive Meshes. *Appl. Numer. Math.*, 113:109–123, 2017.
- [Zar60] E. H. Zarantonello. Solving functional equations by contractive averaging. *Math. Research Center Report*, 160, 1960.
- [Zei90] E. Zeidler. *Nonlinear functional analysis and its applications. Part II/B - Nonlinear monotone operators*. 1990.
- [ZR79] P. Zave and W. C. Rheinboldt. Design of an adaptive, parallel finite-element system. *ACM Trans. Math. Software*, 5(1):1–17, 1979.
- [ZZ87] O. C. Zienkiewicz and J. Z. Zhu. A simple error estimator and adaptive procedure for practical engineering analysis. *Internat. J. Numer. Methods Engrg.*, 24(2):337–357, 1987.

*Email address:* philipp.bringmann@asc.tuwien.ac.at (corresponding author)

*Email address:* ani.miraci@asc.tuwien.ac.at

*Email address:* dirk.praetorius@asc.tuwien.ac.at